

Development of spatially explicit operating models for yellowfin tuna populations in the Indian Ocean

Prepared for the Indian Ocean Tuna Commission

October 2020

Prepared by:

Alistair Dunn, Ocean Environmental Ltd, Wellington, New Zealand.
Simon Hoyle, National Institute of Water and Atmospheric Research (NIWA), Nelson, New Zealand.
Samik Datta, National Institute of Water and Atmospheric Research (NIWA), Wellington, New Zealand.




For any information regarding this report please contact:

Simon Hoyle
Fisheries modeller
Nelson
+64-3-545 7883
simon.hoyle@niwa.co.nz

National Institute of Water & Atmospheric Research Ltd
PO Box 893
Nelson 7040

Phone +64 3 548 1715

NIWA CLIENT REPORT No: 2020300WN
Report date: October 2020
NIWA Project: FAO19401

| Quality Assurance Statement | | |
|---|--------------------------|-----------------|
|  | Reviewed by: | Jeremy McKenzie |
|  | Formatting checked by: | Alex Quigley |
|  | Approved for release by: | Rosemary Hurst |

Dunn, A.; Hoyle, S.; Datta, S. (2020). Development of spatially explicit operating models for yellowfin tuna populations in the Indian Ocean. IOTC-2020-WPT22(AS)-19.

© All rights reserved. This publication may not be reproduced or copied in any form without the permission of the copyright owner(s). Such permission is only to be given in accordance with the terms of the client's contract with NIWA. This copyright extends to all forms of copying and any storage of material in any kind of information retrieval system.

Whilst NIWA has used all reasonable endeavours to ensure that the information contained in this document is accurate, NIWA does not give any express or implied warranty as to the completeness of the information contained herein, or that it will be suitable for any purpose(s) other than those specifically contemplated during the Project or agreed by NIWA and the Client.

Contents

| | |
|---|-----------|
| Abstract | 1 |
| 1 Introduction | 2 |
| 2 Methods | 5 |
| 2.1 Introduction | 5 |
| 2.2 Population and movement dynamics | 6 |
| 2.3 Observations and catch data | 15 |
| 2.4 Estimation of parameters | 29 |
| 2.5 Simulations | 30 |
| 2.6 Evaluation of stock assessment bias..... | 30 |
| 3 Results | 33 |
| 3.1 SPM model results | 33 |
| 3.2 SS3 model fit | 38 |
| 3.3 Examining how tag mixing affects stock assessment bias..... | 39 |
| 4 Discussion | 44 |
| 4.1 Further work | 45 |
| 4.2 Spatial model meeting..... | 46 |
| 5 Acknowledgments | 47 |
| 6 References | 48 |
| Appendix A SS Model Fit | 50 |

Tables

| | |
|---|----|
| Table 1: <i>Annual</i> cycle (i.e. year-in quarter years) of the YFT spatial model, showing the processes taking place at each step and the available observations, and the proportion mortality (natural and fishing) assumed to have taken place at the time the observations were evaluated. | 9 |
| Table 2: Stock synthesis model fishery structure. | 31 |
| Table 3: Estimated parameters values in the preliminary model (selectivity and movement preference functions), labels, priors, and assumed upper and lower bounds in the estimation (note: MLE values do represent a plausible minimum). | 34 |

Figures

| | |
|--|----|
| Figure 1: The Indian Ocean and the regions assumed in the SS3 stock assessment model (labelled R1a, R1b, R2, R3, and R4 from Fu et al., 2018); the region modelled using the spatially explicit model (SPM, grey cells) and the relative amount of catch (number) from each cell over the history of the YFT fishery (blue circles). | 4 |
| Figure 2: The Indian Ocean modelled region using the spatially explicit model (SPM, with 5×5° grey cells), within the total region assumed for the model. | 6 |
| Figure 3: Locations assumed for recruitment of age 1 YFT, where the colour (light blue = low, and dark blue = high) represents the proportion of recruitment occurring in each cell. | 10 |
| Figure 4: Assumed mean length at age (with grey indicating the 95% range) for YFT, taken from Fu et al. | 11 |
| Figure 5: Assumed rates of natural mortality by age for YFT, taken from Fu et al. (2018). | 11 |
| Figure 6: Assumed rates of maturation by age for YFT, taken from Fu et al. (2018). | 12 |
| Figure 7: Assumed recruitment (YCS multiplier) for YFT, taken from Fu et al. (2018). | 12 |
| Figure 8: Total catch (left axis, black line) by number and (right axis, red line) for YFT in the spatial model for 1952–2015. | 13 |
| Figure 9: Total catch (by number) for the seven defined fishery's in the spatial model; Purse Seine, troll, bait boat, gillnet, longline, handline, and all others. | 13 |
| Figure 10: Mean SST over the period 1952–2018 (data source: UK Met Office Hadley Centre (Rayner 2003) analyses with the Levitus et al. (2009) corrections applied). | 14 |
| Figure 11: Mean quarterly Chlorophyll-a over the period 2002–2018 (Data source: NASA Goddard Space Flight Center, Ocean Ecology Laboratory, Ocean Biology Processing Group 2020). | 15 |
| Figure 12: Relative catches by spatial location of the Purse Seine fishery assumed in the YFT spatial model. | 16 |
| Figure 13: Relative catches by spatial location of the Troll fishery assumed in the YFT spatial model. | 17 |
| Figure 14: Relative catches by spatial location of the bait boat fishery assumed in the YFT spatial model. | 18 |
| Figure 15: Relative catches by spatial location of the longline fishery assumed in the YFT spatial model. | 19 |
| Figure 16: Mean raw catch per hook (Japanese longline data only) for the years 1972–2015 by 5×5° spatial cell. | 20 |
| Figure 17: Raw CPUE for the Japanese longline fleet, 1952–2015. The period before 1972 (early CPUE, and not used within the preliminary model) is given in red. | 21 |
| Figure 18: Spatial Japanese longline (a) CPUE indices, standardised by (b) SST, (c) oxygen, and (d) Chlorophyll-a for 1952–2015. | 22 |
| Figure 19: Spatial density of proportions of measured fish of 50-80 cm, over years 1952–2015 and all fleets. | 23 |
| Figure 20: Spatial density of proportions of measured fish 80–120 cm, over years 1952–2015 and all fleets. | 24 |
| Figure 21: Spatial density of proportions of measured fish >120 cm, over years 1952-2015 and all fleets. | 25 |

| | |
|---|----|
| Figure 22: Locations of tag releases of YFT in the RTTP-IO programme between 2005–2007. | 27 |
| Figure 23: Locations of tag recaptures of YFT released in the RTTP-IO programme (2005–2007) and recaptured by purse seine vessels between 2005–2015. | 28 |
| Figure 24: Plot of the distance between release location and recapture location of the RTTP-IO tag releases and subsequent recaptures by purse seine vessels, 2005–2015. | 29 |
| Figure 25: Estimated preference functions for distance for (red) immature and (blue) mature YFT. | 35 |
| Figure 26: Estimated preference functions for SST for (red) immature and (blue) adult YFT. | 35 |
| Figure 27: Estimated preference functions for Chlorophyll-a for (red) immature and (blue) adult YFT. | 36 |
| Figure 28: Estimated SSB trajectory from the preliminary SPM model, compared with estimated SSB trajectory from Fu et al. (2018). Note that time units are pseudo-years (quarters). | 36 |
| Figure 29: Relative density of immature YFT (number) at initialisation (B_0) from the preliminary spatial model. | 37 |
| Figure 30: Relative density of mature YFT (number) at initialisation (B_0) from the preliminary spatial model. | 38 |
| Figure 31: Comparison of SSB estimates between the SSB simulator and SS estimation runs either without tags or with different assumed mixing periods. | 41 |
| Figure 32: Comparison of recruitment estimates between the SSB simulator and SS estimation runs either with (<i>mix4</i>) or without tags (<i>notags</i>). | 42 |
| Figure 33: Variation in estimated quarterly (pseudo-year) movement rates depending on how tags are treated in the SS model, for models without tags (<i>notags</i>) and with mixing periods 1, 4, and 8 quarters (<i>mix1</i> , <i>mix4</i> , <i>mix8</i>). | 43 |

Abstract

A preliminary operating model for Indian Ocean yellowfin tuna was successfully developed with the stock assessment package SPM. The model was spatially explicit at the 5° cell level with a quarterly (3-month) time step. The model was age-structured with many of the same biological characteristics as the 2018 IOTC Stock Synthesis assessment. Fish movements were estimated using preference functions based on distance and time-varying SST and chlorophyll, with independent preference functions for mature and immature fish. The model was fitted with catch, size, CPUE and tagging data. Initial biomass was fixed because biomass scale appeared to be confounded with movement rates.

This preliminary model can be considered a proof of concept for spatially explicit operating models of pelagic species and their potential utility.

As an example of its use, the MPD estimate of the SPM operating model was used to simulate randomised observational data for size, CPUE and tag recoveries, and these observational data were reformatted and loaded into a Stock Synthesis model based on the 2018 IOTC YFT stock assessment. Four versions of the SS assessment were trialled with different approaches to the tagging data, namely mixing periods of 1, 4, and 8 quarters and a version that omitted the tag likelihood.

The model with mixing period of 8 quarters estimated very similar biomass to the 'truth' represented by the operating model, while shorter mixing periods produced lower biomass estimates. Removing the influence of tagging data resulted in biomass estimates approximately twice the true value. These results may be indicative but should be seen as preliminary, since full exploration and validation of the models was beyond the scope of the project.

There is potential to both further develop the SPM model for yellowfin and other tuna species, and to use the operating model to test and improve current assessments. Recommendations are made for further work.

1 Introduction

The Indian Ocean Tuna Commission (IOTC) is mandated to manage 16 species of tuna and tuna-like species, with the primary objective to conserve and provide for optimum utilisation of the stocks while ensuring long-term sustainability. Tropical tuna (yellowfin tuna, skipjack tuna, and bigeye tuna) have accounted for about 55% of total catches of all IOTC managed species in recent years and are of major commercial importance to Indian Ocean coastal states as well as the distant water fishing nations.

Management advice for tropical tuna species is based on integrated statistical catch-at-age stock assessment models that accommodate complex population processes and a diverse range of input observations and data. However, there has been limited research to investigate the uncertainties in the tropical tuna population dynamics. Distribution, movement dynamics, and the underlying population structure are poorly understood, but may have important influences on stock assessment outputs.

A recent YFT assessment is described by Fu et al. (Fu et al. 2018), a preliminary update of the 2015 assessment of Indian Ocean yellowfin tuna (Langley 2015, 2016). From that assessment, Indian Ocean YFT were determined to be overfished and subject to overfishing. The Indian Ocean Tuna Commission (S20) adopted an Interim Plan for Rebuilding the Indian Ocean Yellowfin Tuna Stock in the IOTC area of competence (Resolution 16/01, IOTC 2016). The next full assessment of yellowfin tuna is scheduled for 2021.

The yellowfin tuna (YFT) assessment uses tag-release and recapture data to inform population size and movement dynamics — these data are highly influential for estimates of stock levels and reference quantities (Langley 2015, 2016; Fu et al. 2018). The 2018 YFT assessment (Fu et al. 2018) assumed five regions (see Figure 1), with movement between regions and recruitment in each region estimated within the model. Within each region, the model assumes that the tagged and untagged fish have the same probability of recapture, i.e. are homogeneously mixed. As tag-release and recapture data are highly informative to the assessment, any violation in the homogeneous tag mixing assumption, e.g. due to fish movement and/or distribution changes in fishing effort, is likely to introduce bias into the estimation of fish abundance and distribution.

Spatially explicit assessment models have indicated that the mixing rates of the populations were probably low at the ocean-basin scale for YFT. Most tags collected from the Indian Ocean Tuna Tagging Programme (IOTTP) were released in the local area, and tag recoveries were influenced by the spatial distribution of the catch from the fisheries and variable reporting rates amongst fleet. Langley et al. (2012) found that the tag recoveries of YFT from the FAD purse-seine fishery were not mixed during the 6-month period when their size matched the main selectivity ogive for that fishery. However free-school tag recoveries of larger fish indicate a higher degree of mixing within the fished population. Examination of the tag recoveries of bigeye from the Purse Seine fishery identified considerable differences in the recovery rate amongst latitudinal zones for tags at liberty for at least 12 months (Langley 2016). The low connectivity of skipjack tuna between the East and West Indian Ocean could also be attributed to the apparent differences in reporting rate amongst fleet and tagging programs (Fu et al. 2018). Using different methods, (Kolody & Hoyle 2015) identified incomplete mixing for Indian Ocean skipjack for at least three quarters following their release, and in the Western and Central Pacific Ocean (where tagging programs and fisheries were structured differently, and there are more data) for at least six quarters (1.5 years) after release.

Regional partitioning of sub-populations with different tag dispersion rates, and the discounting of observations during the “non-mixing” period may reduce the bias caused by temporal and spatial heterogeneity of tag mixing. However, to fully quantify the extent of the bias requires understanding of the drivers of tuna migration and movement, and hence the mixing of tags released into the wider population. Simulation experiments using spatial movement models can provide a useful tool to assist in the evaluation of potential bias caused by non-random distribution of tags and/or fishing effort in the context of area-aggregated or spatially explicit stock assessments.

A method to investigate the impact of tagged fish movement and mixing assumptions is through spatial population dynamics modelling. Dunn et al. (2018) developed a generalised spatially explicit statistical catch-at-age population modelling tool (the Spatial Population Model, SPM), that allows estimating and modelling the movement dynamics of fish populations, particularly at finer spatial scales than those typically conducted using standard integrated statistical assessment models. SPM allows for the implementation of a range of spatial modelling assumptions within a common modelling framework. SPM was used to implement a spatially explicit model for Antarctic toothfish in the Ross Sea region (Mormede & Dunn 2013; Mormede et al. 2017), and used to conduct a simulation experiment that evaluated the bias from the assessment model that ignored spatial heterogeneity from tag movement and mixing.

The aim of this project is to develop a preliminary spatially explicit SPM operating model for YFT, and to use this to determine the feasibility of using it to evaluate potential assessment bias from tag mixing heterogeneity. The specific objectives for this project are:

1. To develop a spatially explicit operating model of the tropical yellowfin tuna population for the use of evaluating potential stock assessment bias.
2. To provide a final report describing the developed operating model and preliminary evaluation of stock assessment bias, to be submitted to the IOTC Working Party on Tropical Tunas.

The parameter values used to specify the YFT SPM operating model were derived by fitting the SPM operating model to the available YFT observational data time series.

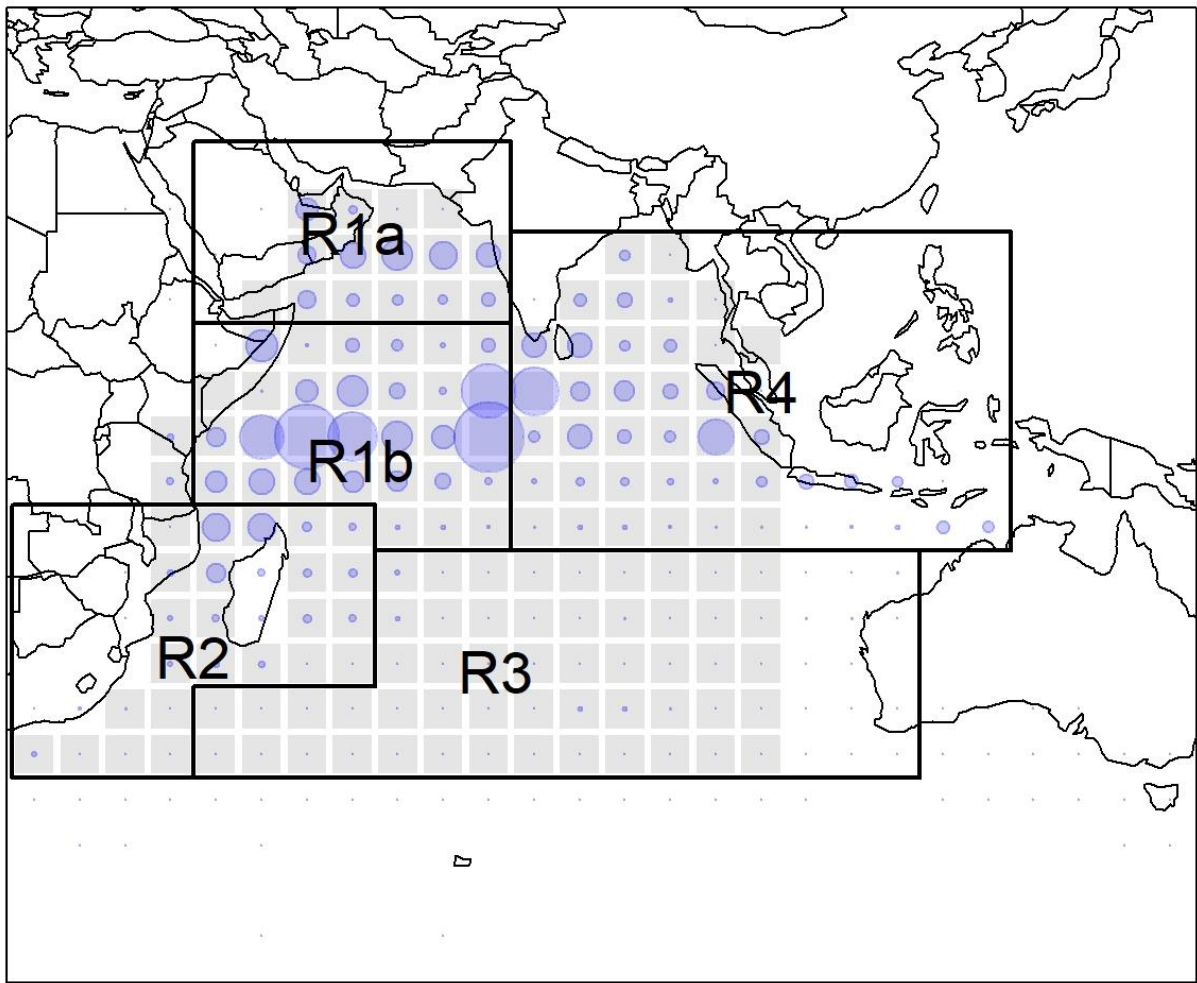


Figure 1: The Indian Ocean and the regions assumed in the SS3 stock assessment model (labelled R1a, R1b, R2, R3, and R4 from Fu et al., 2018); the region modelled using the spatially explicit model (SPM, grey cells) and the relative amount of catch (number) from each cell over the history of the YFT fishery (blue circles).

2 Methods

2.1 Introduction

A preliminary spatially explicit population dynamics model for YFT in the Indian Ocean was developed using SPM (Dunn et al. 2018), approximating the stock assessment model of Fu et al. (2018) but with simplified input data, population processes dynamics, and observations. A simplified population dynamics, fisheries and assumptions were used to develop a preliminary model to evaluate and test SPM as an approach for investigating bias from tag data in an assessment model. The SPM (Dunn et al. 2018) model is available at <https://github.com/alistairdunn1/SPM>, and this preliminary model used version SPMv1.1-2020-02-08 (rev. 2020-02-08 09:30:11 UTC) to evaluate the fits and to undertake the simulations.

The SPM operating model used data and observations from the fishery (longline CPUE, fishery length frequencies, and tag-recapture data) to inform and fit both population (R_0 , and fishery selectivities) and movement parameters using Bayesian MPDs and maximum likelihood estimation, and then this was used to simulate plausible observations for the fishery for use in a non-spatially explicit model. The model structure, assumptions, parameters, bounds, and priors are described below.

In this preliminary model we did not evaluate model fits and observation data weightings, as the objective was to develop the initial model structure and test the application of SPM in estimating model parameters and simulating these population dynamics for tagging into an example SS3 model. Hence, model parameter values are presented here for illustration purposes only, and that these can be improved with additional structural assumptions, data choice, and alternative data weightings.

The SPM model used data and observations from the 2018 YFT stock assessment (Fu et al. 2018) implemented in SS3 (Methot et al. 2018) for the years 1952–2015 (i.e., data available from the IOTC were used in the assessment, but with spatially explicit catch data only available up to 2015). Data from areas between 20–105° E, and 20° N–40° S were included, with areas on land excluded from the model (see Figure 1 above). Data and observations from outside this area were also excluded from the model.

A spatially explicit region was defined between 20–105° E, and 20° N–40° S, modelled as 159 5×5° discrete cells (see Figure 2), with each cell assumed to be square with 556 km width. Spatially explicit scientific catch data from 2016 and 2017 were not available for the development of the SPM operating model at the time, and hence the model was only run up to the end of the 2015 year. These data can be added to the preliminary model, along with other improvements in model structure, data, and assumptions, when required.

Catch and population dynamics were modelled for the years 1952–2015 and were assumed to be in quarter years (i.e., defined as ‘model years’ of 3 month duration where the model periods were the quarters from 1952–2015, with 1952 quarter 1 labelled as model year 1, and 2015 quarter 4 as model year 256). Note that in the assessment of Fu et al. (2018), model years started at 13 (representing 1952 quarter 1), and ended in 277 (representing 2017 quarter 4).

Each spatial cell in the SPM operating model was assigned to a fishery region, using the regions defined for the integrated stock assessment model of Fu et al. (2018) — although these regions were only used for the purposes of reporting simulated observations and outputs from the spatial model in a manner consistent with the SS3 stock assessment assumptions.

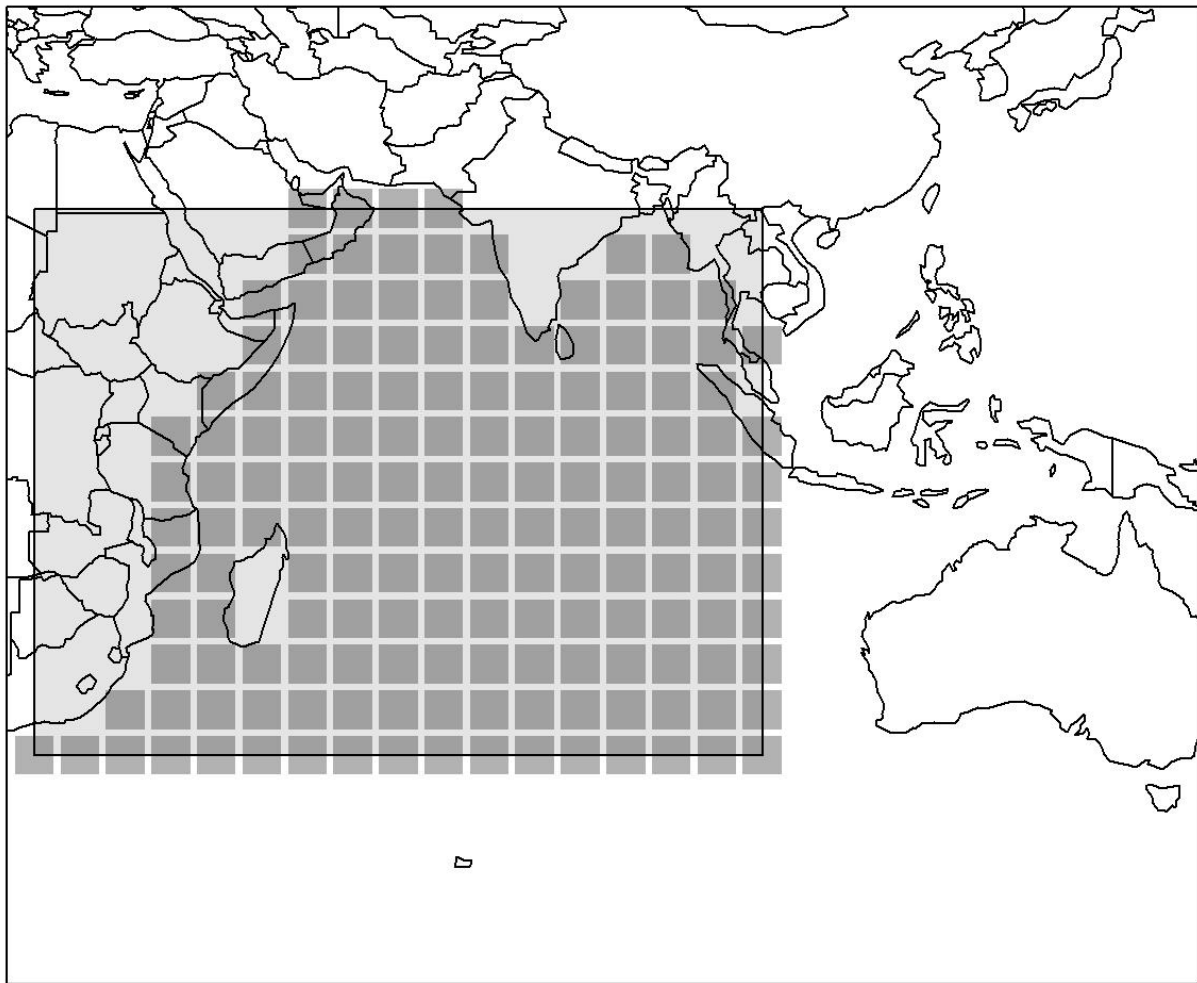


Figure 2: The Indian Ocean modelled region using the spatially explicit model (SPM, with 5×5° grey cells), within the total region assumed for the model. Non-grey cells were excluded from the model and were assumed to exist on land. Areas outside the spatial region defined were ignored, and all the data (catch, CPUE, length frequency, and tag data) from areas outside the modelled region were ignored.

2.2 Population and movement dynamics

The population was assumed to be a single stock contained within the modelled region, with no immigration or emigration to or from outside that region. The population processes assumed were similar to those assumed in the SS3 YFT assessment of Fu et al. (2018) across three time steps: in time step one, recruitment occurred at age 1 and tagging and movement processes took place; in time step two, fishing was applied and observations were evaluated; and in time step three, natural mortality, maturation, and ageing were applied (see Table 1). The processes in each time step were applied in sequence, and repeated for each model year (i.e., quarter years).

Growth rates were assumed to be as described in Fu et al. (2018) derived from Fonteneau & Gascuel (2008), and are given in Figure 4. Natural mortality rates by age were also as assumed in Fu et al. (2018), and are given in Figure 5. Similarly, the rates of maturation were the same as assumed in Fu et al. (2018), and are given in Figure 6.

Recruitment was assumed to occur at age one and was applied in locations where the length frequency data indicated fish of length less than 40 cm were caught over all of the years of available

data (Figure 3 above), and followed a Beverton-Holt relationship with steepness $h=0.8$. Recruitments (R_y) were calculated from the stock recruitment relationship using year class strength multipliers (i.e., annual recruitment strengths were applied on the natural scale using YCS multipliers, rather than log scale as recruitment devs.) with the stock recruitment relationship, i.e.,

$$SR(SSB_y) = \frac{SSB_y}{B_0} / \left(1 - \frac{5h-1}{4h} \left(1 - \frac{SSB_y}{B_0} \right) \right)$$

And

$$R_y = R_0 \times YCS_{y-1} \times SR(SSB_{y-1})$$

In the models applied here, recruitments were assumed as equal to those estimated in the SS3 model by Fu et al. (2018), and are shown in Figure 7.

The population was modelled as two main categories (immature and mature fish, unsexed), with ages from one to seven (1–28 model years) where the last age class was a plus group, and with an initial equilibrium starting state (B_0) with $R_0 = 97.2506 \times 10^6$ (i.e., the value of initial recruitment reported by Fu et al. (2018))

Tagging was applied using the same methods as Fu et al. (2018) and with the assumed age of fish released determined by the size at age from the growth curve and the measured length at release. Tagging was implemented as additional categories (immature and mature tagged fish for each model year where there were releases), in order to model the tagged part of the population. Aside from initial mortality (i.e., the assumed proportion of fish that either lost their tags or died during the tagging process) and ongoing tag loss (i.e., an assumed rate that fish lost tags over time and were no longer identifiable as tagged fish), the population and movement processes applied to these fish were the same as the general population.

Fishing was applied using an exploitation rate equation, rather than an approximation to the Baranov equation, with maximum exploitation rates (U_{max}) set equal to 0.95 in each of the timesteps, model years, and spatial cells where fishing occurred, where

$$U_f = \frac{C_f}{\sum_j \bar{w}_j S_{fj} n_j}$$

Where the catch from fishery f is denoted C_f , S_{fj} is the selectivity for fishery f at age j , \bar{w}_j is the mean weight of a fish at age j , n_j is the pre-mortality number of fish, and U_f is the exploitation rate for fishery f .

The number of fisheries applied in the SS3 model was reduced for the development of this preliminary model, mostly to reduce the number of parameters and the model run time, from 25 fisheries in Fu et al. (2018) to seven (Purse Seine, troll, bait boat, gillnet, longline, handline, and all others categorised as other). Total catch for each model year is given in Figure 8, and the relative catch reported from each of the modelled fisheries is given in Figure 9. Catches were modelled using the number of fish caught, rather than biomass (as per Fu et al. (2018)), again, to reduce computation complexity in the model. In further development, these assumptions and simplifications

may be relaxed to investigate their relative importance on conclusions and outcomes. We note that there may be some discrepancy between the time series of catch as biomass and catch as numbers (see Figure 8) that should be considered in future model developments.

Catches from each of the seven fisheries in each model period (quarter years) from 1952 to 2015 were allocated among $5 \times 5^\circ$ cells, with all except longline having a selectivity that was assumed to follow a double normal function, defined separately for each of the fisheries. The longline fishery was assumed to have a logistic selectivity. See Dunn et al. (2018) for details about the functions and parametrisation used for these selectivities.

SPM allows for movement between cells to be parameterised using preference functions, defined as estimable probability functions of spatial attributes. A preference function is parameterised as a probability density function based on attributes specified at each time and location (i.e., environmental layers). The distances between locations also operate as preference functions. (Note that alternative movement functions are available in SPM, but in this case, preference-based movement using environmental layers was determined as the one most likely to be tractable for YFT — see Dunn et al. (2018)).

Here, we define the preference for each spatial attribute $A_i(x)$ in each cell x as the function $f_i(\theta_i, A_i(x))$, where i are the parameters for some function f_i . Each spatial attribute $A_i(x)$ can be time varying and is cell specific. Given a set of n attributes for the domain, we can define an aggregated or total preference function for each individual cell x in the model as the weighted product of individual preference functions f_i , i.e.,

$$P_x = f_1(\theta_1, A_1(x))^{\alpha_1} \times f_2(\theta_2, A_2(x))^{\alpha_2} \times \dots \times f_n(\theta_n, A_n(x))^{\alpha_n}$$

where α_i is the weighting factor for each function f_i .

Then for each cell we define the probability of moving from cell a to any cell b (where b is defined as the set of all possible cells, including a), as the ratio of the preference of being in cell a to the sum of the preference in all the cells, i.e.,

$$P\left(a \xrightarrow{\text{moves}} b\right) = \frac{P_a}{\sum_{i \in \forall b} P_i}$$

The movements of immature and mature YFT were estimated through three separate preference functions based on the environmental variables — quarter year SST by $5 \times 5^\circ$ cell, mean quarter chlorophyll by $5 \times 5^\circ$ cell, and straight-line distance (kms) between source and sink locations. The movement from each cell for either immature or mature fish was assumed to be constant by age of fish and through time, i.e., all fish within a category (immature or mature) responded in the same manner to the environmental layers or the distance, regardless of their age or the model year. All movement parameters were estimated within the model by fitting the model to the available data.

Preference movement for both immature and mature fish had the same parameterisation, but parameters were estimated separately for each category. Tagged fish (immature and mature) were assumed to be the same as the untagged fish (immature and mature, respectively).

The underlying environmental data of the layers for the attributes used in movement were:

- A. Monthly $1 \times 1^\circ$ SST data from 1952–2015 from the UK Met Office Hadley Centre (Rayner 2003) analyses with the Levitus et al. (2009) corrections applied. Quarterly $5 \times 5^\circ$ SST data were derived by assuming the centre cell of the $1 \times 1^\circ$ grid that was closest to the centre of the $5 \times 5^\circ$ grid assumed in the spatial model, at the month in the middle of the quarter period, represented the best approximation of the SST for each $5 \times 5^\circ$ grid cell in each of the model years (Figure 10).
- B. Mean quarterly Chlorophyll-a from the period 2002–2018, at the 4 km scale and averaged for each quarter (winter, spring, summer, and autumn) (NASA Goddard Space Flight Center, Ocean Ecology Laboratory, Ocean Biology Processing Group 2020). Mean 3×3 block estimates were applied to before assigning the value of chlorophyll-a at the location nearest the centre of each $5 \times 5^\circ$ cell, and values were applied on a log scale within the spatial model (Figure 11).

Distance between cells was estimated using the linear distance between each of the cell centres, assuming a 556 km square width for each cell.

Preference functions assumed for distance used an exponential decay function parameterised by λ ; and for SST and the Chlorophyll-a environmental layers, a double normal function parameterised by the mean, and left and right variance terms. In this model, equal weight was assumed for each of the three preference functions (i.e., relative function weights were not estimated).

Table 1: Annual cycle (i.e. year-in quarter years) of the YFT spatial model, showing the processes taking place at each step and the available observations, and the proportion mortality (natural and fishing) assumed to have taken place at the time the observations were evaluated.

| Time step | Process | Observations | Proportion mortality |
|-----------|--------------------------------|----------------------|----------------------|
| 1 | Recruitment | | |
| | Tagging | | |
| | Movement (immature and mature) | | |
| 2 | | CPUE | 0.5 |
| | Fishing mortality | Fishery catch-at-age | 0.5 |
| | | Tag-recapture | 0.5 |
| 3 | Natural mortality (M) | | |
| | Maturation | | |
| | Ageing | | |

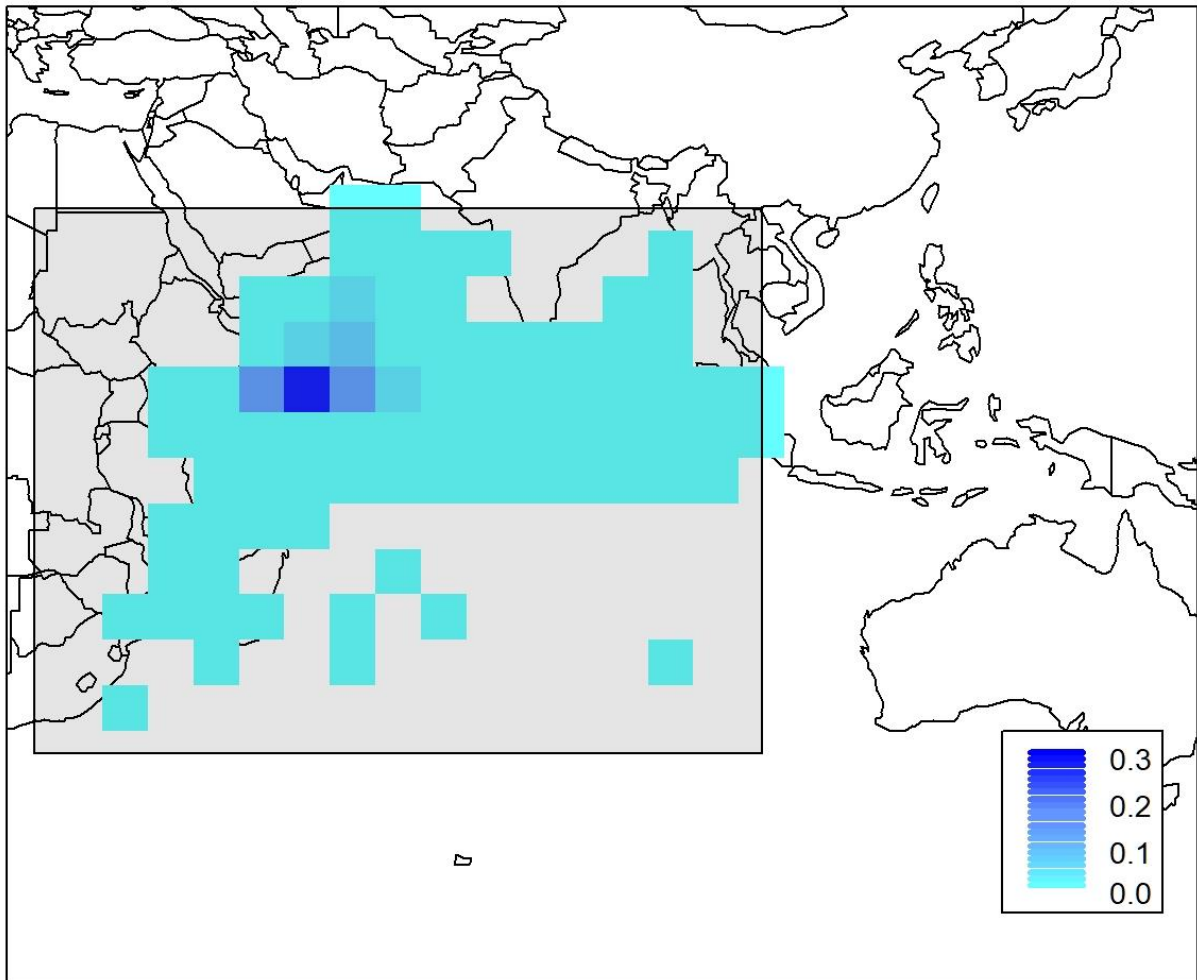


Figure 3: Locations assumed for recruitment of age 1 YFT, where the colour (light blue = low, and dark blue = high) represents the proportion of recruitment occurring in each cell.

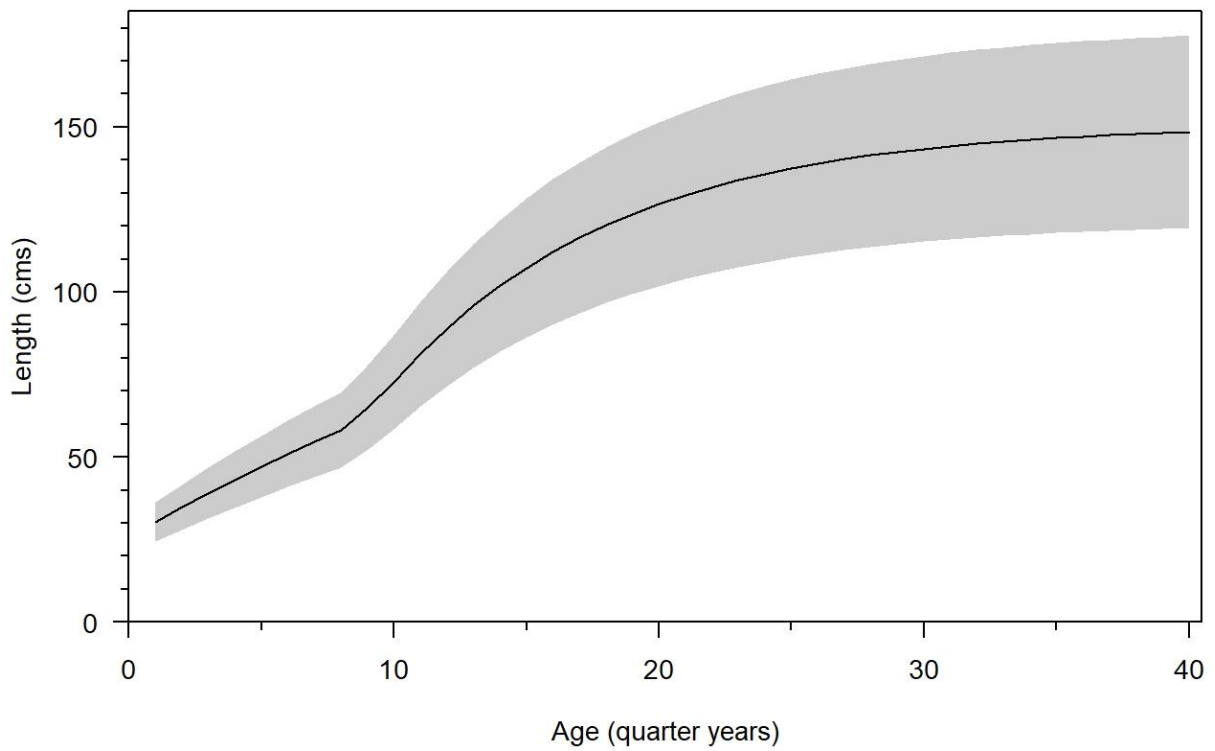


Figure 4: Assumed mean length at age (with grey indicating the 95% range) for YFT, taken from Fu et al. (2018). Note that x-axis age units are pseudo-years (quarters).

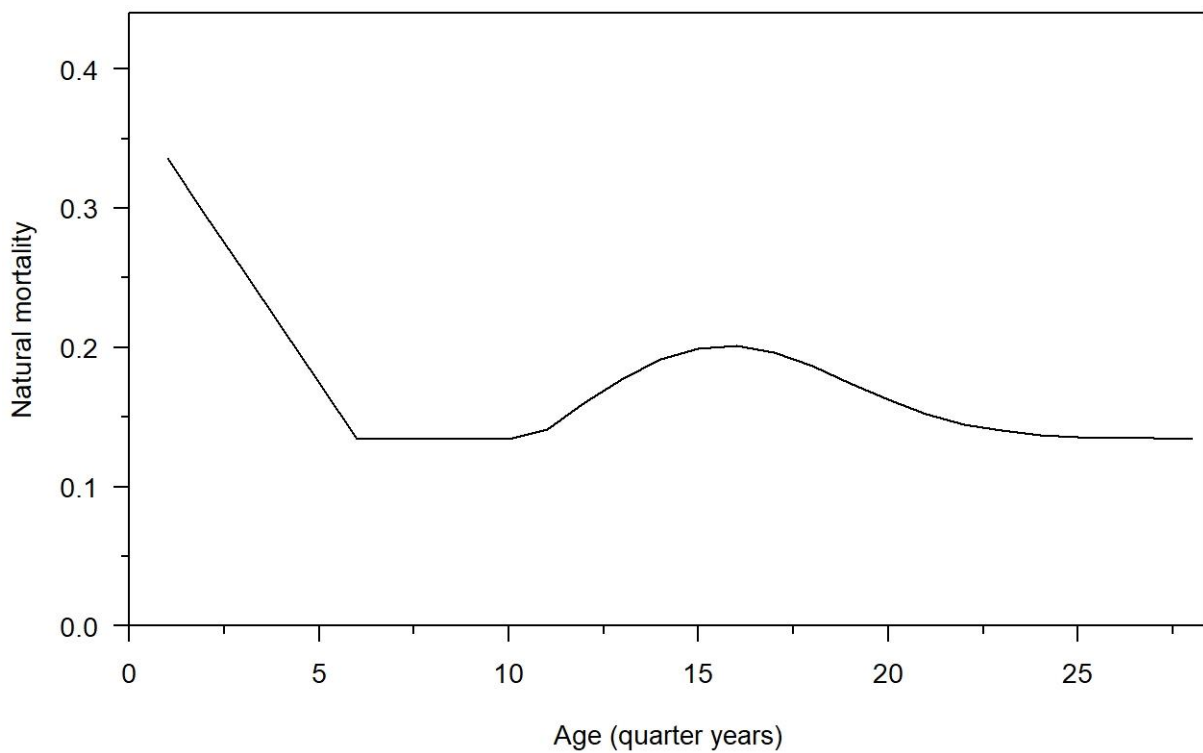


Figure 5: Assumed rates of natural mortality by age for YFT, taken from Fu et al. (2018). Note that x-axis age units are pseudo-years (quarters).

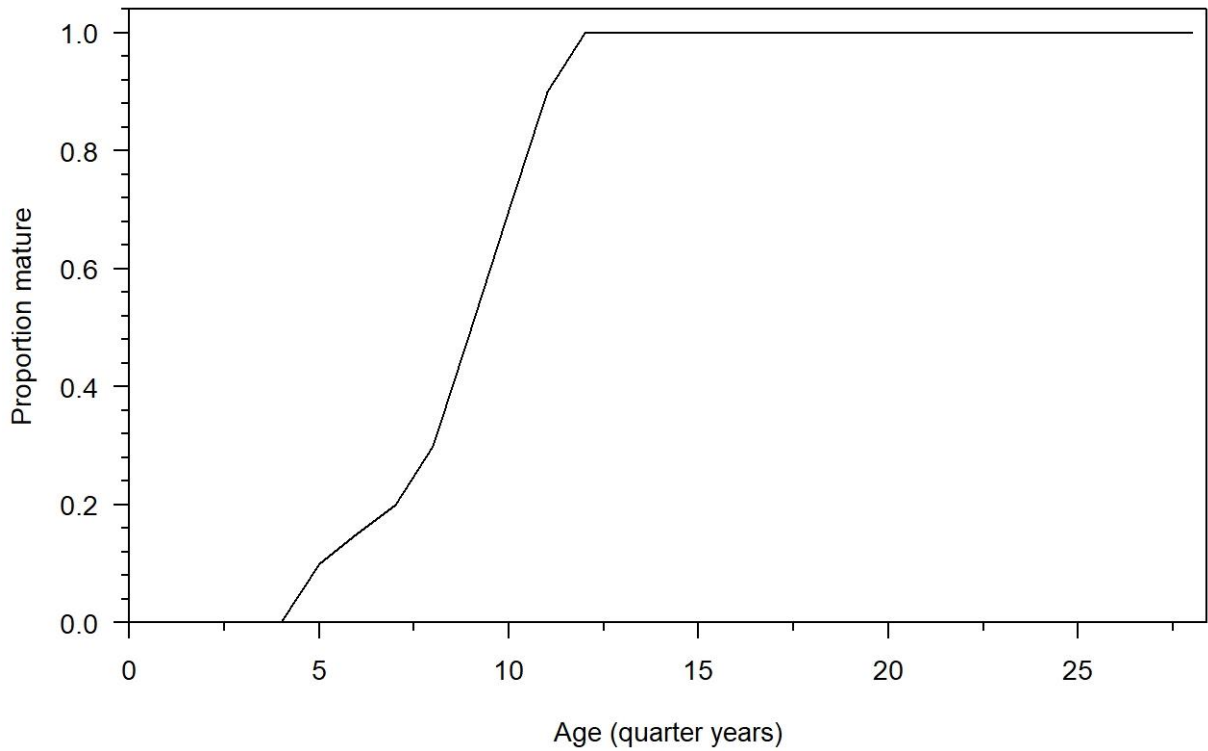


Figure 6: Assumed rates of maturation by age for YFT, taken from Fu et al. (2018). Note that x-axis age units are pseudo-years (quarters).

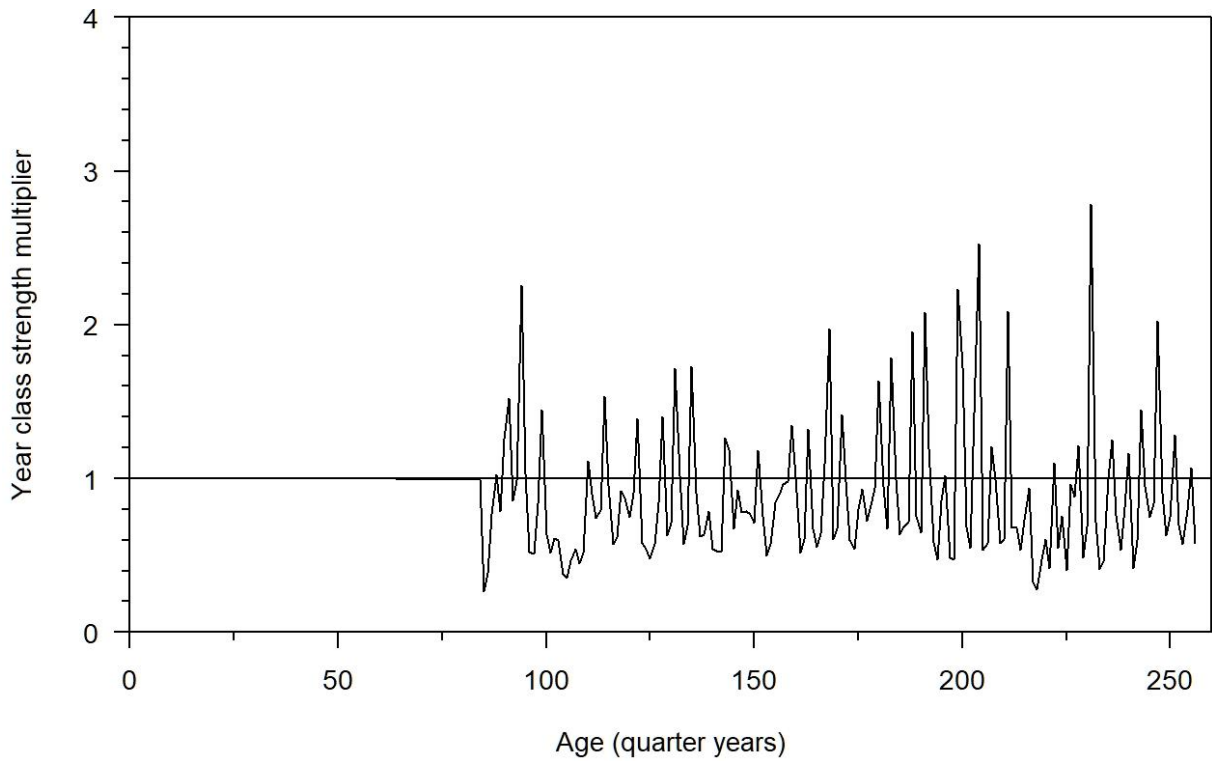


Figure 7: Assumed recruitment (YCS multiplier) for YFT, taken from Fu et al. (2018). Note that x-axis time units are pseudo-years (quarters).

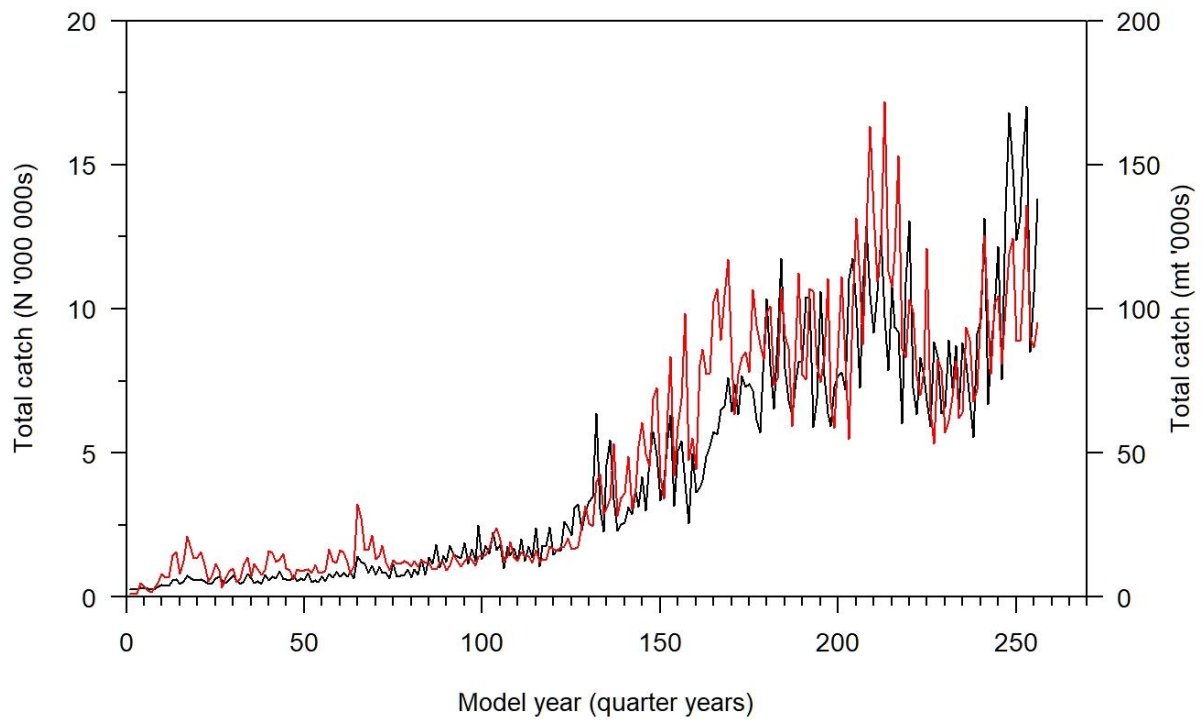


Figure 8: Total catch (left axis, black line) by number and (right axis, red line) for YFT in the spatial model for 1952–2015. Note that x-axis time units are pseudo-years (quarters).

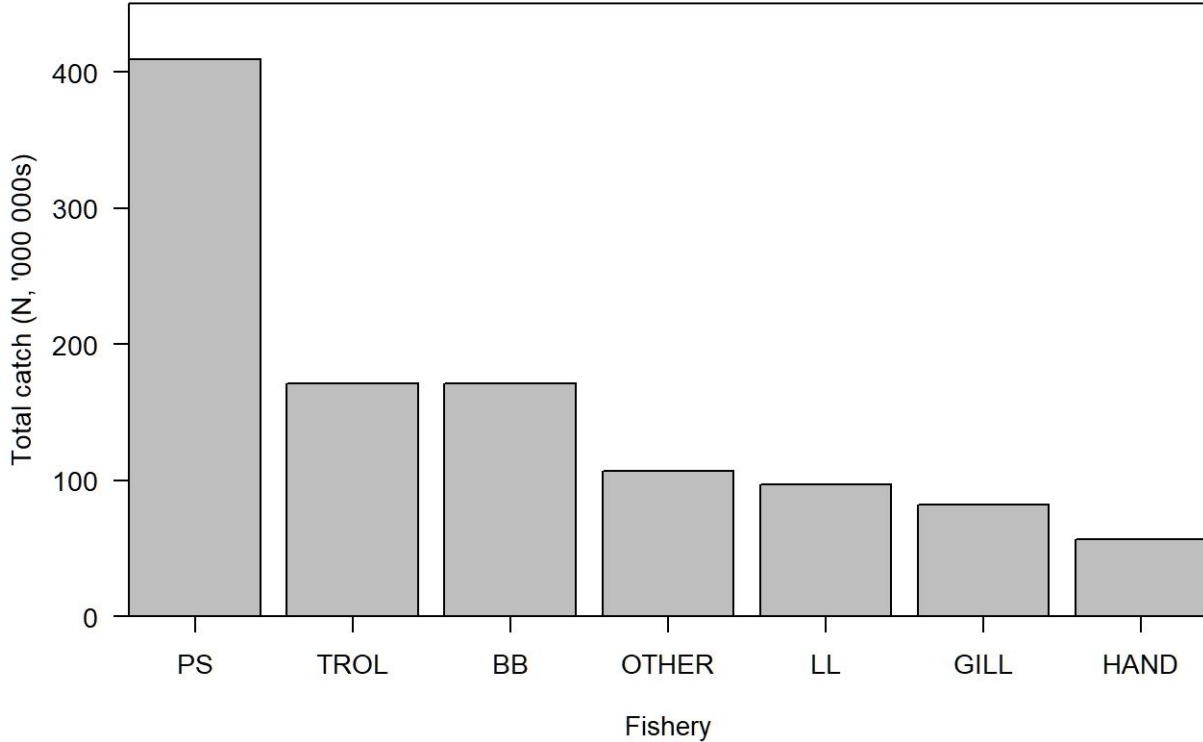


Figure 9: Total catch (by number) for the seven defined fishery’s in the spatial model; Purse Seine, troll, bait boat, gillnet, longline, handline, and all others.

Mean SST

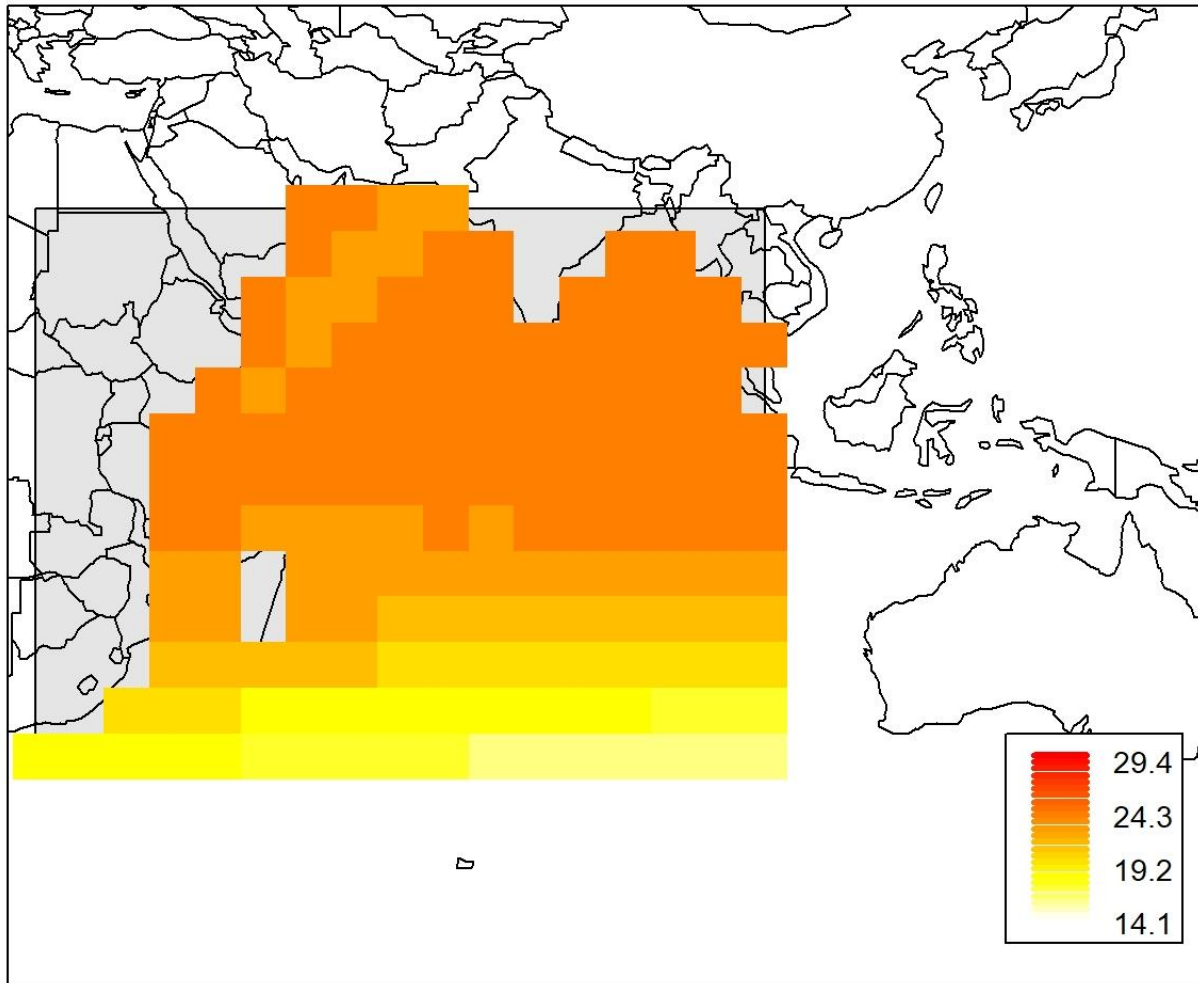


Figure 10: Mean SST over the period 1952–2018 (data source: UK Met Office Hadley Centre (Rayner 2003) analyses with the Levitus et al. (2009) corrections applied).

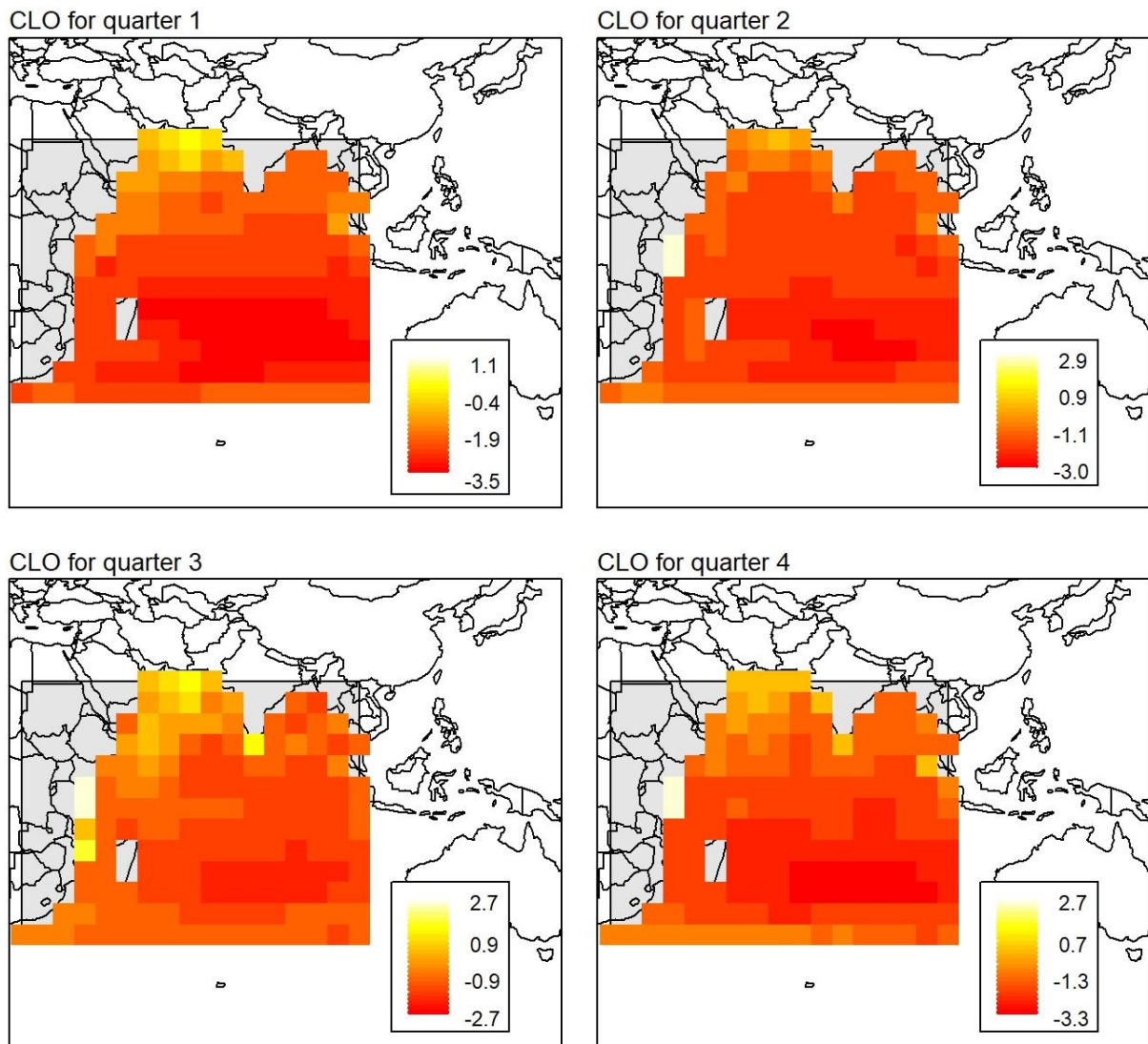


Figure 11: Mean quarterly Chlorophyll-a over the period 2002–2018 (Data source: NASA Goddard Space Flight Center, Ocean Ecology Laboratory, Ocean Biology Processing Group 2020).

2.3 Observations and catch data

Spatially explicit catch data made available by IOTC (Dan Fu, pers. comm, February 2020) were the same data used for the integrated SS3 stock assessment model of Fu et al. (2018) for the years 1952–2015. Total catches are shown in Figure 8 above. The catch data by fleet (in numbers of fish caught) were allocated to one of the seven fisheries — Purse Seine (Figure 12), troll (Figure 13), bait boat (Figure 14), gillnet, longline (Figure 15), handline, and all others categorised as other — in quarter years (i.e., model years) and within the 5×5° spatial cells.

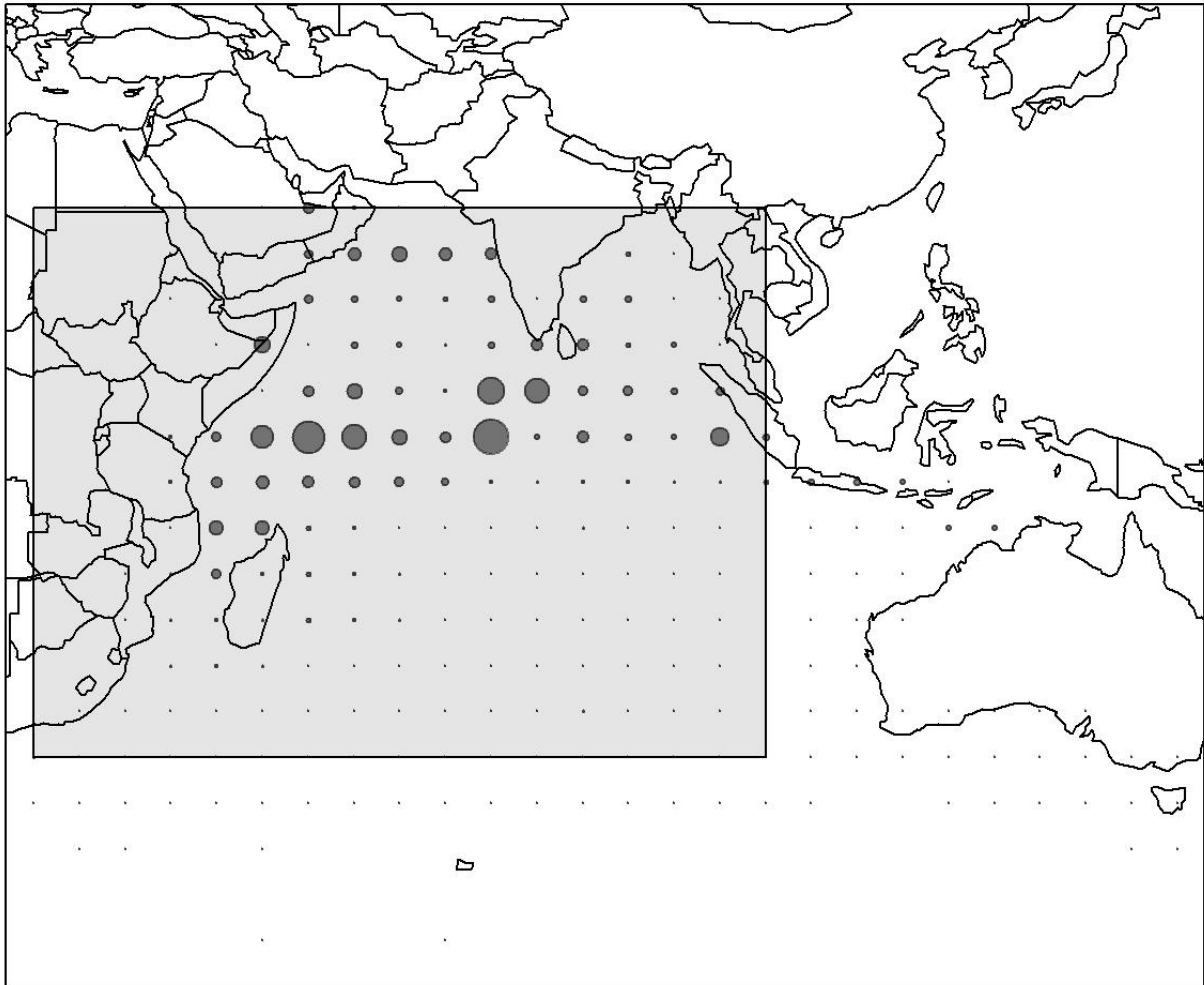


Figure 12: Relative catches by spatial location of the Purse Seine fishery assumed in the YFT spatial model.

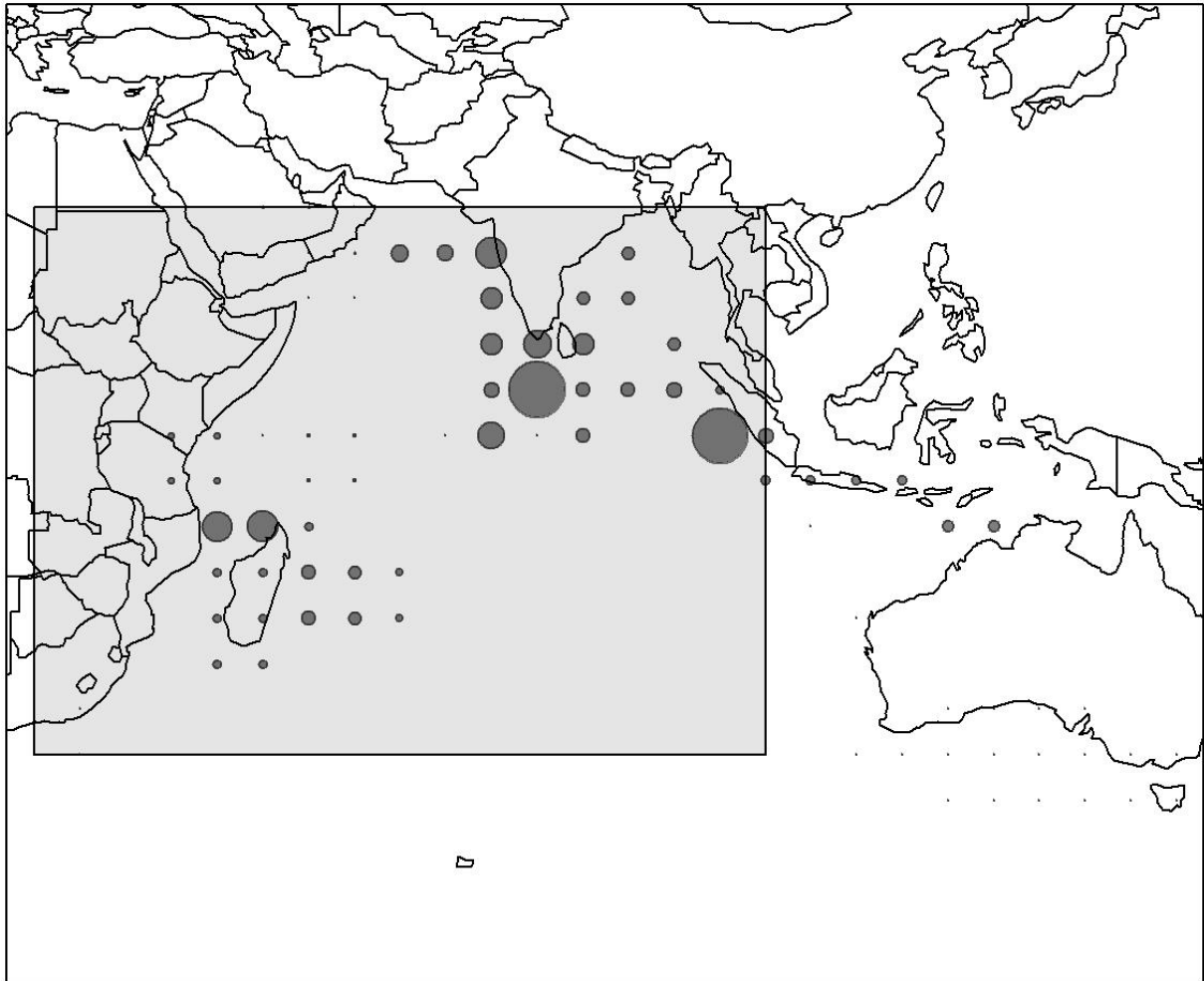


Figure 13: Relative catches by spatial location of the Troll fishery assumed in the YFT spatial model.

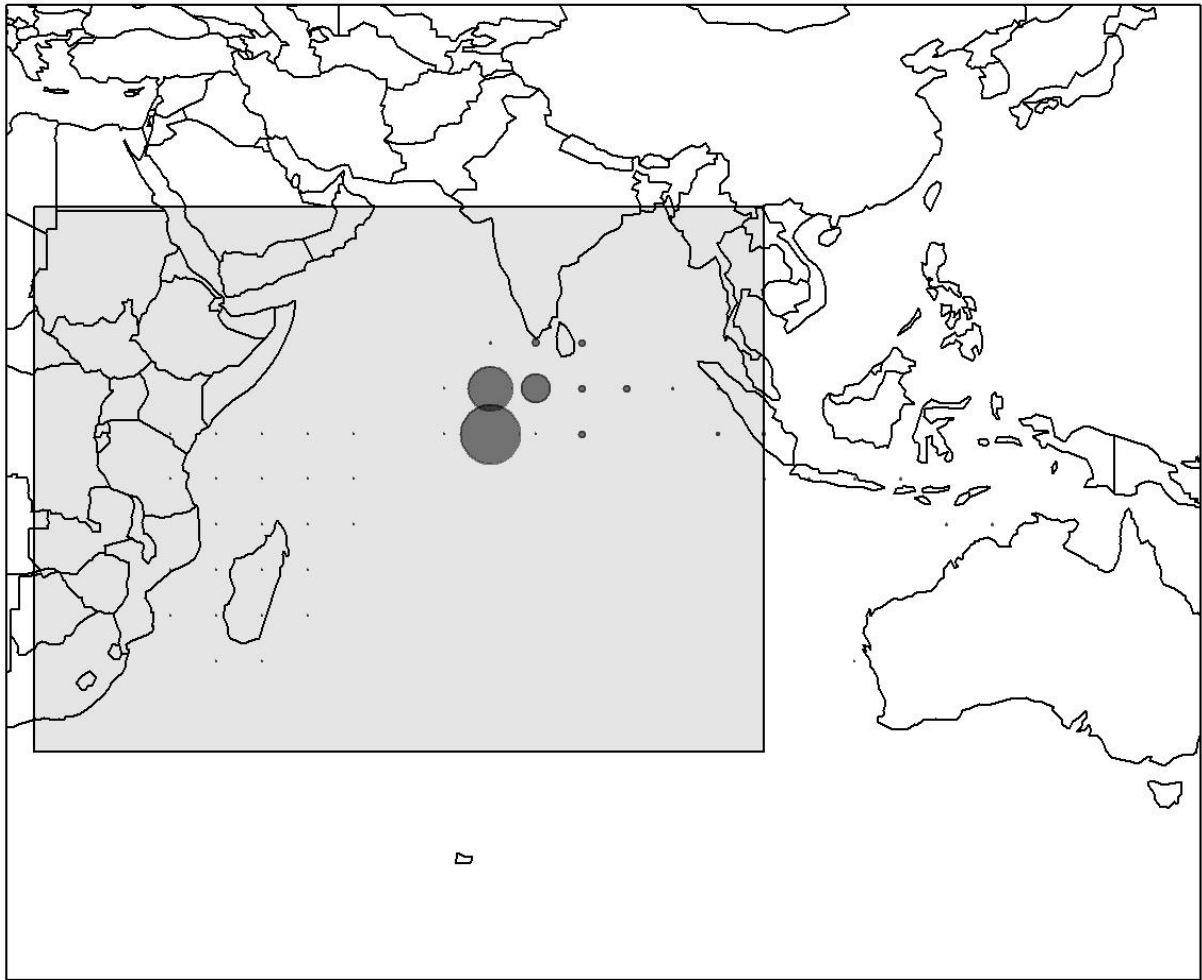


Figure 14: Relative catches by spatial location of the bait boat fishery assumed in the YFT spatial model.

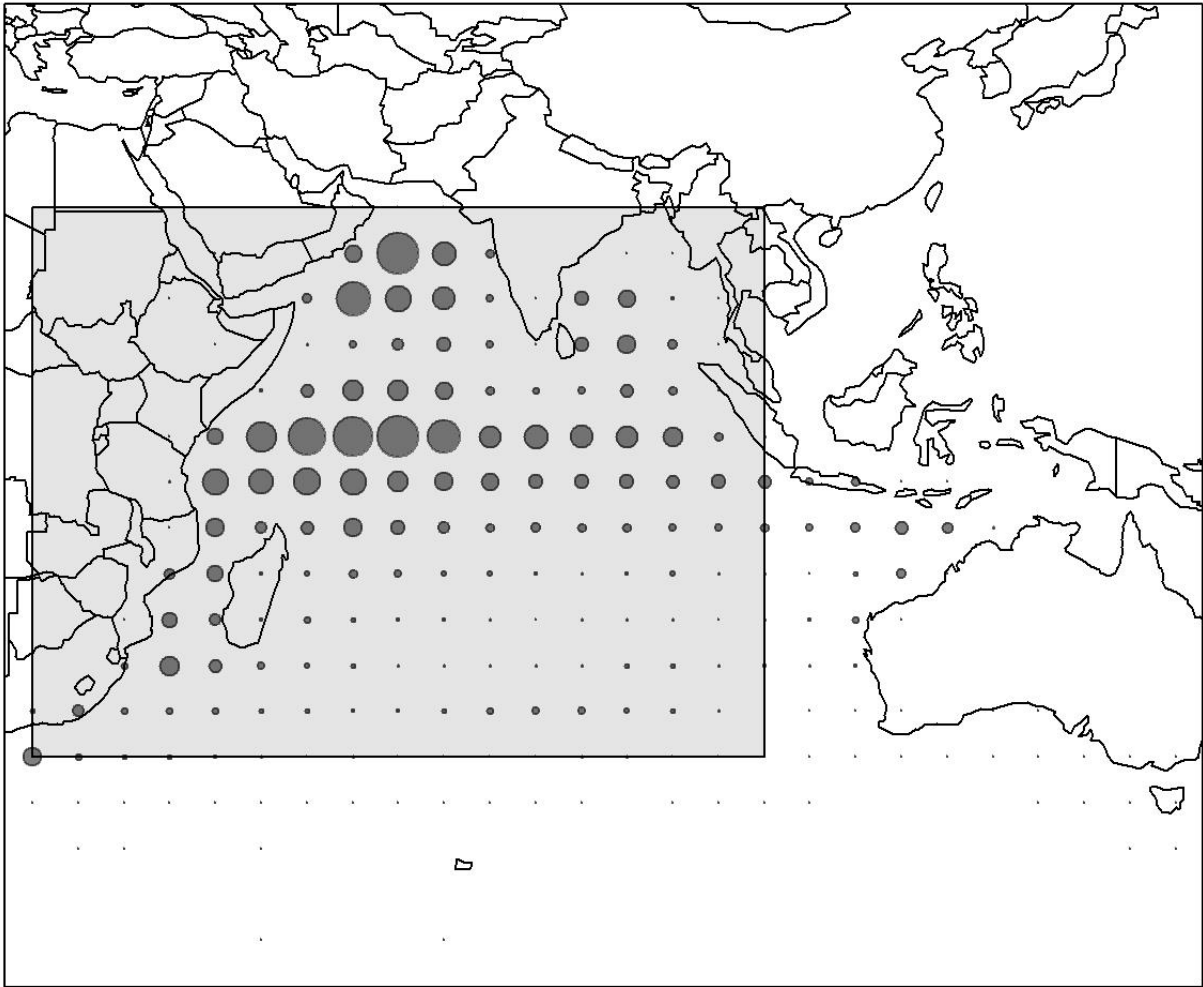


Figure 15: Relative catches by spatial location of the longline fishery assumed in the YFT spatial model.

2.3.1 CPUE

Unstandardised CPUE indices were derived for each cell in each quarter, using data from the Japanese longline fishery only. The unstandardised CPUE was calculated as simply the number of fish caught divided by the number of hooks in each cell (Figure 16). Note that the calculation of raw CPUE used in this model may not reflect actual changes in abundance, and that further work to generate spatially explicit CPUE indices by cell and quarter should be undertaken in any future model developments. The SS3 model by Fu et al. (2018) used CPUE indices from 1972 as the indices before this period were not thought to reflect abundance, hence we also ignore CPUE for the years before 1972 in the preliminary model.

Aggregated CPUE indices are given in Figure 17, and simple standardised CPUE indices (i.e., using SST, oxygen, and Chlorophyll-a only for the years 1952–2015) are given in Figure 18. The standardisation suggests that SST and Chlorophyll-a provide a relationship with CPUE that is dome-shaped, with peaks for SST at about 30° and for Chlorophyll-a at a concentration of about 0.5 mg m⁻³. While there was some relationship between CPUE and SST, the correlation between oxygen and SST variables was high (Pearson's correlation = 0.94, $P < 0.001$), and hence oxygen was not investigated further in these models. These functional forms were assumed as the shape of the preference functions used to model movement in the SPM model.

Raw catch-effort indices for the Japanese longline fleet by spatial cell were fitted within the model assuming a lognormal likelihood with constant c.v. = 0.2. Note that future improvements to the model would need to carefully evaluate the choice of the CPUE index, method of standardisation, and the associated uncertainty (c.v.) for use in the spatial model.

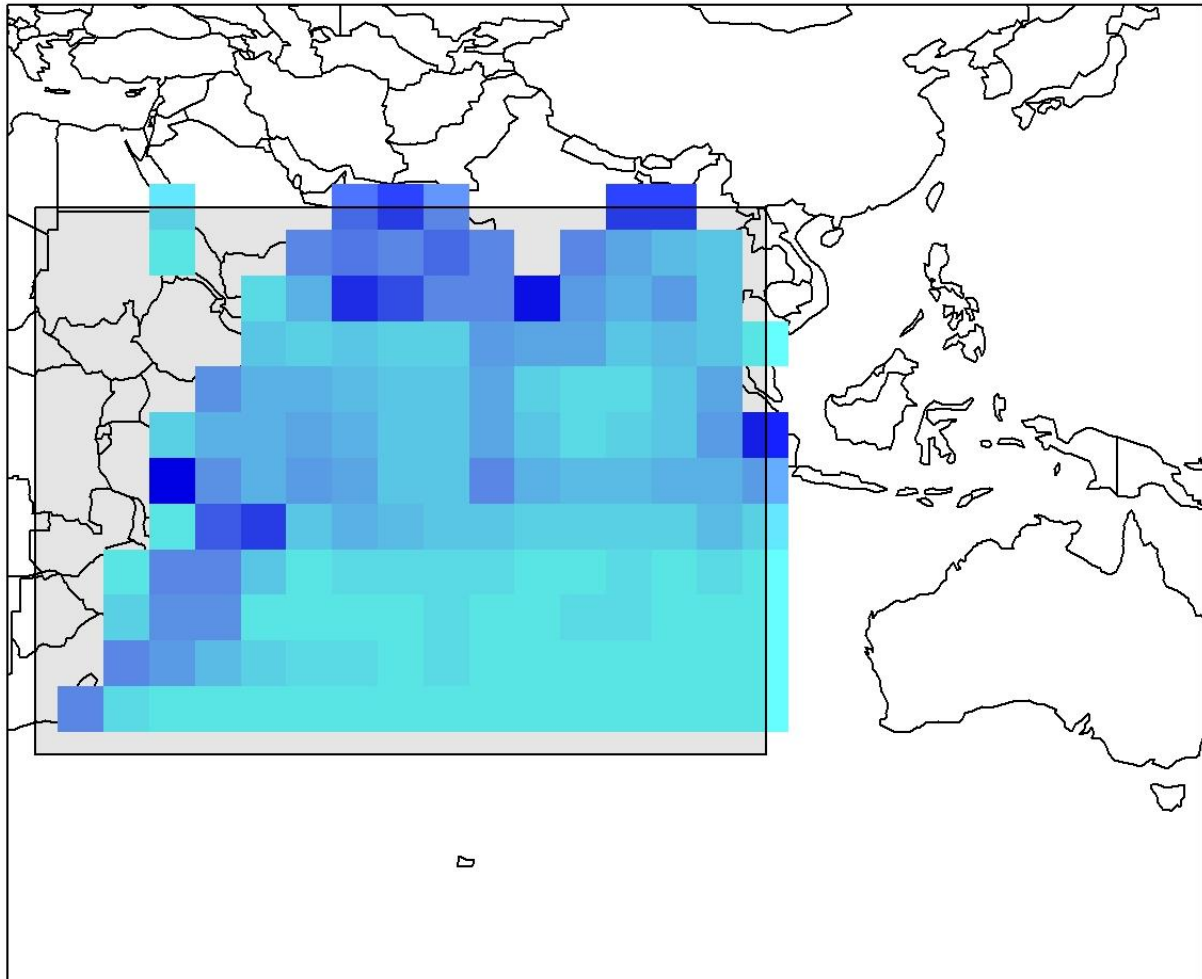


Figure 16: Mean raw catch per hook (Japanese longline data only) for the years 1972–2015 by 5×5° spatial cell.

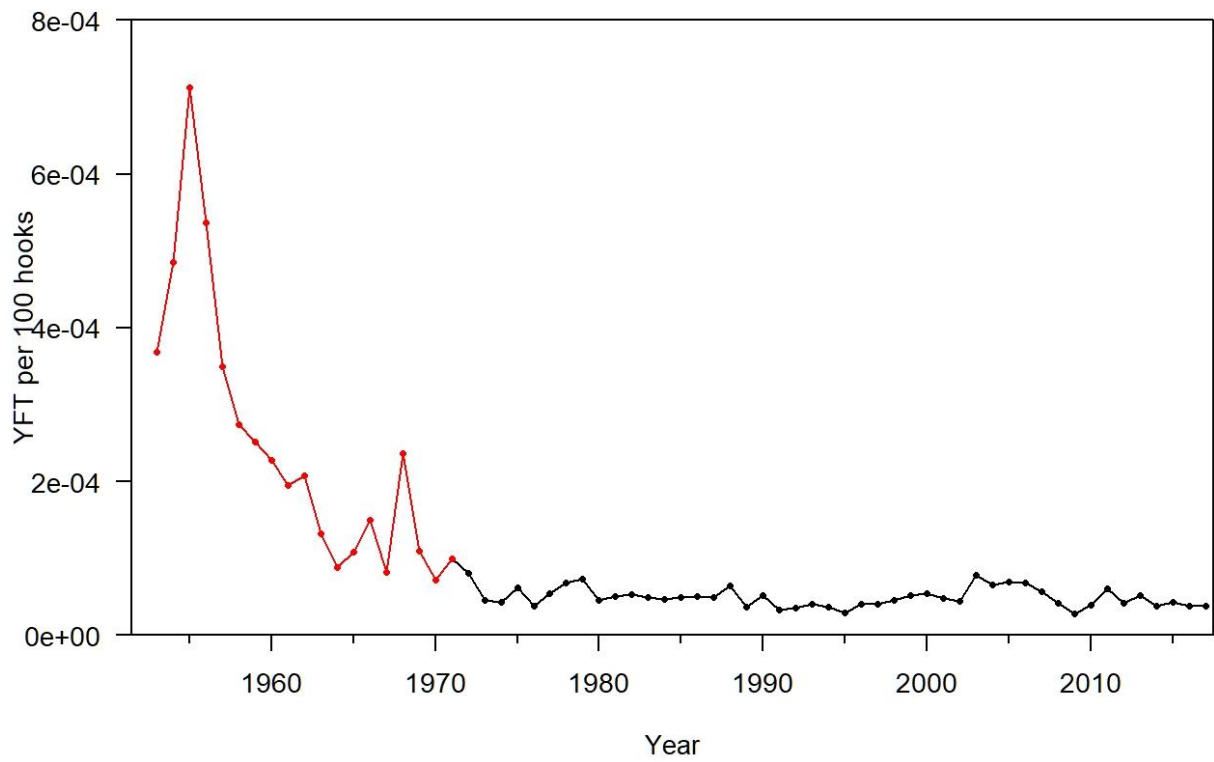


Figure 17: Raw CPUE for the Japanese longline fleet, 1952–2015. The period before 1972 (early CPUE, and not used within the preliminary model) is given in red.

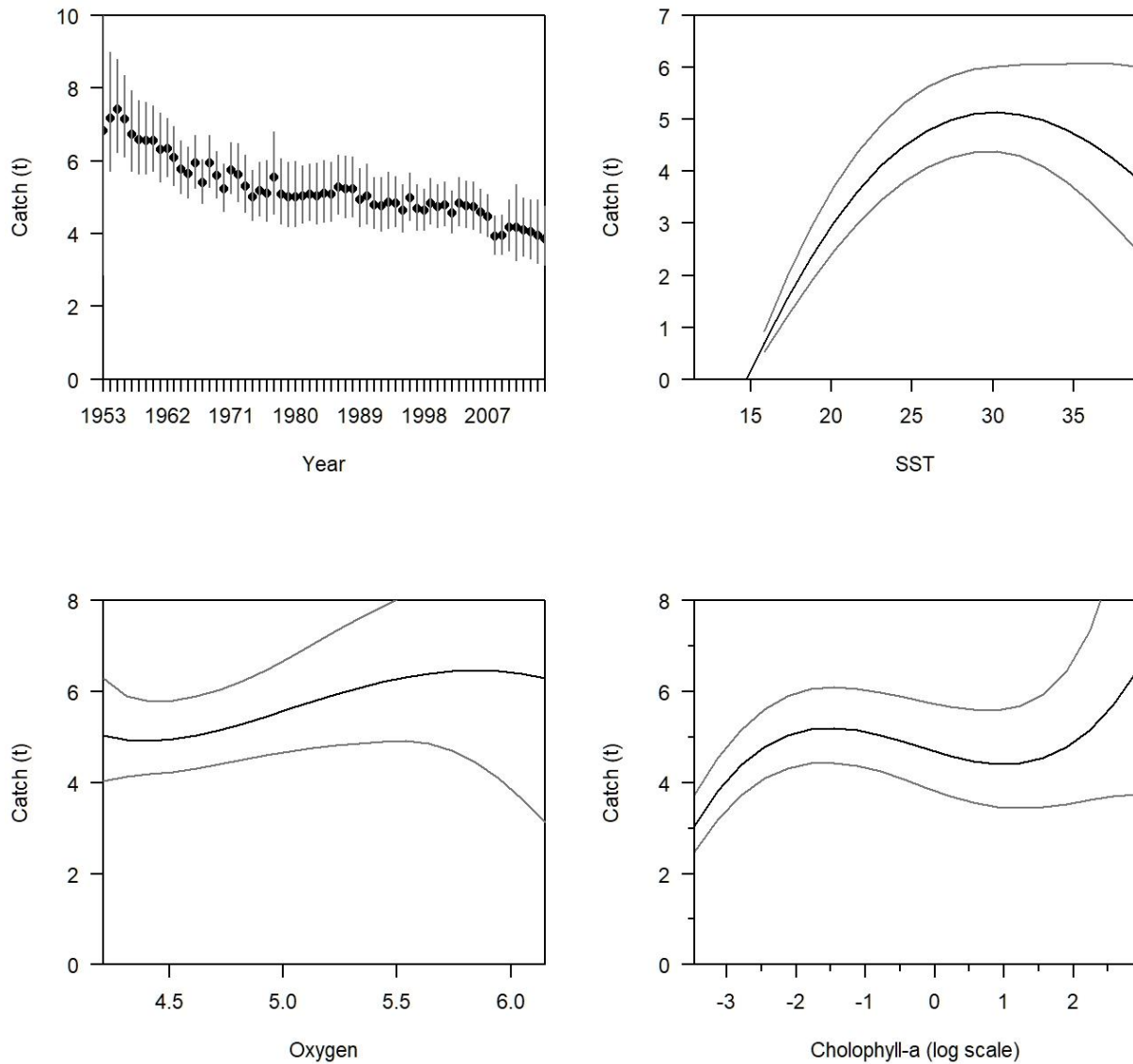


Figure 18: Spatial Japanese longline (a) CPUE indices, standardised by (b) SST, (c) oxygen, and (d) Chlorophyll-a for 1952–2015.

2.3.2 Length frequencies

Length frequencies were developed from the raw length frequency data available. The length frequencies were fitted using multinomial likelihood with effective sample size (N) defined as,

$$N_{effective} = 1 / \left(\frac{1}{N_{observed}} + \frac{1}{N_{PE}} \right)$$

Where $N_{observed}$ was the number of fish observed in the length frequency for each cell, fishery, and quarter; and N_{PE} was set equal to 5. We note that the impact of this value may be too high in the model, as the aggregated likelihood weight associated with this may unduly influence the model towards fitting the length frequencies at the expense of the observational data.

Length data were applied by fleet (in proportions at length in 5 cm length bins between 10 and 195+ cm, with the lengths less than 10 cm aggregated into a minus group, and fish >195 cm aggregated

into the 195–200 cm plus group). Lengths frequencies were allocated to one of the seven fisheries — Purse Seine, troll, bait boat, gillnet, longline, handline, and all others categorised as other — in quarter years (i.e., model years) and within the 5×5° spatial cells. Note that the data used for each fishery was all the available data in the length frequency data set except that for the longline data, only data for the Japanese fleet was used. The choice of length frequency range and bins were to approximate the overall length frequencies of the longline fishery, but in future developments should be extended and modified to be more appropriate for each of the fishery groups. Summary figures of the spatial distributions of length frequencies, aggregated for all years and fisheries are plotted in Figure 19 (for lengths 50–80 cm), Figure 20 (for lengths 80–120 cm), and Figure 21 (for lengths >120 cm).

Note that future improvements to the model would need to carefully evaluate the method of determining the most appropriate length frequencies for each fleet, and the associated uncertainty (multinomial N, including additional process error) for use in the spatial model.

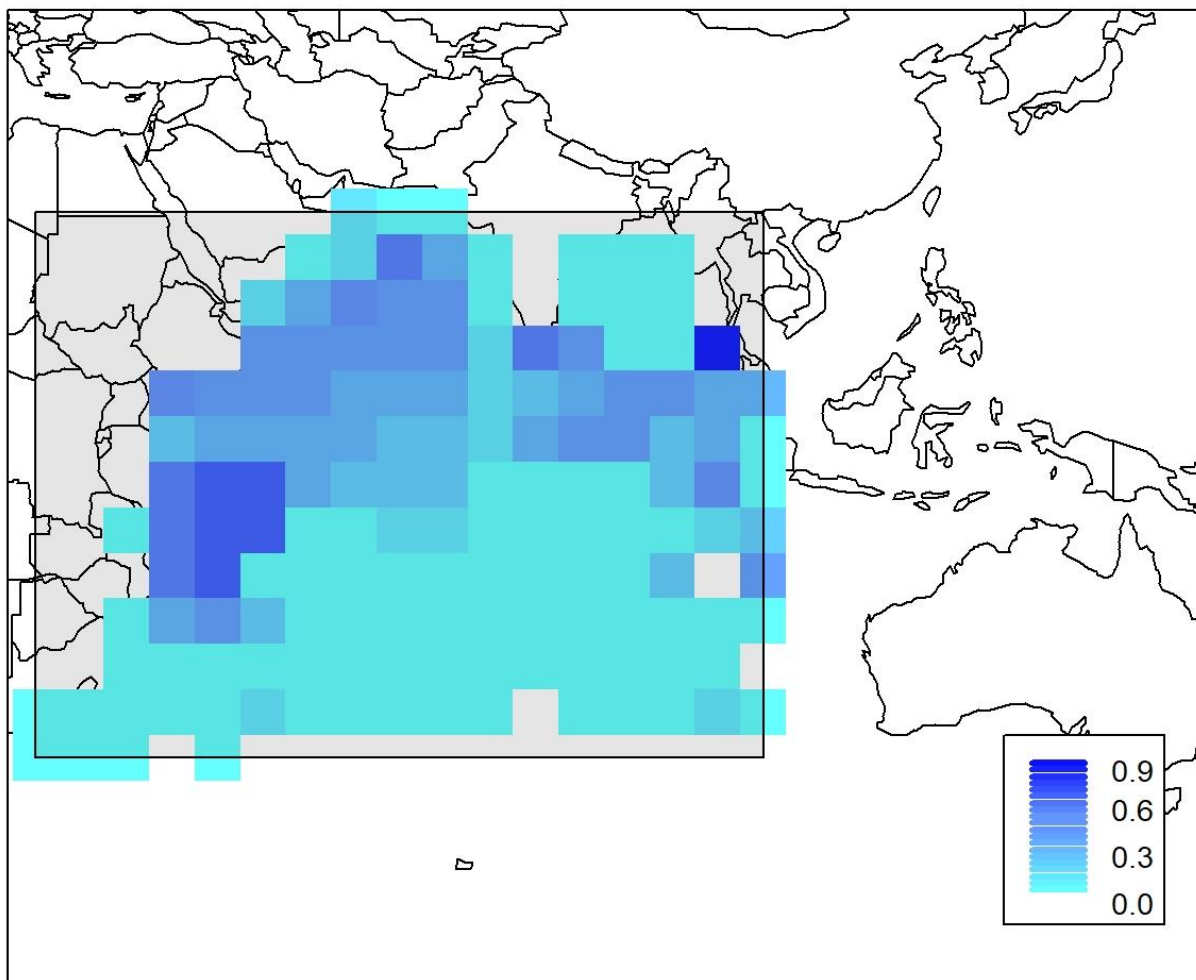


Figure 19: Spatial density of proportions of measured fish of 50-80 cm, over years 1952–2015 and all fleets.

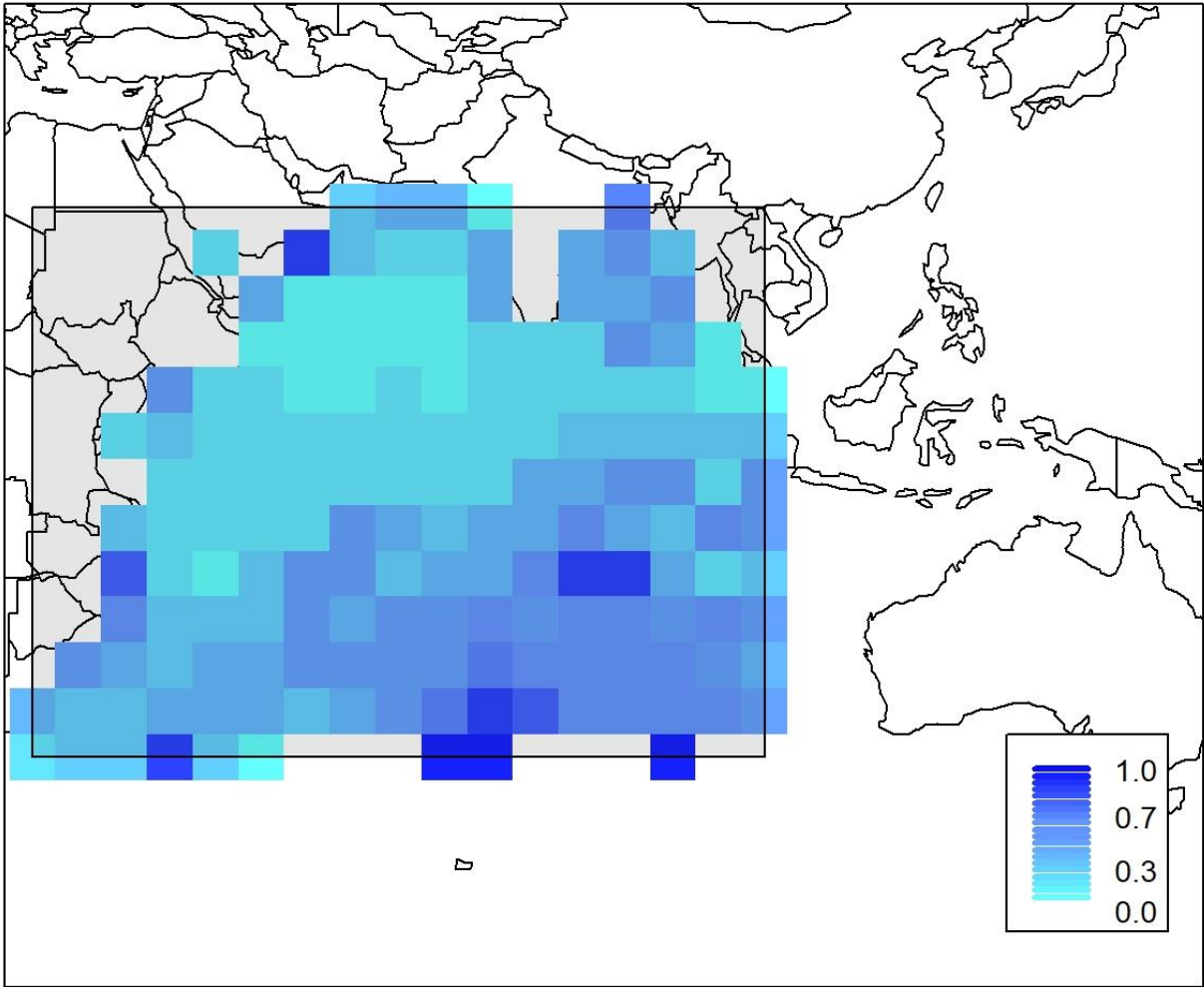


Figure 20: Spatial density of proportions of measured fish 80–120 cm, over years 1952–2015 and all fleets.

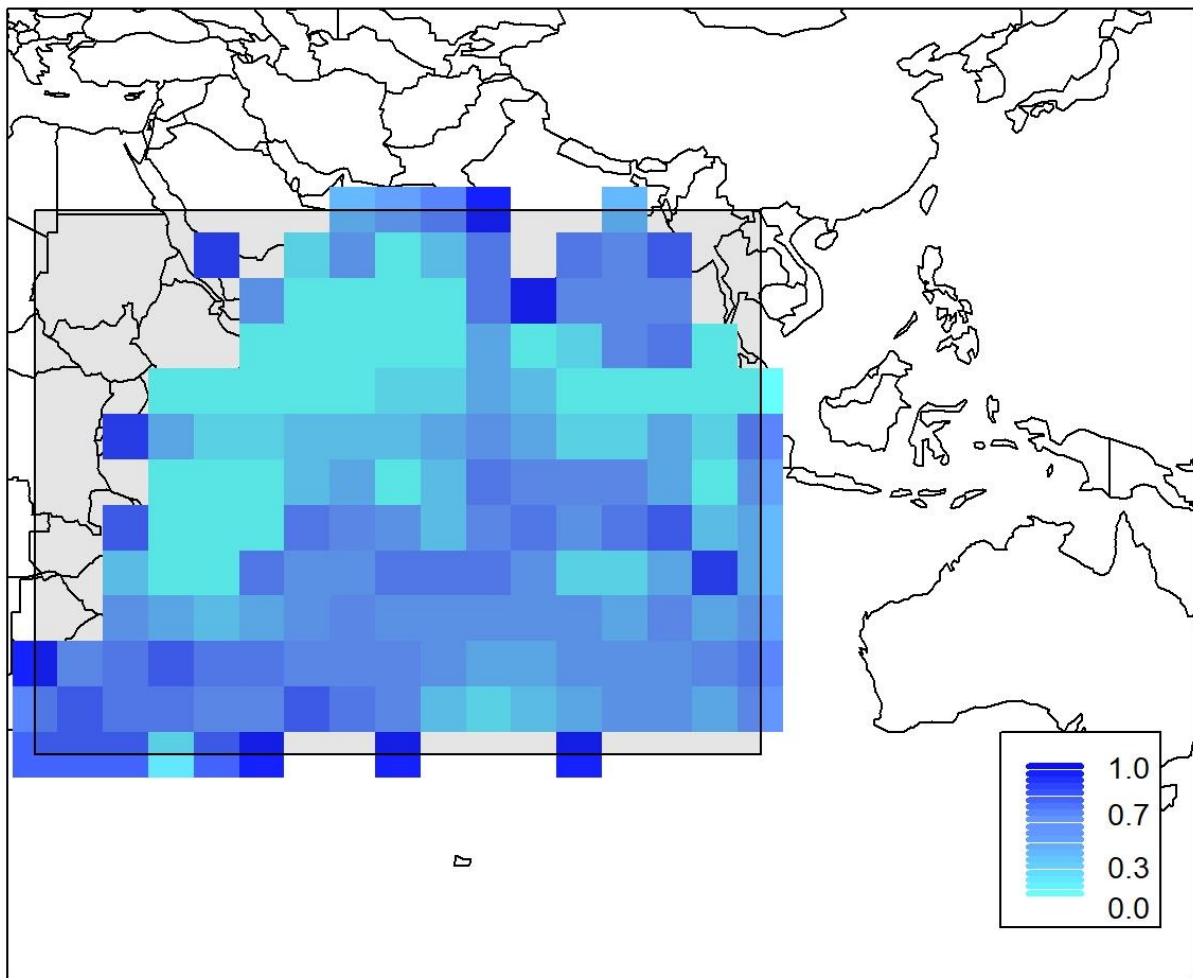


Figure 21: Spatial density of proportions of measured fish >120 cm, over years 1952-2015 and all fleets.

2.3.3 Tag release and recapture data

A total of 54 688 YFT were tagged and released by the RTTP-IO program. Most of the tag releases occurred within the western equatorial region (Figure 22) and a high proportion of these releases occurred in the second and third quarters of 2006 (IOTC 2008). The model included all tag recoveries up to the end of 2015 (Figure 23). Most tags were recaptured within 2000–3000 km of their release position (Figure 24) and within 2–3 years of the time of release.

Tag releases were assigned as released in time step one, in the model year (i.e., quarter year) that they were reported as released. Tagged fish were assigned to immature or mature in proportion the ratios of immature or immature in the population at the time of release and were assigned an age equal to the mean age of their length at time of release as per Fu et al. (2018). Tagged fish from each quarter were aggregated into either the immature or mature tag category, and tag releases from different quarters or years were not maintained as separate partitions within the model for the estimation model. However, the tag releases were categorised within their own categories, defined as the release model year, in generating the simulations. Maintaining the tag releases within categories determined by their release period would introduce additional time requirements when estimating the model but should be considered in future developments to evaluate if this is found to introduce bias.

Tag retention was assumed to be 0.9 (i.e., 10% of fish with tags were assumed to have discarded their tag, or otherwise were not identifiable as tagged fish in the population), implemented by discounting the numbers of released fish when included within the model (note that this is below the level of 27% used in current assessments but, since the same value is assumed in both simulation and estimation models, it has no impact on results). Ongoing tag loss rates were assumed to be 20% per 2000 days (Fu et al. 2018), and was implemented as a model (quarter) year mortality of 0.91%. Note that Fu et al. (2018) adjusted the reporting rates of EU purse seine catch landed in the Seychelles based on the reporting rates of Hillary (2008) and Hillary et al. (2008), but that adjustment was not applied in here.

Tag recaptures were used as observations, with the age of recaptured fish set equal to the age of that individuals release plus its time at liberty. The number of scanned fish was determined from the purse seine fishery and was estimated using a binomial likelihood (Dunn et al. 2018), with no overdispersion assumed. The binomial likelihood assumed that the number of tags recovered was a binomial proportion of the number of fish scanned in each length bin in each cell in each quarter, with the effective sample size equal to the number scanned.

Tag detection was assumed for the purse seine fishery only, and a 100% tag detection rate was assumed. Scanned fish for detection was assumed to be the number of fish reported by the purse seine fishery. While tag detection rates can be introduced by discounting the number of fish scanned to detect the tags in the data provided to the model, an alternative is to modify SPM to allow for this. Future models would need to consider the alternative methods of including tag detection rates.

Note that future improvements to the model would need to carefully evaluate the most appropriate method for including tag releases and recaptures, including if these should be included as length-based observations rather than aged-based, and the associated overdispersion associated with the observations.

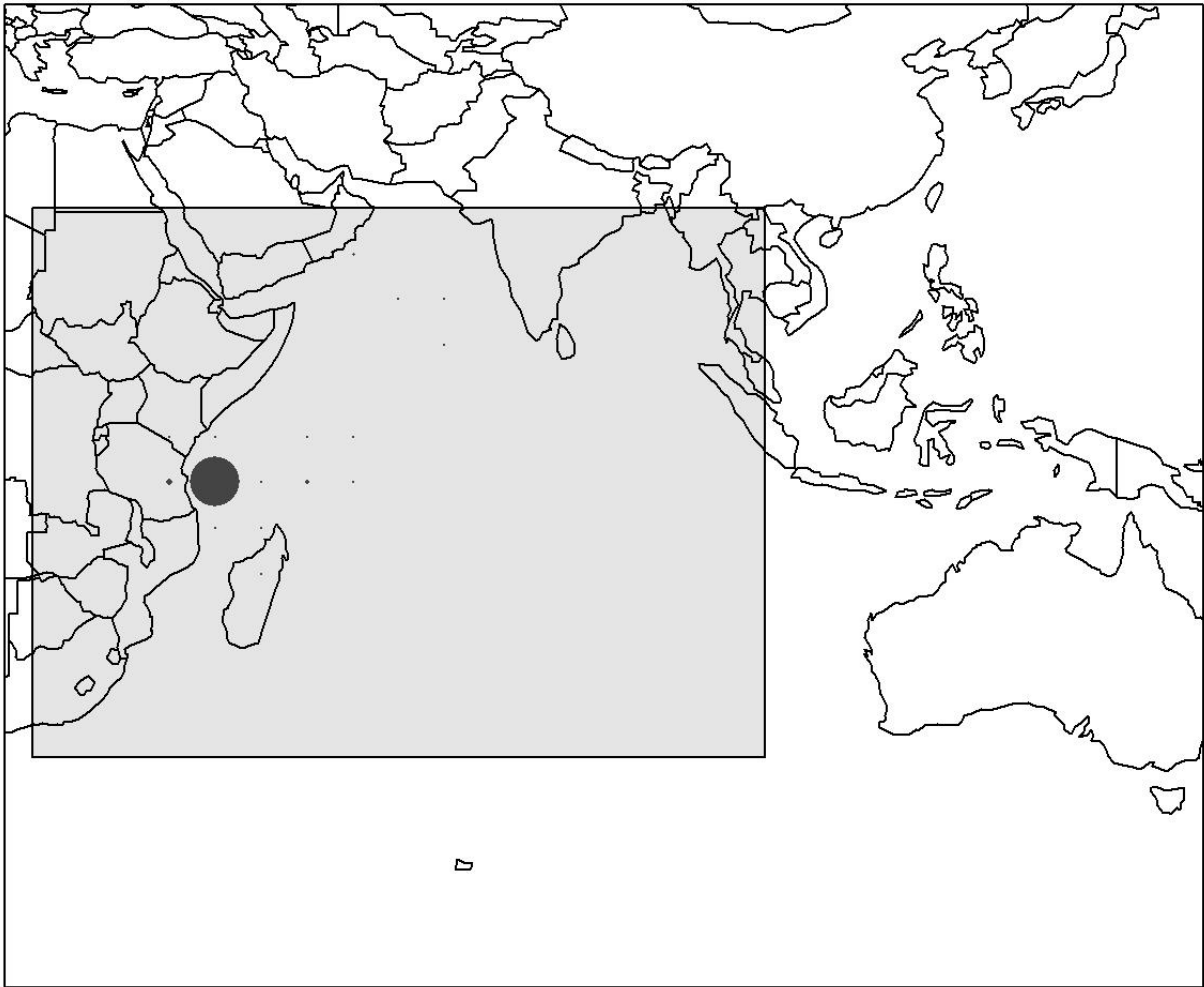


Figure 22: Locations of tag releases of YFT in the RTP-IO programme between 2005–2007.

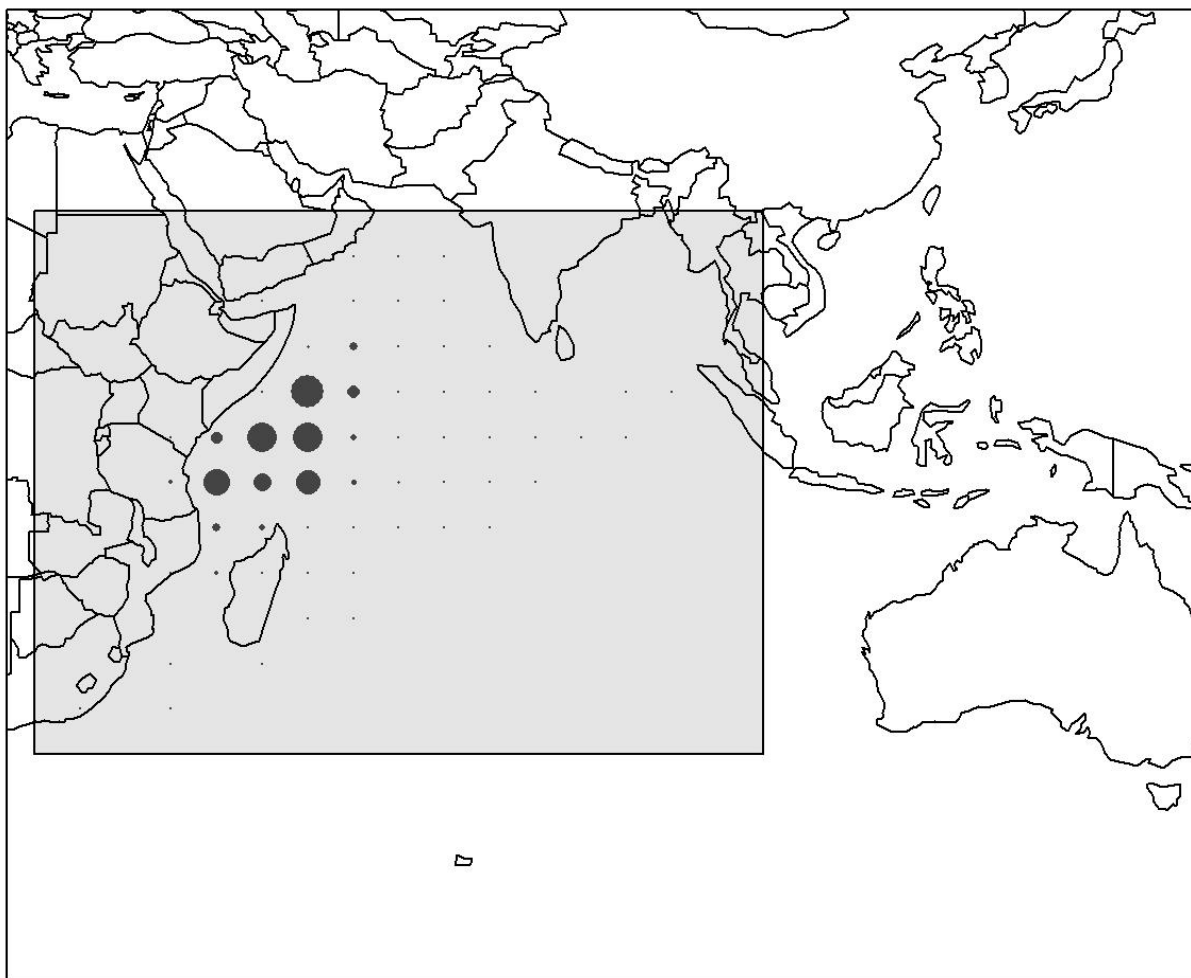


Figure 23: Locations of tag recaptures of YFT released in the RTTP-IO programme (2005–2007) and recaptured by purse seine vessels between 2005–2015.

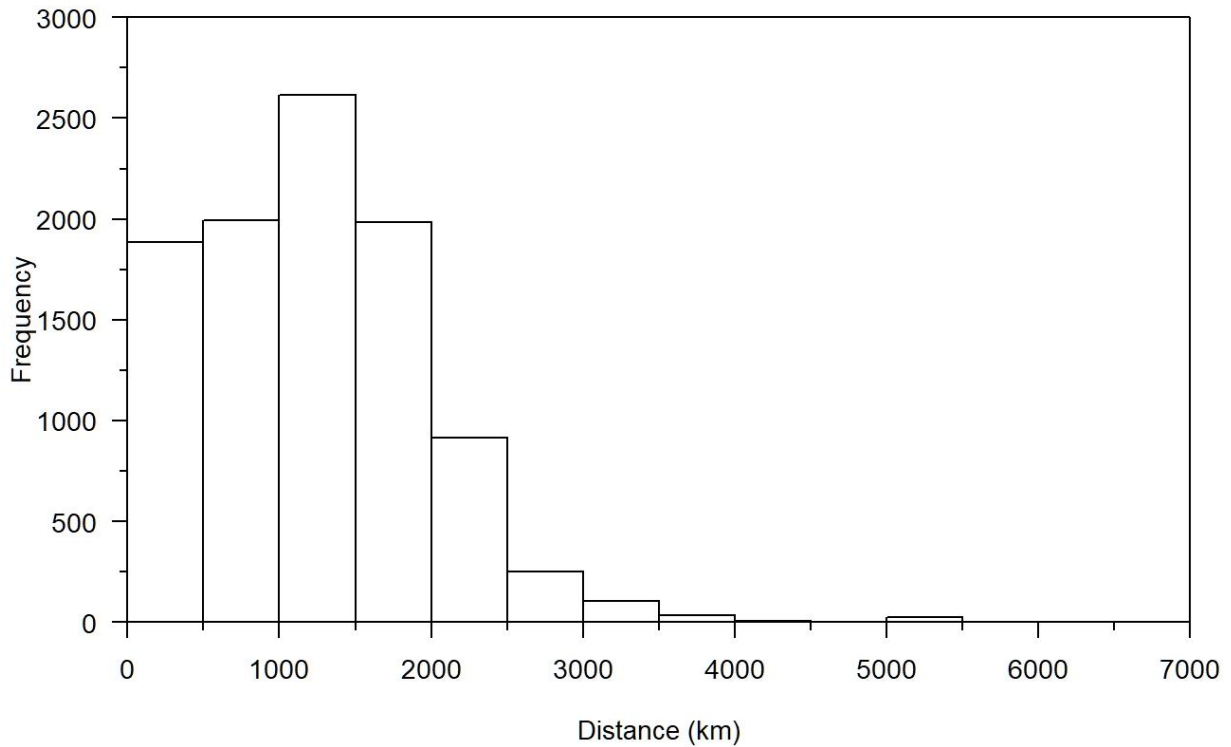


Figure 24: Plot of the distance between release location and recapture location of the RTTP-IO tag releases and subsequent recaptures by purse seine vessels, 2005–2015.

2.4 Estimation of parameters

Preliminary model estimates were fitted assuming a known initial recruitment (R_0) set equal to the value assumed in the SS3 model by Fu et al. (2018). Parameters estimated were the selectivity parameters for each fishery, and the movement parameters for immature and mature fish. The estimated parameters, assumed bounds, and their priors are given in Table 3.

Catch penalties were assumed in order to encourage the model to reject parameter space where there was not enough abundance in each cell in each quarter to ensure the catch could be taken, assuming a maximum exploitation rate of 0.95. In the preliminary estimation, catch penalties were applied to about 11% of all fished cells over all quarters and fishery groups, suggesting that the model was unable to correctly allocate enough fish into every cell in each fishery and each quarter to account for the reported catch. Further evaluation of the spatial cells, length classes, and quarters where this occurred would need to be evaluated in future developments.

Model fits were evaluated by minimising a total objective function, the sum of the log-likelihoods from observations, priors, and of the catch penalties, i.e.,

$$\text{Objective}(\mathbf{p}) = - \sum_i \log[L(\mathbf{p}|O_i)] - \log[\pi(\mathbf{p})]$$

where π is the joint prior density of the parameters \mathbf{p} .

Observations were fitted using the multinomial likelihood for length frequencies, lognormal for CPUE indices, and binomial for the tag recaptures. Equations for these observation likelihoods are given in Dunn et al. (2018).

While SPM was formulated as a Bayesian model, the priors used in this model were assumed to be non-informative — priors for all parameters were set as uniform, i.e., where

$$-\log(\pi(\mathbf{p})) = 0$$

And the priors had no contribution to the overall objective function, and hence the estimates from the model can be considered Maximum Likelihood Estimates (MLE), albeit with the addition of penalties.

2.5 Simulations

Simulations were run using SPM as a simulator (see Dunn et al. 2018), from a single point estimate, set equal to the preliminary MPD for the estimation run (as described above). Simulated observations were generated for the CPUE, length frequency, and tag-recapture data with the same observation error as was assumed for the fitted model (and including process error) and with stochastic error dependent on the assumed likelihood (i.e., log-normal for CPUE, multinomial for the length frequencies, and binomial for the tag-recapture at length), assuming the model parameters were the same as that estimated in the fitted point estimate.

In the simulations, an additional structural change was made to record tag releases by the model year that they were released. Here, releases from 2005–2007 were included within the simulation model as categories (immature and mature), with simulated observations for the number of recaptured fish from each of the release categories in each year for periods immediately following the model year of release. Recapture information was simulated for each model year following release up to 2015. Recaptures were recorded by year of release, year of recovery, age, and cell.

Stochastic error arising from model structure was ignored, and hence the only additional error introduced into the simulations was the stochastic error arising from observational uncertainty.

The simulated length frequencies, CPUE, and tag data were reported after being aggregated into the regions defined for the SS3 assessment model (i.e., regions R1a, 1b, R2, R3, R4, and R5 — see Figure 1 above).

2.6 Evaluation of stock assessment bias

The effect of tagging data on assessment bias was evaluated by taking the data generated from the SPM simulation model and using an SS model to estimate the stock size both with and without the tagging data. The objective was to compare stock size and management parameters from the SPM assessment with the SS estimates, both with and without tagging data.

Simulated data were processed in R to produce Stock Synthesis stock assessment input files.

The SS assessment structure was based on the 2018 IOTC yellowfin tuna stock assessment (Fu et al. 2018), adapted as needed.

The spatial structure of the SS model was the same as the 2018 SS assessment (Fu et al. 2018), with four regions (Figure 1). Data from subregions R1a and R1b were combined by summing catches, length frequencies, tag releases and tag recoveries, and using the CPUE trend from region R1b.

The model was run with quarters standing in for years, as in the operating model. The time series in both models ran from pseudo-year 1 (=1952, quarter 1) to 256 (=2015, quarter 4).

Fishery structures were simplified from the 2018 assessment to reflect the simplified fishery structure of the SPM model. The 25 fisheries in the 2018 assessment were aggregated into 16 fisheries (Table 2).

Selectivities were shared within each fishing method (all longline fisheries shared the same selectivity). Time blocks in longline selectivity were removed. Catchability of the longline surveys was also shared. Regional scaling was implemented since all CPUE series were proportional to the vulnerable biomass of the region. The CPUE for region R1 was adjusted to represent the whole region rather than just subregion R1b, by multiplying all R1b index values by the average of $(R1a + R1b) / R1b$, for all pseudo-years with indices for both R1a and R1b.

Table 2: Stock synthesis model fishery structure.

| Number | Gear | Region |
|--------|-------------|--------|
| 1 | Gillnet | 1 |
| 2 | | 4 |
| 3 | Handline | 1 |
| 4 | Longline | 1 |
| 5 | | 2 |
| 6 | | 3 |
| 7 | | 4 |
| 8 | Other | 1 |
| 9 | | 4 |
| 10 | Baitboat | 1 |
| 11 | Purse seine | 1 |
| 12 | | 2 |
| 13 | | 4 |
| 14 | Troll | 1 |
| 15 | | 2 |
| 16 | | 4 |

Catches were those used in the estimation phase of the operating model. In a few cases these differed from the catches simulated by the operating model when insufficient biomass was available in the operating model to take the catch. However, the realised catches were not available because the simulator does not currently report them.

Size bins in the estimation model were at 5 cm intervals, from 10-200 cm. and the tag mixing period was assumed to be 4 quarters. Initial values and fixed values for all parameters were in general the same as used in the 2018 assessment, with some exceptions such as the fisheries that were removed. Environmental effects on movement parameters were not included in the estimation process.

Three additional estimation runs were included as steps towards examining how tag mixing affects yellowfin stock assessment results. These involved a) *mix1*: mixing period reduced to 1 quarter (pseudo-year) rather than 4 quarters, b) *mix8*: mixing period increased to 8 quarters, c) *notags*: tag likelihood lambda set to zero so tags had no influence on the model fit.

3 Results

3.1 SPM model results

Model fits were made using MLE of the preliminary model with initial recruitment (R_0) fixed at the value in the SS3 assessment and with the structure and assumptions described above. A small number of movement assumptions were assessed, using various combinations of preference functions and their functional forms for immature and mature fish, including logistic and double normal preference functions. However, at the time of this report the estimated MLE was unclear as to the extent this represented a true minimum, and the model fits may be inadequate. Hence, we note that this should not be considered as a model that reliably represents the yellowfin tuna population. We note that further development of the input data, model structure, and model assumptions will be required to develop an operating model that can be used for inference about this population, rather than as a general tool for model testing.

The total objective function was dominated by the likelihoods, with catch exploitation rate penalties having only a small impact on the total objective function. Estimated initial relative density for immature and mature YFT at B_0 is given in Figure 29 and Figure 30 respectively, and the resulting SSB trajectory in Figure 28.

The parameters of the preliminary operating model are presented in Table 3. Preliminary estimates of the model fits to the observational data gave estimates of the selectivities and preference movement parameters that were potentially plausible, with the preference-based movement suggested movement of YFT was related to distance, SST, and chlorophyll-a. Distance estimates suggested that movement was over a relatively short distance in each model year — immature fish were estimated to move further than mature fish in each quarter, an estimate that was broadly consistent with the distances moved for the tagged fish when recaptured (see Figure 25). The preference function for SST (Figure 26) suggested some evidence for a relationship with spatial location and underlying SST for mature fish, but less so for immature fish. Similarly, the preference function for chlorophyll-a (Figure 27) suggested some evidence of a relationship for immature fish, but the relationship for mature fish was less clear. However, we note that the current MLE estimates of the parameters for the preliminary model may be unstable and further work is required.

Table 3: Estimated parameters values in the preliminary model (selectivity and movement preference functions), labels, priors, and assumed upper and lower bounds in the estimation (note: MLE values do represent a plausible minimum).

| | Type | Label | Parameter | Preliminary MLE | Lower bound | Upper bound |
|----|---------------------|-------------------|-----------|-----------------|-------------|-------------|
| 1 | Selectivity | fishing_ps_sel | mu | 9.31 | 1.00 | 30.00 |
| 2 | Selectivity | fishing_ps_sel | sigma_l | 3.40 | 1.00 | 100.00 |
| 3 | Selectivity | fishing_ps_sel | sigma_r | 22.31 | 1.00 | 100.00 |
| 4 | Selectivity | fishing_trol_sel | mu | 5.29 | 1.00 | 30.00 |
| 5 | Selectivity | fishing_trol_sel | sigma_l | 1.00 | 1.00 | 100.00 |
| 6 | Selectivity | fishing_trol_sel | sigma_r | 10.38 | 1.00 | 100.00 |
| 7 | Selectivity | fishing_bb_sel | mu | 3.59 | 1.00 | 30.00 |
| 8 | Selectivity | fishing_bb_sel | sigma_l | 1.00 | 1.00 | 100.00 |
| 9 | Selectivity | fishing_bb_sel | sigma_r | 7.28 | 1.00 | 100.00 |
| 10 | Selectivity | fishing_gill_sel | mu | 7.34 | 1.00 | 30.00 |
| 11 | Selectivity | fishing_gill_sel | sigma_l | 1.00 | 1.00 | 100.00 |
| 12 | Selectivity | fishing_gill_sel | sigma_r | 9.42 | 1.00 | 100.00 |
| 13 | Selectivity | fishing_ll_sel | a50 | 9.59 | 1.00 | 30.00 |
| 14 | Selectivity | fishing_ll_sel | ato95 | 5.91 | 1.00 | 100.00 |
| 15 | Selectivity | fishing_hand_sel | mu | 7.67 | 1.00 | 30.00 |
| 16 | Selectivity | fishing_hand_sel | sigma_l | 1.00 | 1.00 | 100.00 |
| 17 | Selectivity | fishing_hand_sel | sigma_r | 10.24 | 1.00 | 100.00 |
| 18 | Selectivity | fishing_other_sel | mu | 8.50 | 1.00 | 30.00 |
| 19 | Selectivity | fishing_other_sel | sigma_l | 4.35 | 1.00 | 100.00 |
| 20 | Selectivity | fishing_other_sel | sigma_r | 9.17 | 1.00 | 100.00 |
| 21 | Preference function | distanceMature | lambda | 0.00991 | 1.0E-6 | 10 |
| 22 | Preference function | SSTmature | a50 | 25.93 | 5.00 | 60.00 |
| 23 | Preference function | SSTmature | ato95 | 1.58 | 1.00 | 100.00 |
| 24 | Preference function | CLOmature | a50 | -2.69 | -20.00 | 20.00 |
| 25 | Preference function | CLOmature | ato95 | 0.10 | 0.10 | 100.00 |
| 26 | Preference function | distancelmmature | lambda | 0.00164 | 1.0E-6 | 10 |
| 27 | Preference function | SSTimmature | a50 | 9.79 | 5.00 | 60.00 |
| 28 | Preference function | SSTimmature | ato95 | 3.81 | 1.00 | 100.00 |
| 29 | Preference function | CLOimmature | a50 | -2.60 | -20.00 | 20.00 |
| 30 | Preference function | CLOimmature | ato95 | 0.64 | 0.10 | 100.00 |
| 31 | Catchability | ll_jpn_q | q | 0.00010 | 1.0E-7 | 0.50 |

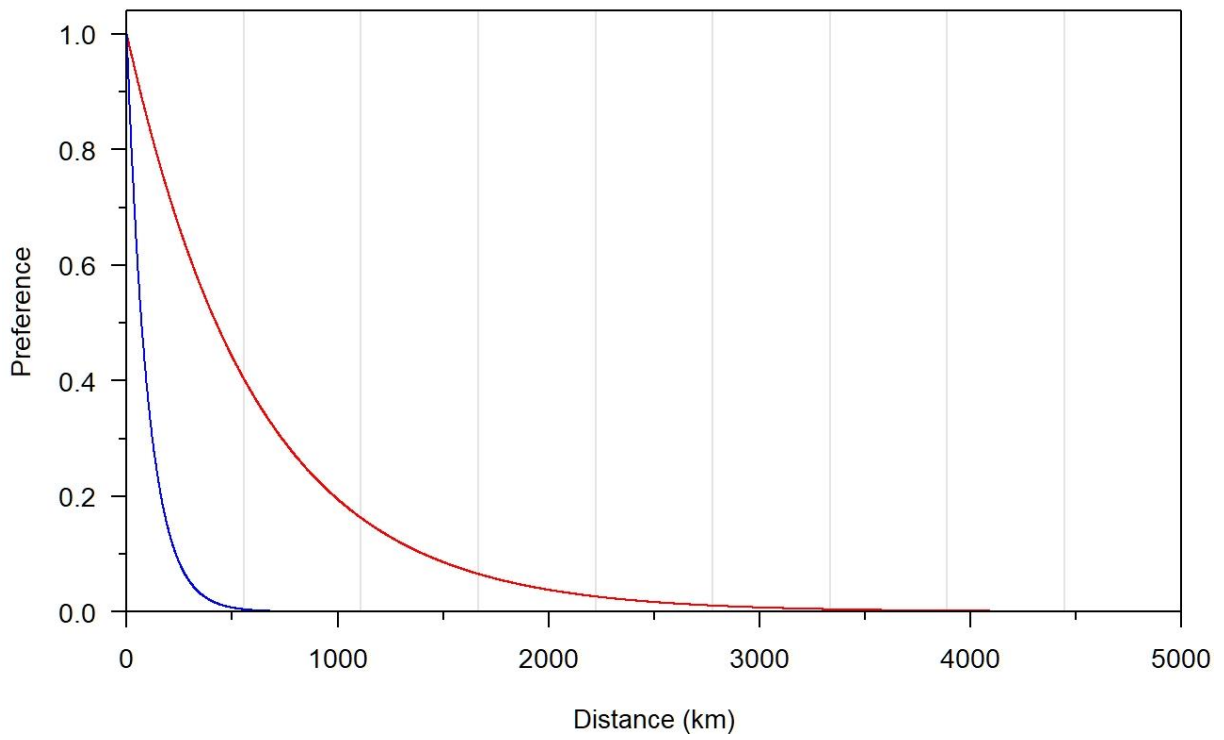


Figure 25: Estimated preference functions for distance for (red) immature and (blue) mature YFT.

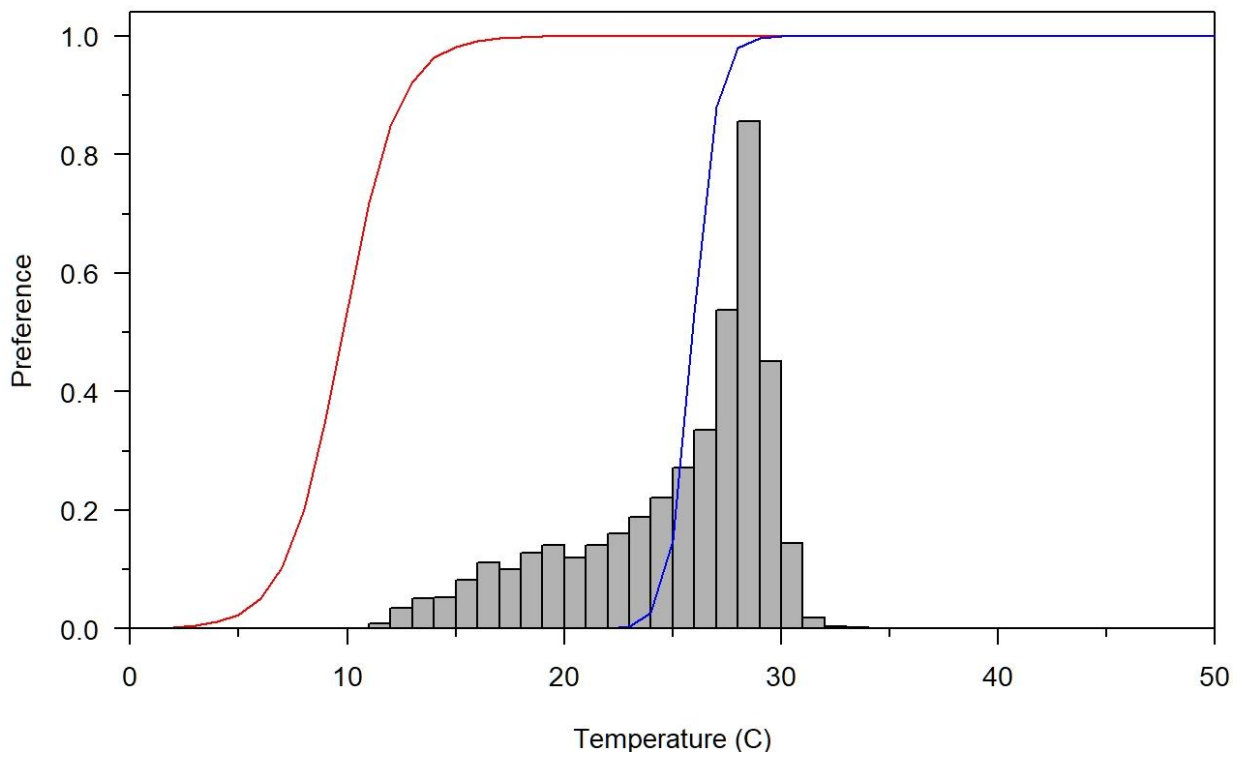


Figure 26: Estimated preference functions for SST for (red) immature and (blue) adult YFT.

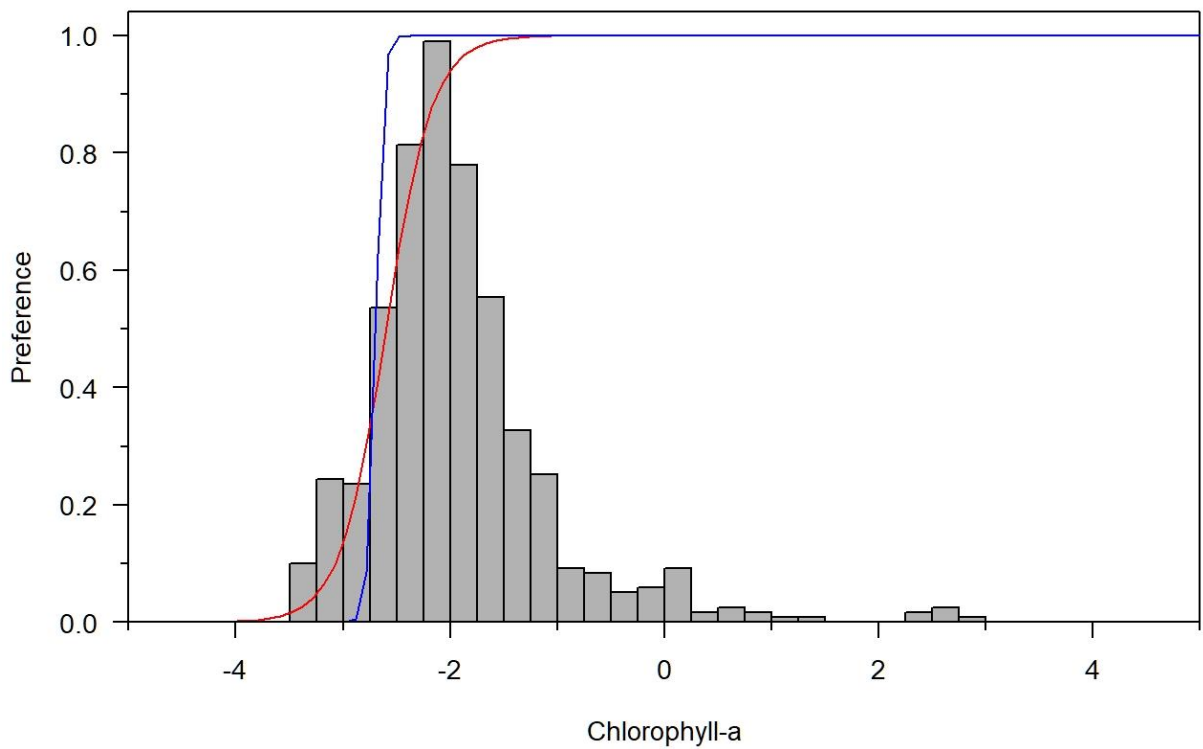


Figure 27: Estimated preference functions for Chlorophyll-a for (red) immature and (blue) adult YFT.

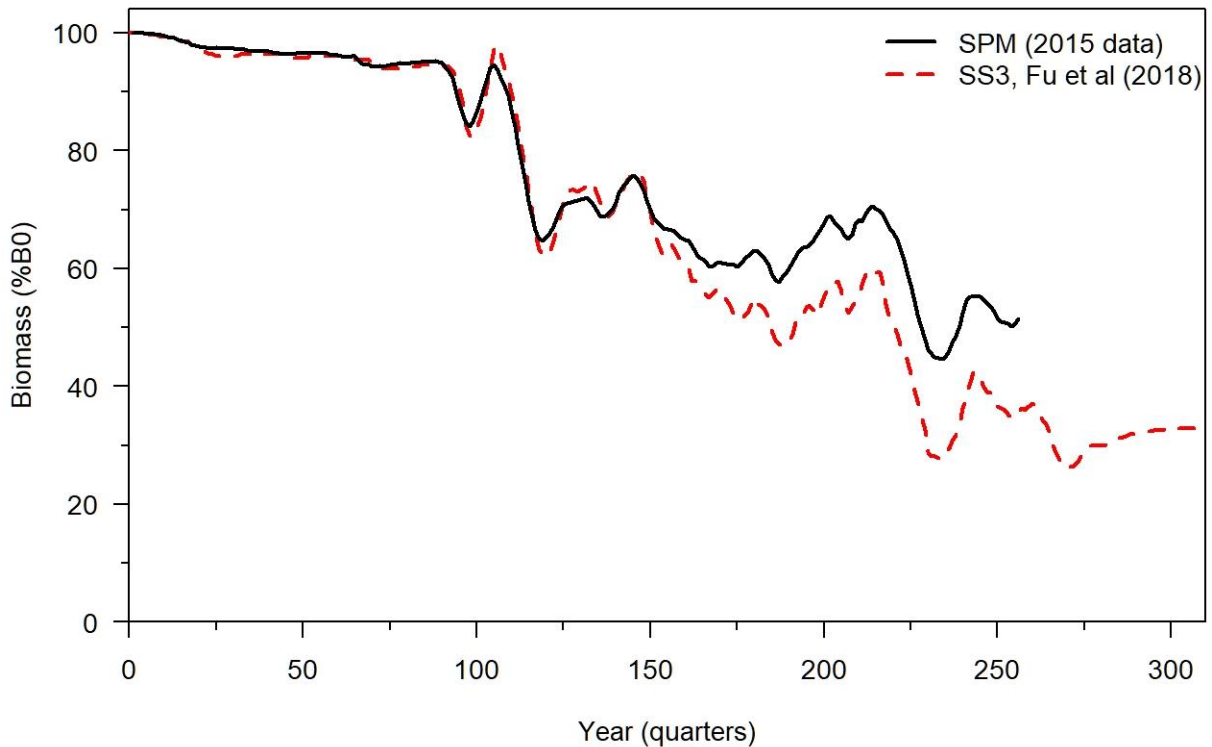


Figure 28: Estimated SSB trajectory from the preliminary SPM model, compared with estimated SSB trajectory from Fu et al. (2018). Note that time units are pseudo-years (quarters).

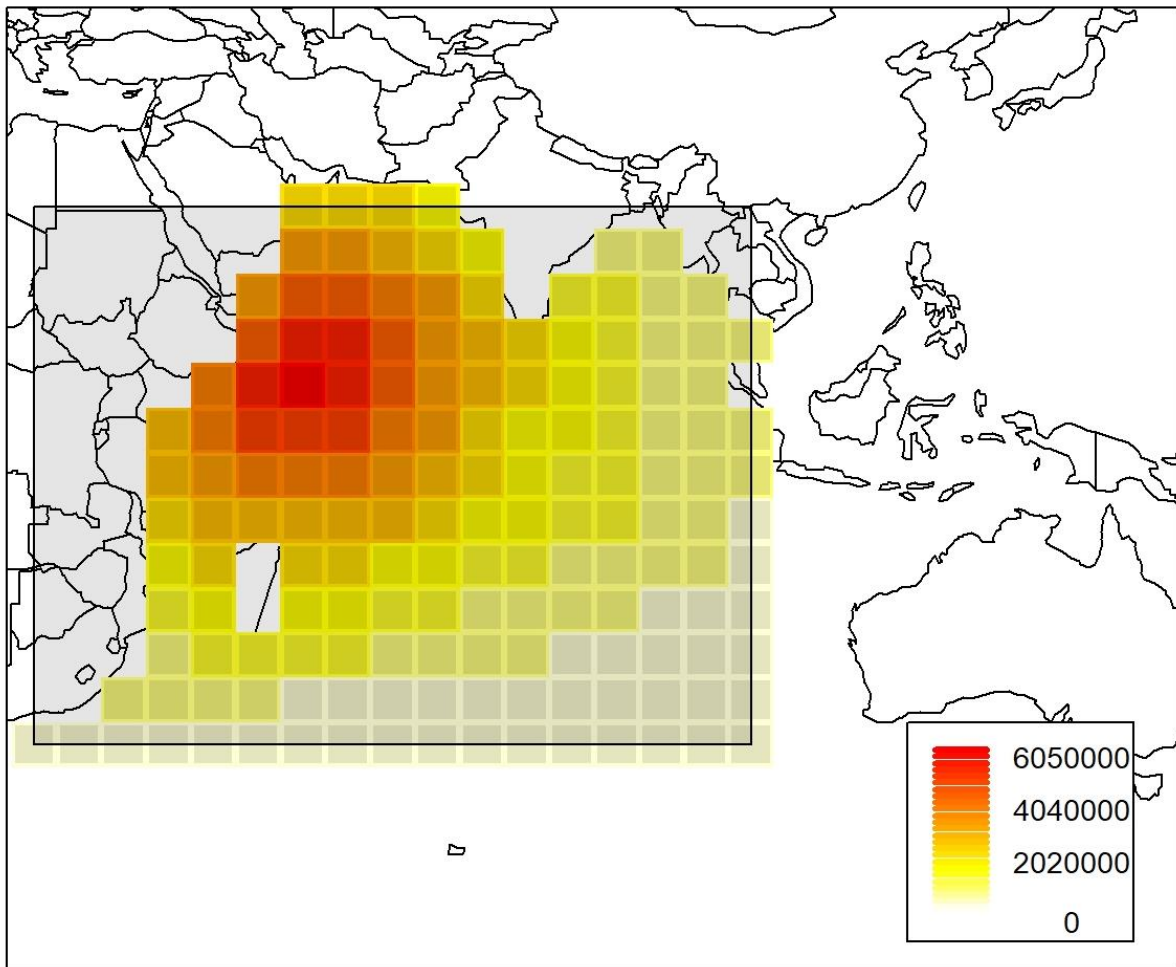


Figure 29: Relative density of immature YFT (number) at initialisation (B_0) from the preliminary spatial model.

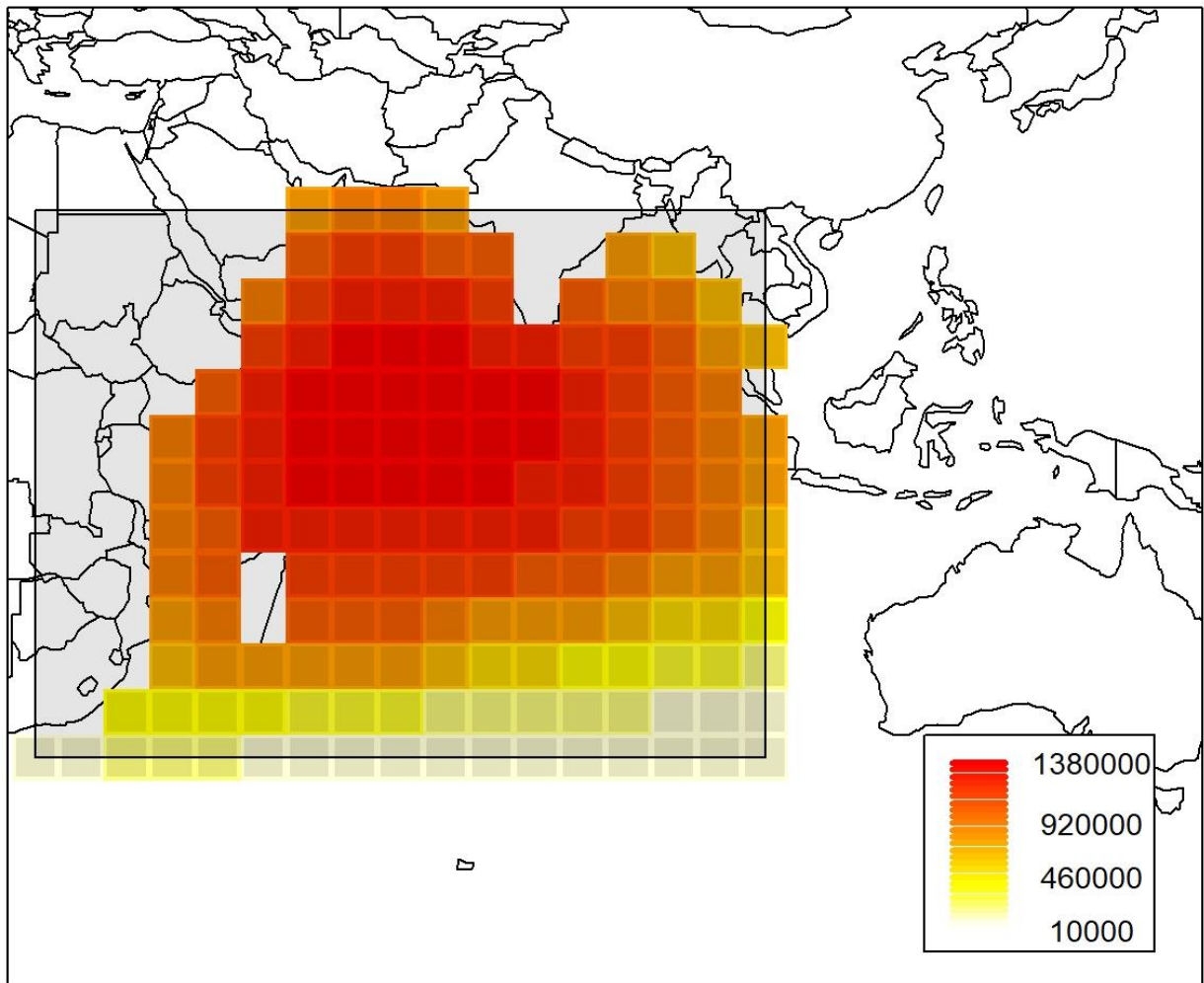


Figure 30: Relative density of mature YFT (number) at initialisation (B_0) from the preliminary spatial model.

3.2 SS3 model fit

The simulated data generated from the SPM operating model were fitted by the Stock Synthesis assessment application. Models converged with gradient less than 0.001.

Example results are provided for the model run with full tagging data and mixing period set to 4 quarters (pseudo-years). This was the mixing assumption used in the original assessment (Fu et al 2018), so represents a test of that approach, albeit a preliminary test given the preliminary nature of both the operating model and the estimation models.

There were many differences between the ‘true’ parameter values of the operating model that generated the data, and those estimated by the SS estimating model. A thorough exploration of these differences and their causes is beyond the scope of this report, but we provide some examples.

Plots for the SS models were generated using the standard plotting functions in r4ss (Taylor et al. 2019). A subset of the plots is provided in Appendix A to facilitate comparison with the full SS assessment. Estimated parameters (apart from deviates), along with priors and bounds, are provided in Table A.1. Availability through time of data inputs by fishery is presented in Figure A.1, and landings in numbers in Figure A.2.

An example of the fit to the length frequency data is presented in Figure A.3. There are some indications from the residuals that the SS model tended to predict more large fish than were generated the operating model throughout the time series.

Fits to the CPUE time series (Figures A.4 to A.7) show that the data generated by the operating model were generally fitted very well by the SS model, apart from the early period up to pseudo-year 100, when predicted catch rates were generally higher than observed catch rates.

Aggregate fits to the tag data were relatively good early in the time series apart from a slight tendency to overestimate the number of observed tags (Figure A.8). Towards the end of the time series the SS model tended to underestimate the number of tags.

Estimated movement rates from the SS model were very high, predicting for example that 100% of 2 to 8-year-old fish in area 2 would move to area 1, while 70% of 2 to 8-year-old fish in area 1 would move to area 2 (Figure A.9). The age structure at equilibrium was not smooth (Figure A.10), reflecting the lack of recruitment into the southern regions and the very high movement rates.

Recruitments showed an increasing trend (Figure A.11), with large declines at the end of the time series. Most of the increasing trend occurs in area 1 (Figure A.12). Recruitments were also presented in the context of the assumed stock recruitment relationship (Figure A.13).

Age-based selectivities were estimated for all fisheries (Figure A.14). In all models the longline selectivity parameter *AgeSel_4P_2_fishing_II_1* was estimated at the lower bound of 2 pseudo-years. This suggests the need for a steeper logistic selectivity curve, in contrast to the operating model's 95% selectivity width of 5.9 pseudo-years. The cause of this difference will need to be further investigated in future work.

Fishing mortalities as expected showed an increasing trend throughout the time series, with a spike up at the end reflecting the decline in estimated biomass (Figure A.15). Total (Figure A.16) and spawning biomass (Figure A.17) by area were tightly constrained by the CPUE series and by the use of regional scaling.

3.3 Examining how tag mixing affects stock assessment bias

Four models were run with alternative treatments of tags, including the base model (*mix4*) with mixing period of 4 quarters, models *mix1* and *mix8* with mixing periods of 1 and 8 quarters respectively, and model *notags* with the influence of tagging data removed from the likelihood.

The models with mixing period of 1 and 4 quarters generated spawning biomass estimates that were very similar to one another, and somewhat smaller than the spawning biomass of the operating model (Figure 31). Increasing the mixing period to 8 quarters produced a higher spawning biomass estimate that was very similar to the operating model for much of the time series, including the period when tags were in the population. This result suggests that, given the movement rates of the simulated population in the operating model, mixing is not complete by 4 quarters. The fact that the *mix-4* SS biomass estimates are negatively biased suggests that, between 4 and 8 quarters, the fleets are catching more tags than SS expects under the assumption that tags are mixed.

The lack of fit by model *mix-8* to the CPUE in the early part of the time series is curious and needs further investigation. It may be an artefact of the fact that the SS estimation model starts estimating recruitment deviates four quarters later than the operating model starts generating them. There may also be an effect of the treatment of the lognormal bias correction through time. Similarly, the

anomalously low recruitment estimates at the end of the time series should be investigated and may have relevance for similar recruitment patterns in other assessments.

The model without tags (*notags*) generated a much higher estimate of spawning biomass than the 'true' value, almost twice the level of the operating model. Without tags, this model obtains most population scaling information from size and CPUE data. This pattern may be a consequence of poor fit to the size data. A likelihood profile on R_0 would be useful to explore which fisheries and datasets are involved.

The overall scales of the recruitment estimates between models were consistent with the relative biomass estimates, indicating that the higher biomass estimates were generated by higher recruitments (Figure 32). Recruitment patterns show similarities but there is considerable variation in scale and timing through the time series. As mentioned above there is also a decline for model *mx4* (with tags) at the end of the time series. The correlation coefficient between recruitments from the operating model and model *mx4* is 0.42.

Mixing is related to movement, and the estimated movement rates varied among models with different treatment of tags. Movement rates overall were lowest in the model that did not fit to the tag data (Figure 33), and were highest in the model that assumed a mixing period of 8 quarters. Average movement rates tended to increase with the length of the mixing period.

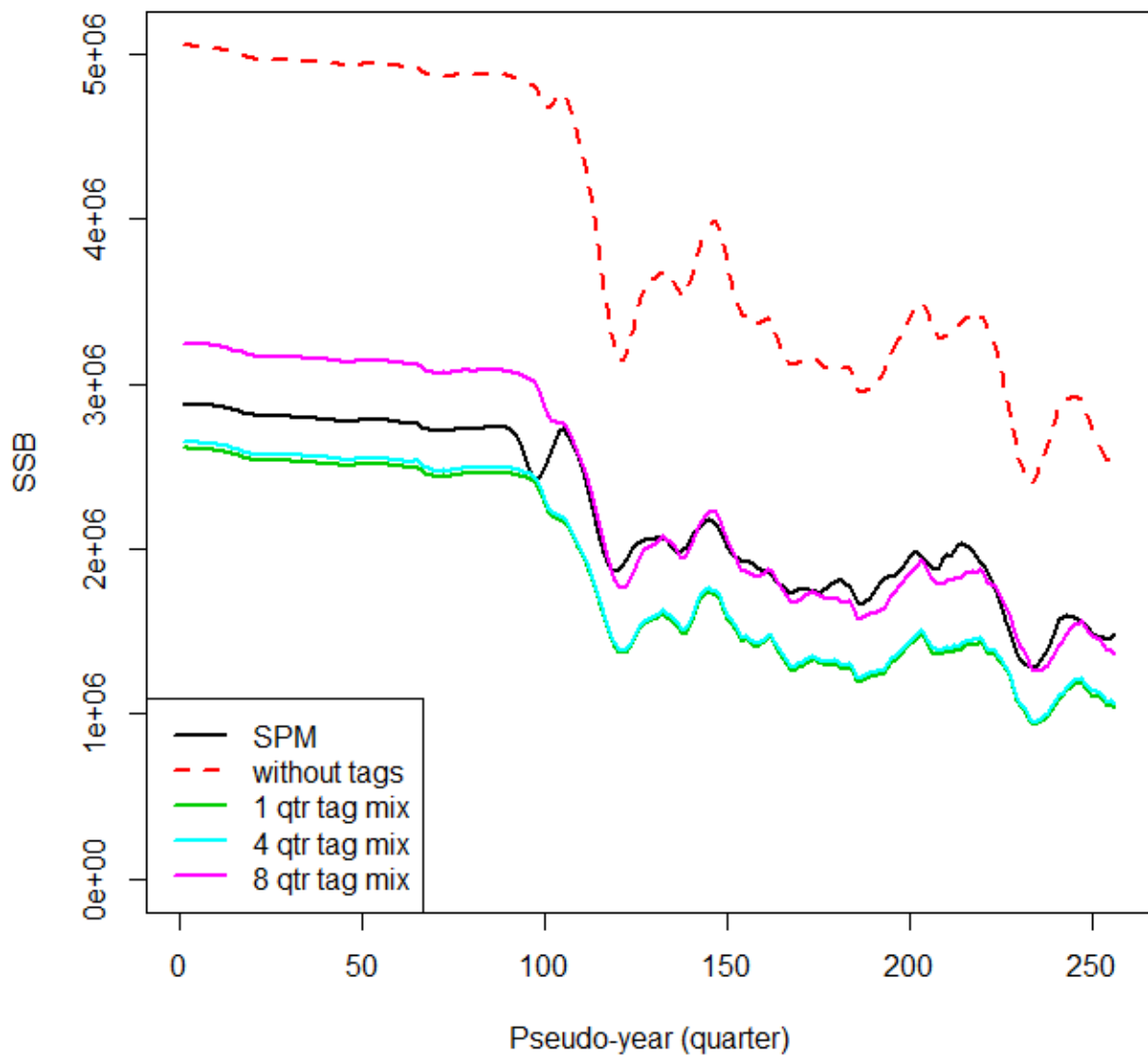


Figure 31: Comparison of SSB estimates between the SSB simulator and SS estimation runs either without tags or with different assumed mixing periods.

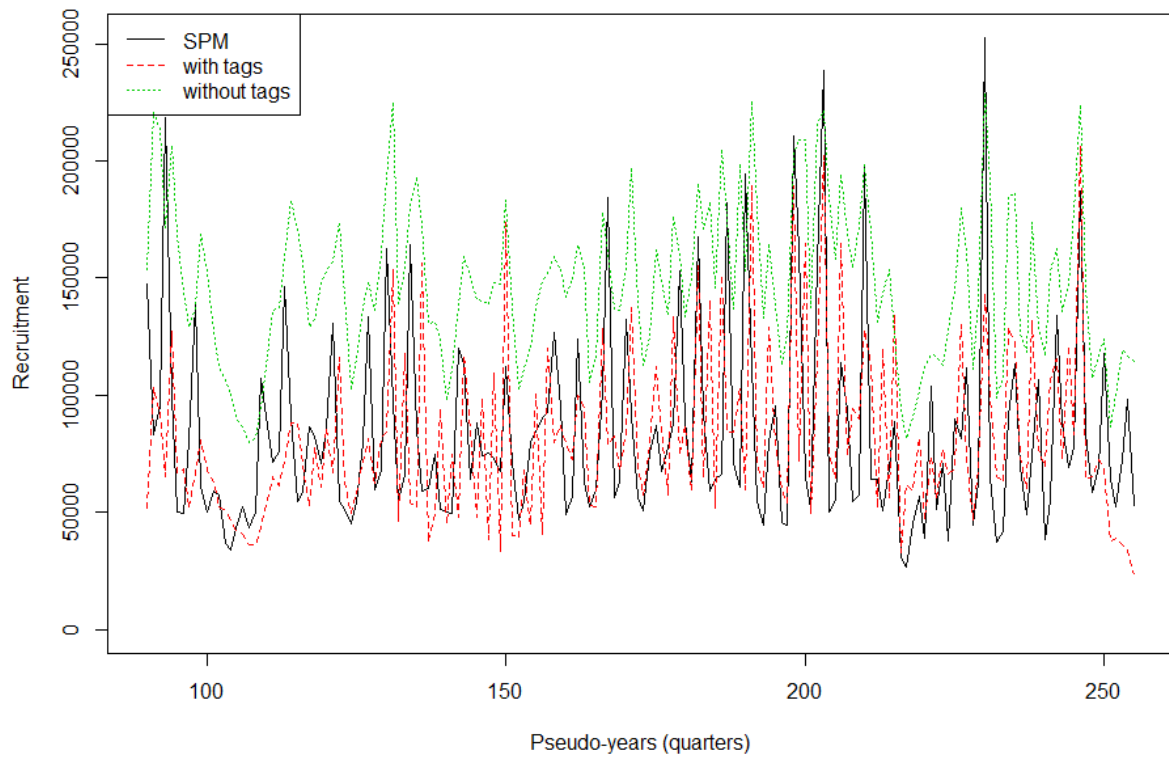
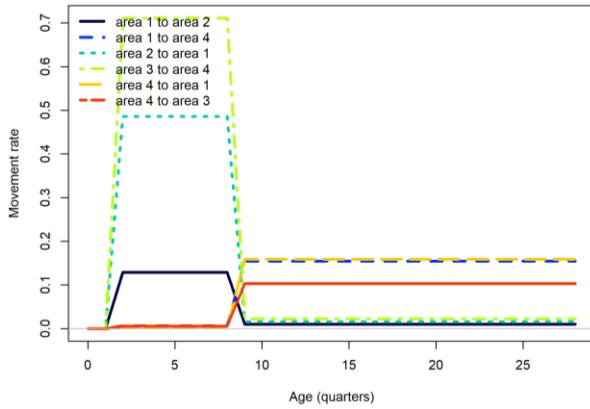
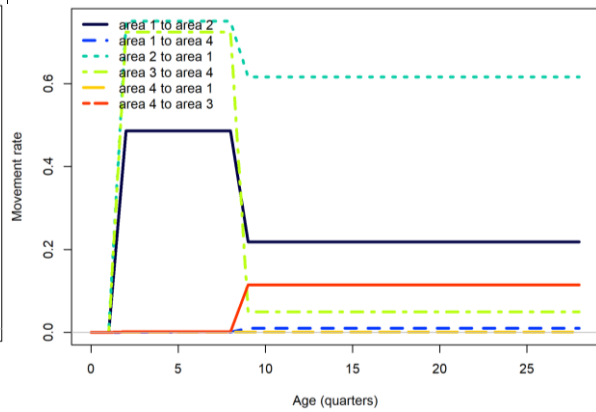


Figure 32: Comparison of recruitment estimates between the SSB simulator and SS estimation runs either with (*mix4*) or without tags (*notags*).

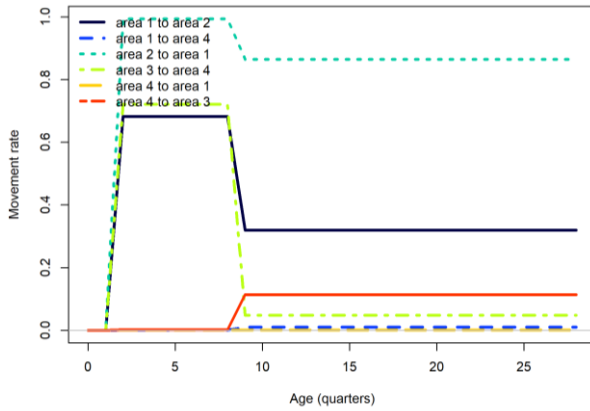
notags



mix1



mix4



mix8

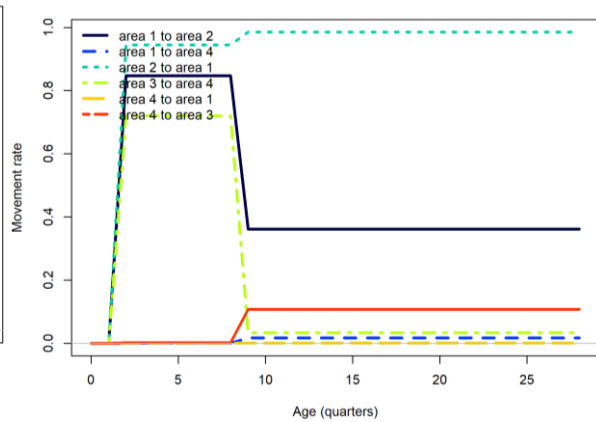


Figure 33: Variation in estimated quarterly (pseudo-year) movement rates depending on how tags are treated in the SS model, for models without tags (*notags*) and with mixing periods 1, 4, and 8 quarters (*mix1*, *mix4*, *mix8*).

4 Discussion

Development of a preliminary model spatially explicit model for YFT in the Indian Ocean suggests that plausible operating models may be developed that allow analysts to investigate and validate many aspects of stock assessment methods, including spatial features such as movement, the treatment of tagged fish, and spatial size variation.

While these preliminary models require further development, SPM can be used both to estimate (approximately) MLE estimates of movement and distribution with the population dynamics of YFT, and to generate simulated data from an operating model where population dynamics are known, for use in alternative SS3 models.

Estimates from the preliminary model suggested that the mixing rates of the populations may be low at the ocean-basin scale for YFT and was broadly consistent with the tagging observations collected from the Indian Ocean Tuna Tagging Programme (IOTTP). Spatial population models, while requiring further development in the preliminary model, have the potential to provide a method to investigate the impact of tagged fish movement and mixing assumptions.

Further development of these models is, however, required. There are underlying differences in model structures between SS3 and SPM which should be addressed to better simulate the population dynamics in a manner consistent with both packages. Some additional functionalities in SPM may also improve its utility for both estimation and simulation, including:

- Improve model run time. Estimation time for large spatial models is typically slow — mostly due to the requirement to evaluate likelihoods for the large number of length frequency observations (i.e., length frequencies by cell, fishery, and quarter) and CPUE (CPUE indices for the longline fleet, by cell and quarter) observations. Model speed could be significantly improved by using threaded CPU processes (e.g., by using large numbers of CPU cores to parallelise minimisation algorithms).
- Implement an overdispersion parameter for tag recapture observations, and potentially introduce additional likelihoods (e.g., Poisson, negative binomial, or the zero inflated binomial likelihood).
- Implement a likelihood multiplier term to modify relative likelihoods in a manner consistent with SS3.
- Implement a tag detection rate into the observation class for tag data.
- Modify the output reports from SPM to enable formats more consistent with SS3 input files.

Most of these modifications to SPM are relatively minor, except for the introduction of threading processes which would require significant code development.

Within the analyses, further development of the YFT models is required. Including:

- Development of standardised CPUE indices by spatial cell and fleet, including development of optimal initial variance estimates.
- Development of standardised length frequencies by cell and fleet, including estimation of optimal effective sample sizes.
- Aggregate length frequencies in cases where only lower resolution data are available (currently assumed to all be at $5 \times 5^\circ$ spatial cell)
- Catch data removals where data is only available at a resolution lower than $5 \times 5^\circ$ spatial cell.

The data simulated from the SPM operating model were successfully fitted by a Stock Synthesis assessment application, demonstrating the potential to test the performance of Stock Synthesis applications in situations where the ‘true’ population dynamics are known, and compare its performance with different configurations.

Results from the SS3 model had similar scale and trend to the biomass of the operating model, particularly for the model with mixing period of 8 quarters. We should be cautious about over-interpreting these results, which are preliminary and require further work to refine both the operating model and the assessment model. Nevertheless, these results are consistent with the hypotheses that, a) when catch, reporting rates, natural mortality and selectivities are known, fully mixed tags can provide reliable evidence about biomass, and b) tag mixing in the SPM operating model is incomplete after 1 and 4 quarters, but the simulated population is relatively well-mixed after 8 quarters.

It is unclear why the estimates of biomass scale and trend were similar for the models with mixing periods of 1 and 4 quarters. This is surprising and requires further investigation but may indicate that tags recaptured between 1 and 4 quarters after release have little influence on population scaling in this realisation of the simulation.

When tag data were not included in the estimation model, spawning biomass estimates were approximately twice the true level of the simulated population. This indicates conflict between the information in the tagging data and other datasets (size frequency and CPUE) and priors. It would be useful to explore the factors causing this discrepancy, via a full exploration of model diagnostics such as likelihood profiles on virgin recruitment.

4.1 Further work

As noted above, further development of the input data, model structure, and model assumptions will be required to develop an operating model that can be used for inference about this population, rather than as a general tool for model testing.

The availability of a spatially explicit operating model provides opportunities to explore many difficult and important issues in stock assessment. For example:

- Recent genetic work reported at SC22 in 2019 (Davies et al. 2019) suggested the presence of more than one genetically isolated yellowfin tuna population in the Indian Ocean. It is unclear how such population substructure would affect estimates from the current stock assessment, which assumes a single

interbreeding population. An SPM operating model with multiple sub-stocks could be used to explore the potential for bias, and to identify which approaches are most likely to give reliable estimates.

- Spatial and seasonal size variation within model fisheries can cause stock assessment bias. There are methods to address these problems including new methods for modelling size and CPUE data (Maunder et al. 2020), or adding additional fisheries to the model, but it is unclear which approaches are most effective and how important this problem is. Size data generated from the current SPM operating model could be used to test and compare these alternative assessment approaches.
- Spatial variation in growth has recently been identified as a potential concern for the Indian Ocean yellowfin tuna assessment, and also for WCPO bigeye and yellowfin tuna. Spatially varying growth could be simulated with a modified version of the SPM operating model and used to identify likely biases and compare ways to mitigate them.

There is also potential for more direct applications to management. Current approaches for assessing and managing the yellowfin tuna population have limited ability to allow for the viscosity of the population, and the potential for fishing impacts and interactions to reduce with distance. SPM could be used to explore the potential for spatial management of yellowfin tunas, which may lead to higher yields and other benefits.

In addition, there is potential to develop SPM operating models for other species, such as bigeye, skipjack and albacore tunas.

4.2 Spatial model meeting

The SPM operating model for yellowfin tuna will be used as one of two case studies in a spatial modeling workshop planned for September 2021 in association with the World Fisheries Congress. The aim of the meeting is to explore and compare the approaches that analysts use to include spatial effects in different stock assessment platforms.

The modeling team will simulate data from the operating model and distribute it to analysts using different stock assessment platforms, who will then fit the data. A refined version of the SS assessment presented here will be one of the key assessments.

There is a need for additional funding to support the meeting, since we have lost some expected funding due to covid-19. This will be used to pay for time to improve the operating model, validate and improve the SS assessment, help generate data files for analysts, and prepare reports for the meeting.

5 Acknowledgments

Development of this report was funded by the Food and Agriculture Organization of the United Nations.

Thanks to Jeremy McKenzie (NIWA) for providing constructive comments on an earlier draft of the report.

6 References

- Davies, C.; Marsac, F.; Murua, H.; Fraile, I.; Farley, J.; Grewe, P.; Proctor, C.; Clear, N.; Aulich, J.; Feutry, P.; Cooper, S.; Foster, S.; Artetxe-Arrate, I.; Nikolic, N.; Krug, I.; Leone, A.; Labonne, M.; Darnaude, A.; Ruchimat, T.; Satria, F.; Lestari, P.; Taufik, M.; Priatna, A.; Zamroni, A. (2019). Estimation with Next Generation Sequencing Technologies and Otolith Micro-chemistry. Working paper submitted to the IOTC 22nd Scientific Committee Meeting IOTC-2019-SC22-INF05_Re. IOTC, Karachi, Pakistan, 47 p.
- Dunn, A.; Rasmussen, S.; Mormede, S. (2018). Spatial Population Model User Manual, SPM v1.1-2018-05-31 (rev. 1291). NIWA Technical Report 138. NIWA, Wellington, New Zealand, 210 p.
- Fonteneau, A.; Gascuel, D. (2008). Growth rates and apparent growth curves, for yellowfin, skipjack and bigeye tagged and recovered in the Indian Ocean during the IOTTP. IOTC-2008-WPTDA-08. Indian Ocean Tuna Commission, Victoria, Seychelles, 23 p.
- Fu, D.; Langley, A.; Merino, G.; Ijurco, A.U. (2018). Preliminary Indian Ocean Yellowfin Tuna Stock Assessment 1950-2017 (Stock Synthesis). IOTC-2018-WPTT20-33., Working Party on Tropical Tunas. Indian Ocean Tuna Commission, Mahé, Seychelles, 116 p.
- Hillary, R.M. (2008). Defining tag rates and TACs to obtain suitably precise abundance estimates for new and exploratory fisheries in the CCAMLR Convention Area 7-7.
- Hillary, R.M.; Million, J.; Anganuzzi, A.; Areso, J.J. (2008). Tag shedding and reporting rate estimates for Indian Ocean tuna using double-tagging and tag-seeding experiments. IOTC-2008-WPTDA-04. Indian Ocean Tuna Commission, Victoria, Seychelles, 11 p.
- IOTC (2008). Report of the Second Session of the IOTC Working Party on Temperate Tunas. IOTC-2008-WPTe-R[E]. Indian Ocean Tuna Commission, Bangkok, Thailand, 36 p.
- IOTC (2016). Resolution 16/01: on an interim plan for rebuilding the Indian Ocean yellowfin tuna stock in the IOTC area of competence. Resolution 16/01. Indian Ocean Tuna Commission, Victoria, Seychelles, 3 p.
- Kolody, D.; Hoyle, S. (2015). Evaluation of tag mixing assumptions in western Pacific Ocean skipjack tuna stock assessment models. *Fisheries Research* 163, 127–140. <https://doi.org/10.1016/j.fishres.2014.05.008>
- Langley, A. (2015). Stock assessment of yellowfin tuna in the Indian Ocean using Stock Synthesis. IOTC-2015-WPTT17-30. IOTC, Victoria, Seychelles, 82 p.
- Langley, A. (2016). An update of the 2015 Indian Ocean Yellowfin Tuna stock assessment for 2016. IOTC-2016-WPTT18-27. IOTC, Victoria, Seychelles, 14 p.
- Langley, A.; Herrera, M.; Million, J. (2012). Stock assessment of yellowfin tuna in the Indian Ocean using MULTIFAN-CL. IOTC-2012-WPTT14-38 rev. 1. IOTC, Victoria, Seychelles, 72 p.
- Levitus, S.; Antonov, J.I.; Boyer, T.P.; Locarnini, R.A.; Garcia, H.E.; Mishonov, A.V. (2009). Global ocean heat content 1955–2008 in light of recently revealed instrumentation problems. *Geophysical Research Letters* 36. <https://doi.org/10.1029/2008GL037155>

- Maunder, M.N.; Thorson, J.T.; Xu, H.; Oliveros-Ramos, R.; Hoyle, S.D.; Tremblay-Boyer, L.; Lee, H.H.; Kai, M.; Chang, S.-K.; Kitakado, T.; Albertsen, C.M.; Minte-Vera, C.V.; Lennert-Cody, C.E.; Aires-da-Silva, A.M.; Piner, K.R. (2020). The need for spatio-temporal modeling to determine catch-per-unit effort based indices of abundance and associated composition data for inclusion in stock assessment models. *Fisheries Research* 229, 105594. <https://doi.org/10.1016/j.fishres.2020.105594>
- Methot, R.D.; Wetzel, C.R.; Taylor, I.G. (2018). *Stock Synthesis User Manual Version 3.30.12*. NOAA Fisheries, Seattle WA, 235 p.
- Mormede, S.; Dunn, A. (2013). The Investigation of potential biases in the assessment of Antarctic toothfish in the Ross Sea fishery using outputs from a spatially explicit operating model. *WG-SAM-13/36*. CCAMLR, Hobart, Australia, 21 p.
- Mormede, S.; Dunn, A.; Parker, S.; Hanchet, S. (2017). Using spatial population models to investigate the potential effects of the Ross Sea region Marine Protected Area on the Antarctic toothfish population. *Fisheries Research* 190, 164–174. <https://doi.org/10.1016/j.fishres.2017.02.015>
- NASA Goddard Space Flight Center, Ocean Ecology Laboratory, Ocean Biology Processing Group (2020). Moderate-resolution Imaging Spectroradiometer (MODIS) Aqua Chlorophyll Data; 2018 Reprocessing. NASA OB.DAAC, Greenbelt, MD, USA.
- Rayner, N.A. (2003). Global analyses of sea surface temperature, sea ice, and night marine air temperature since the late nineteenth century. *Journal of Geophysical Research* 108, 4407. <https://doi.org/10.1029/2002JD002670>
- Taylor, I.G.; Stewart, I.J.; Hicks, A.C.; Garrison, T.M.; Punt, A.E.; Wallace, J.R.; Wetzel, C.R.; Thorson, J.T.; Takeuchi, Y.; Ono, K.; Monnahan, C.C.; Stawitz, C.C.; A’mar, Z.T.; Whitten, A.R.; Johnson, K.F.; Emmet, R.L.; Anderson, S.C.; Lambert, G.I.; Stachura, M.M.; Cooper, A.B.; Stephens, A.; Klaer, N.L.; McGilliard, C.R.; Mosqueira, I.; Iwasaki, W.M.; Doering, K.; Havron, A.M. (2019). *r4ss: R Code for Stock Synthesis*.

Appendix A SS Model Fit

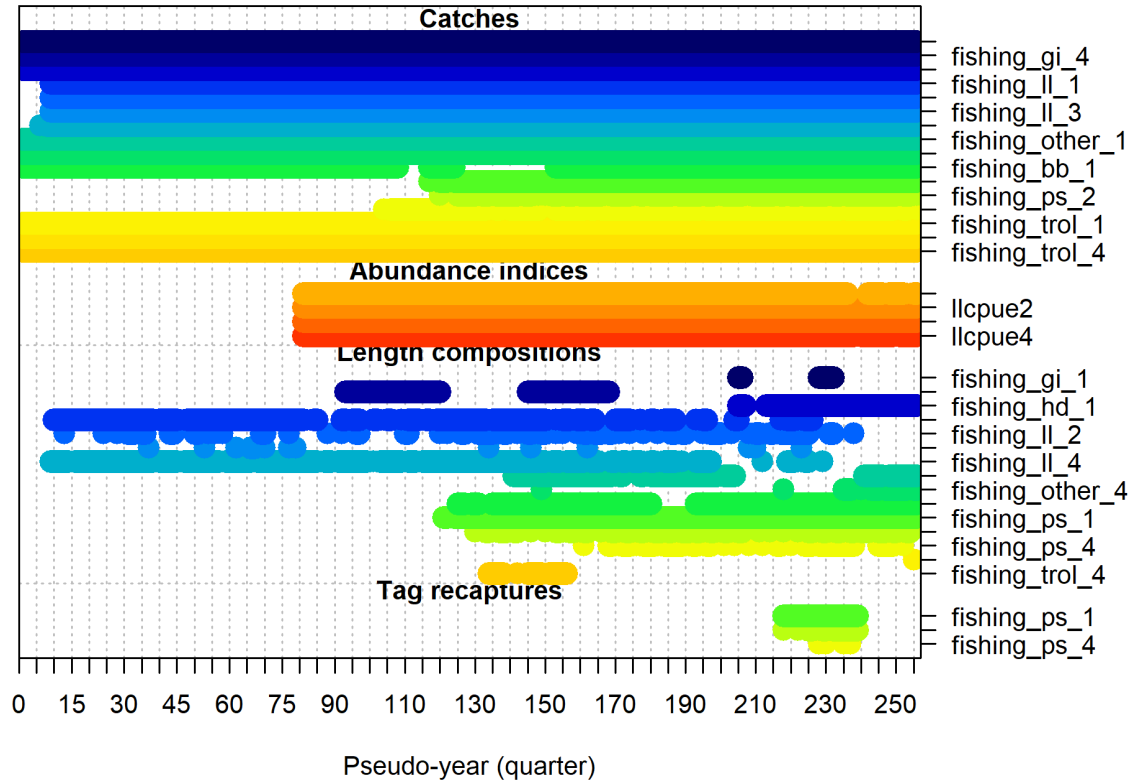


Figure A.1: Simulated data included in the SS model by pseudo-year (quarter).

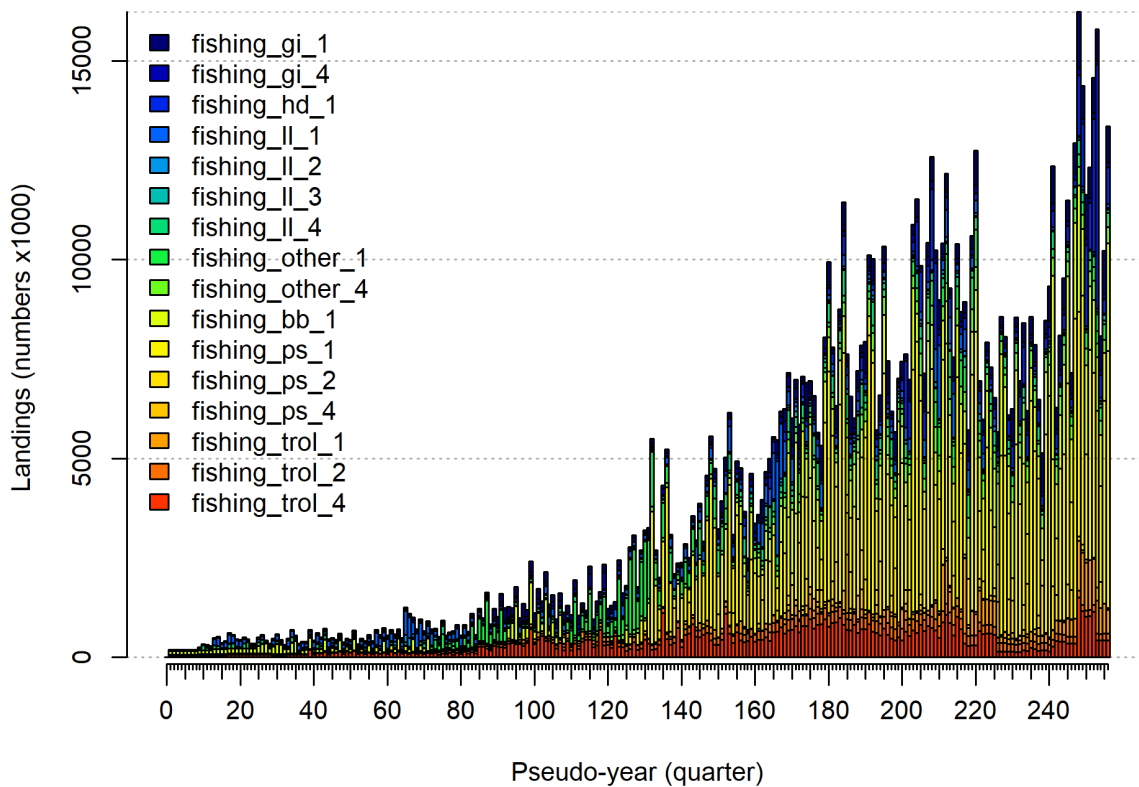


Figure A.2: Catch by pseudo-year (quarter) and fishery.

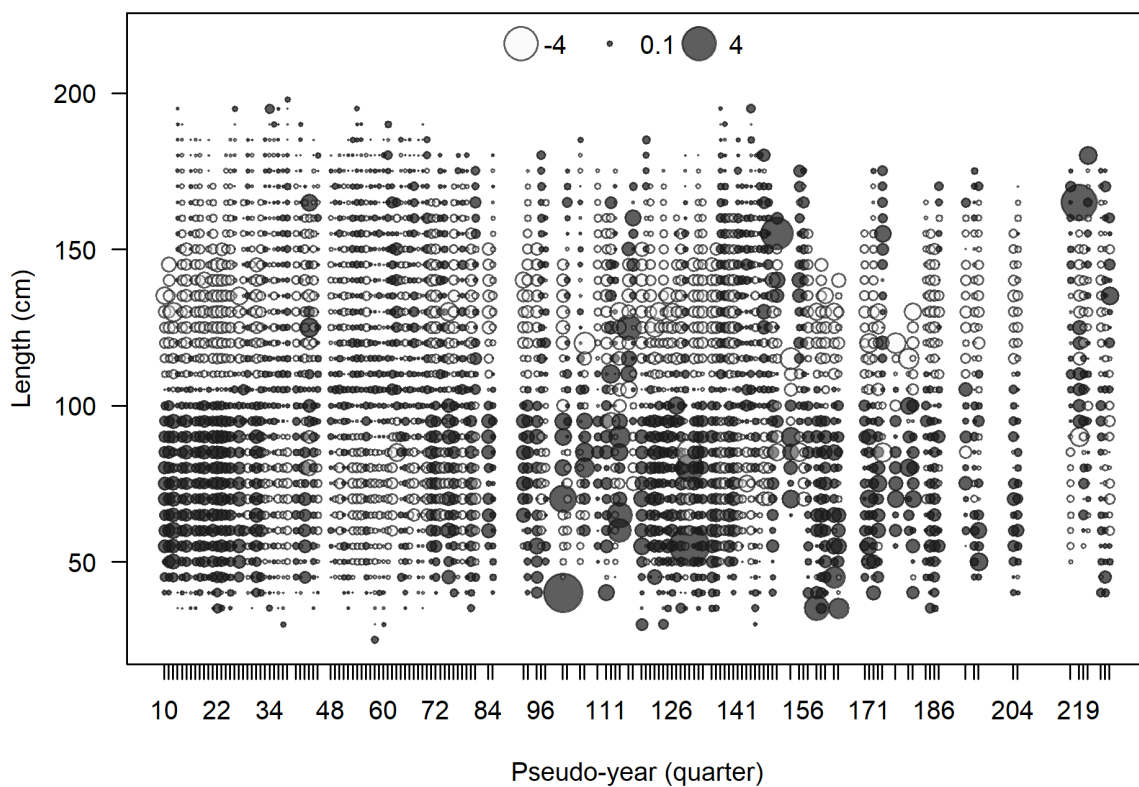


Figure A.3: Bubble plot of Pearson residuals associated with length frequency data from the longline fishery in Region 1, provided as an example.

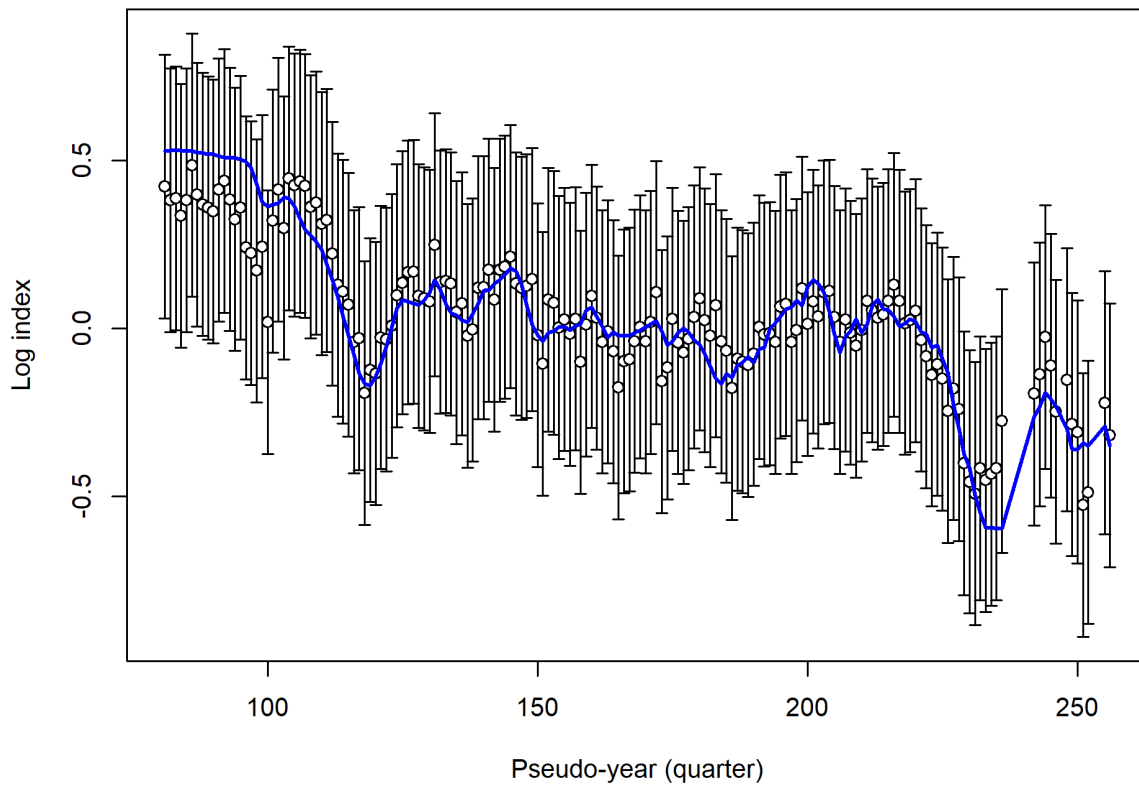


Figure A.4: Log scale fit of the model to the CPUE time series for the longline fishery in region 1.

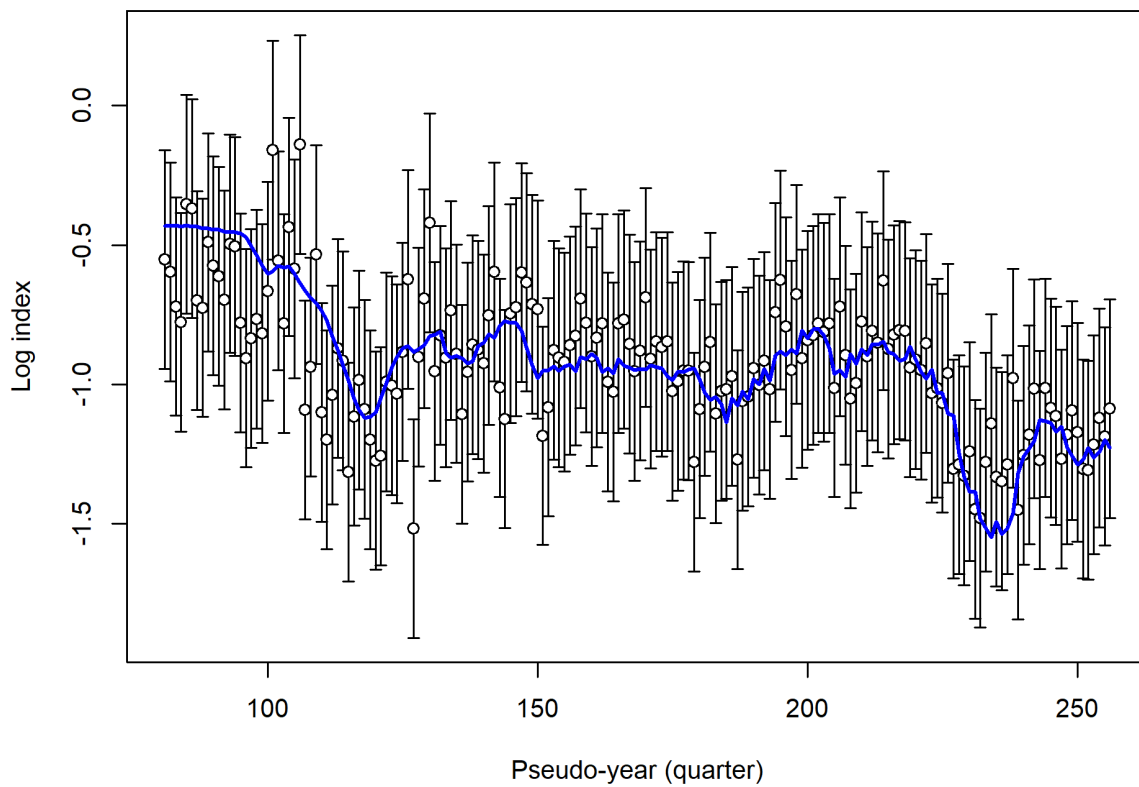


Figure A.5: Log scale fit of the model to the CPUE time series for the longline fishery in region 2.

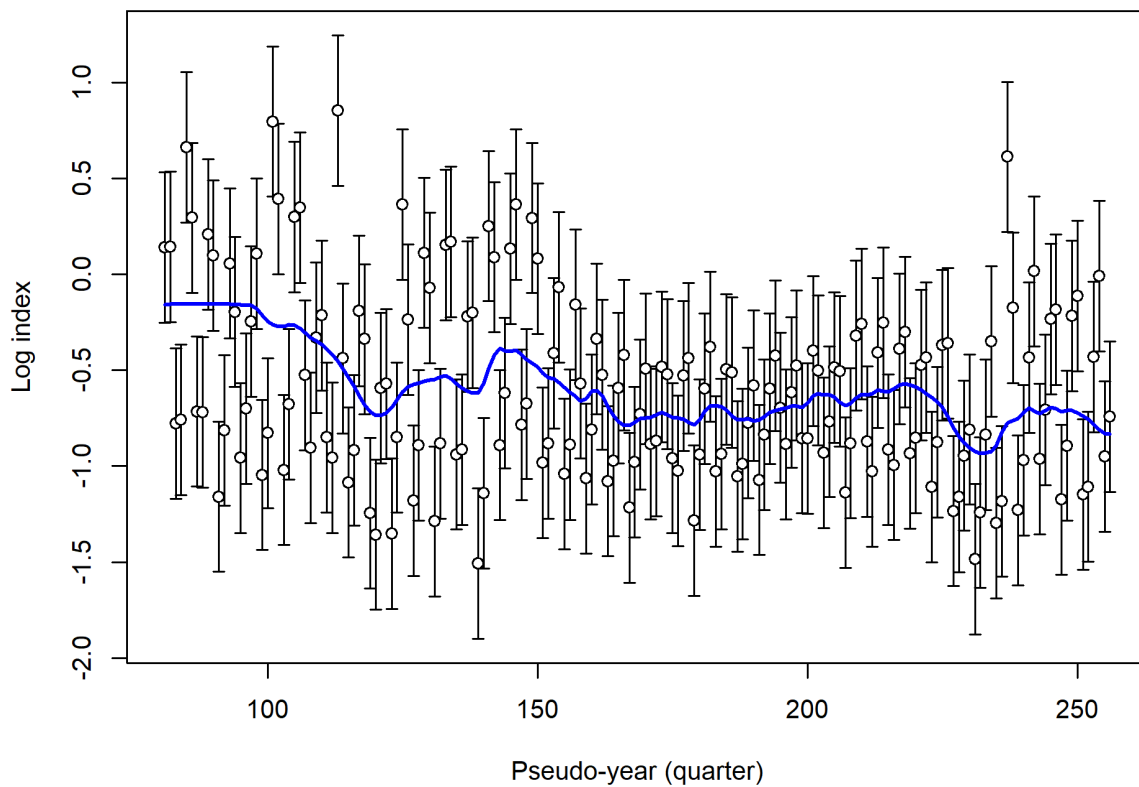


Figure A.6: Log scale fit of the model to the CPUE time series for the longline fishery in region 3.

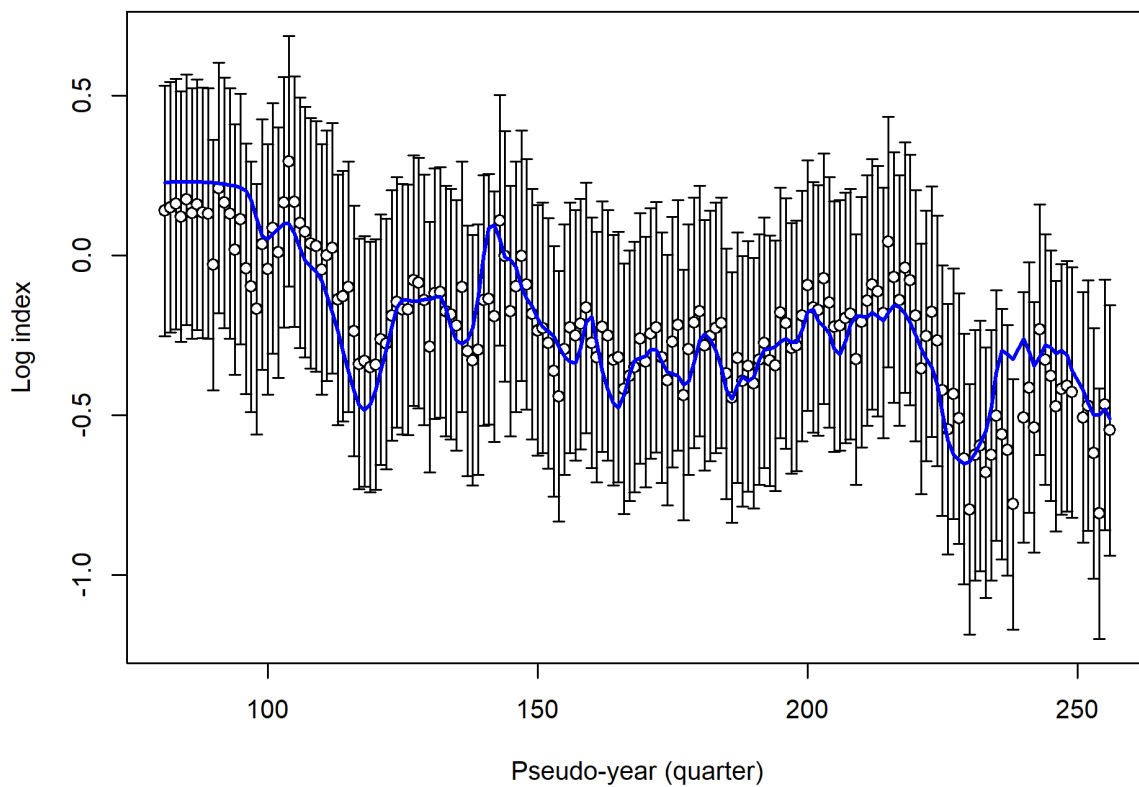


Figure A.7: Log scale fit of the model to the CPUE time series for the longline fishery in region 4.

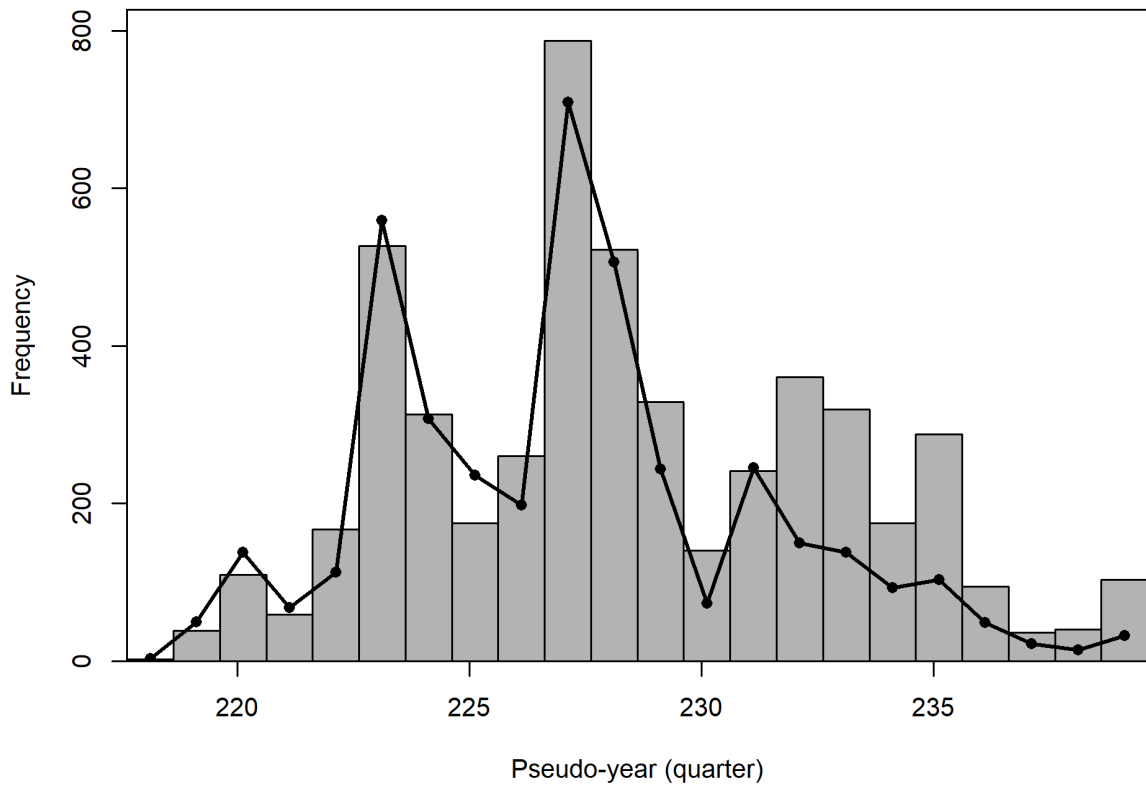


Figure A.8: Observed (bars) and expected (line) tag recaptures aggregated across tag groups and fleets.

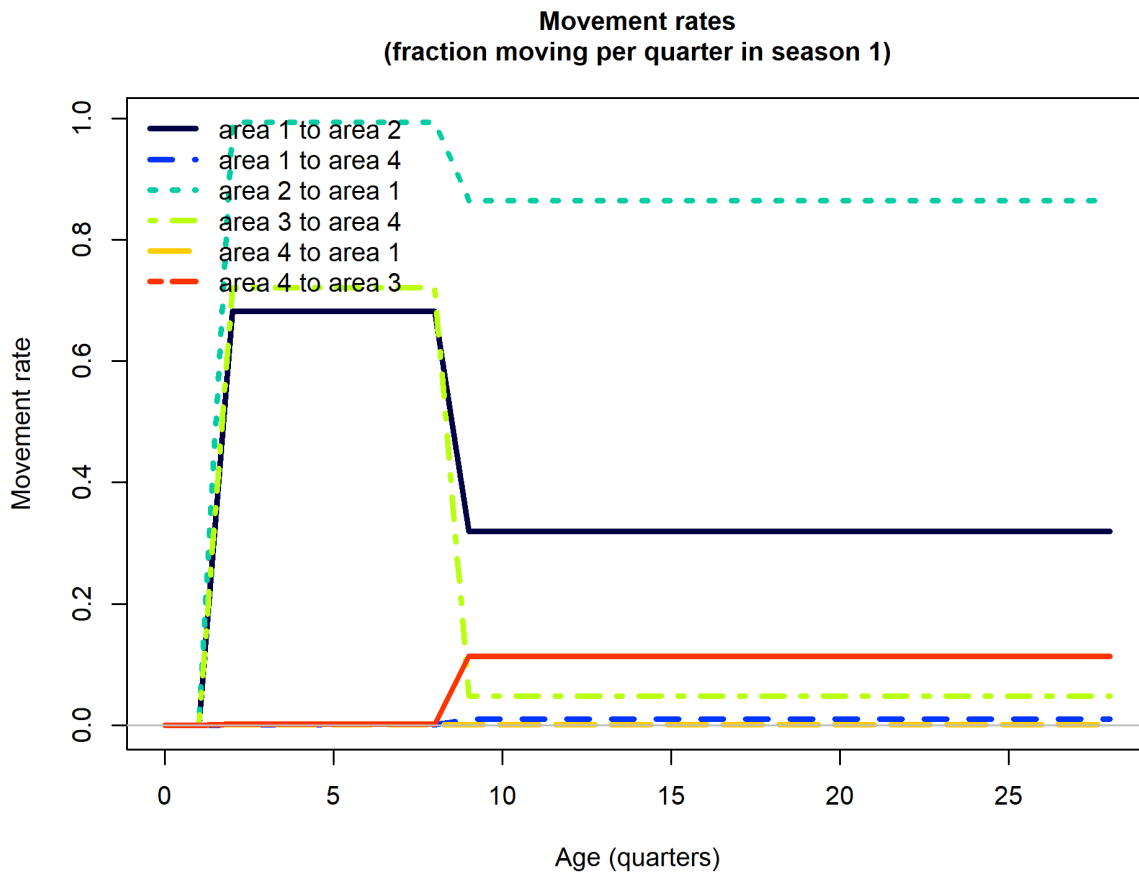


Figure A.9: Estimated quarterly (pseudo-year) movement rates by age and region pair. Note that ages are in pseudo-years, i.e. quarters, and each year has one season.

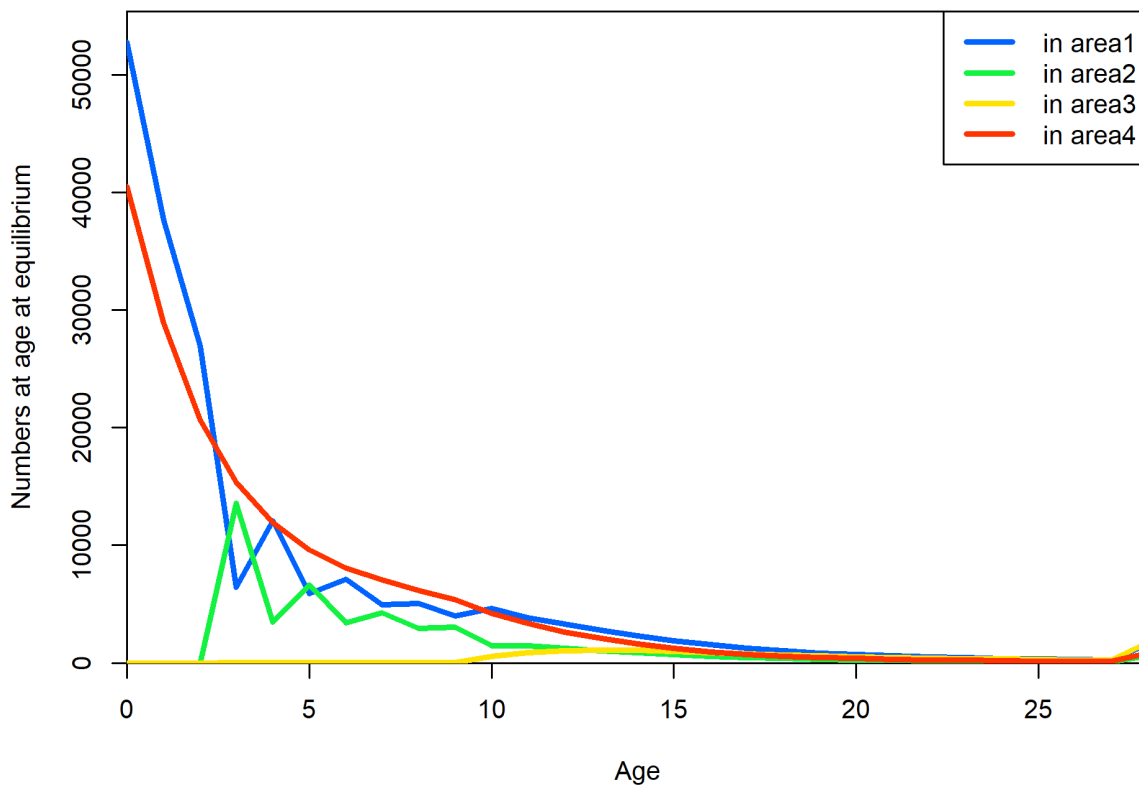


Figure A.10: Equilibrium numbers at age in each region. Note that ages are in pseudo-years, i.e. quarters.

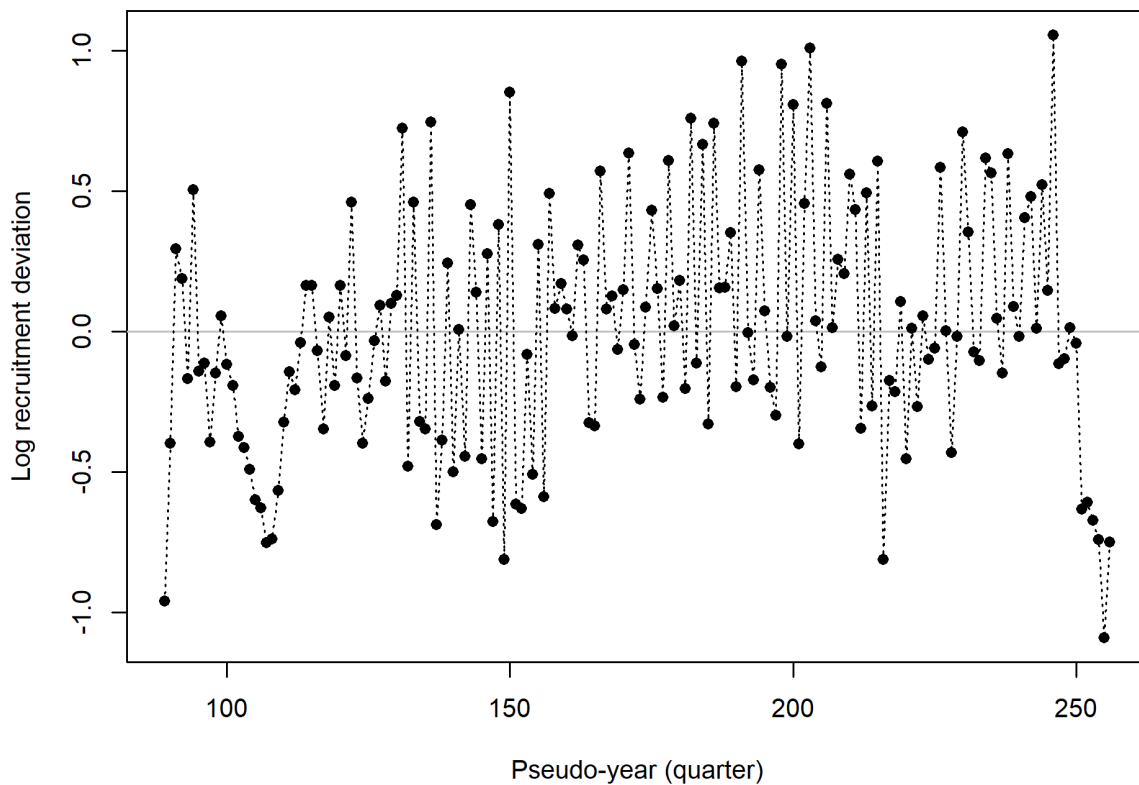


Figure A.11: Log recruitment deviates by pseudo-year.

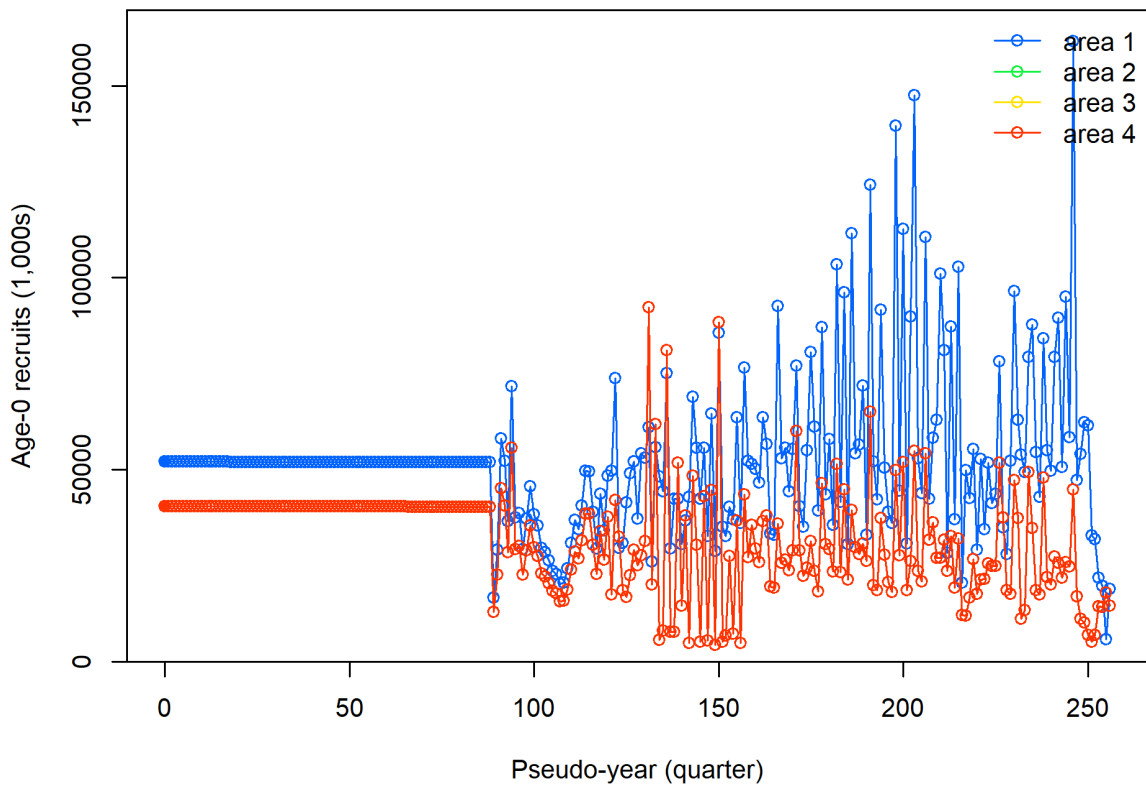


Figure A.12: Estimated recruitment output per pseudo-year by region.

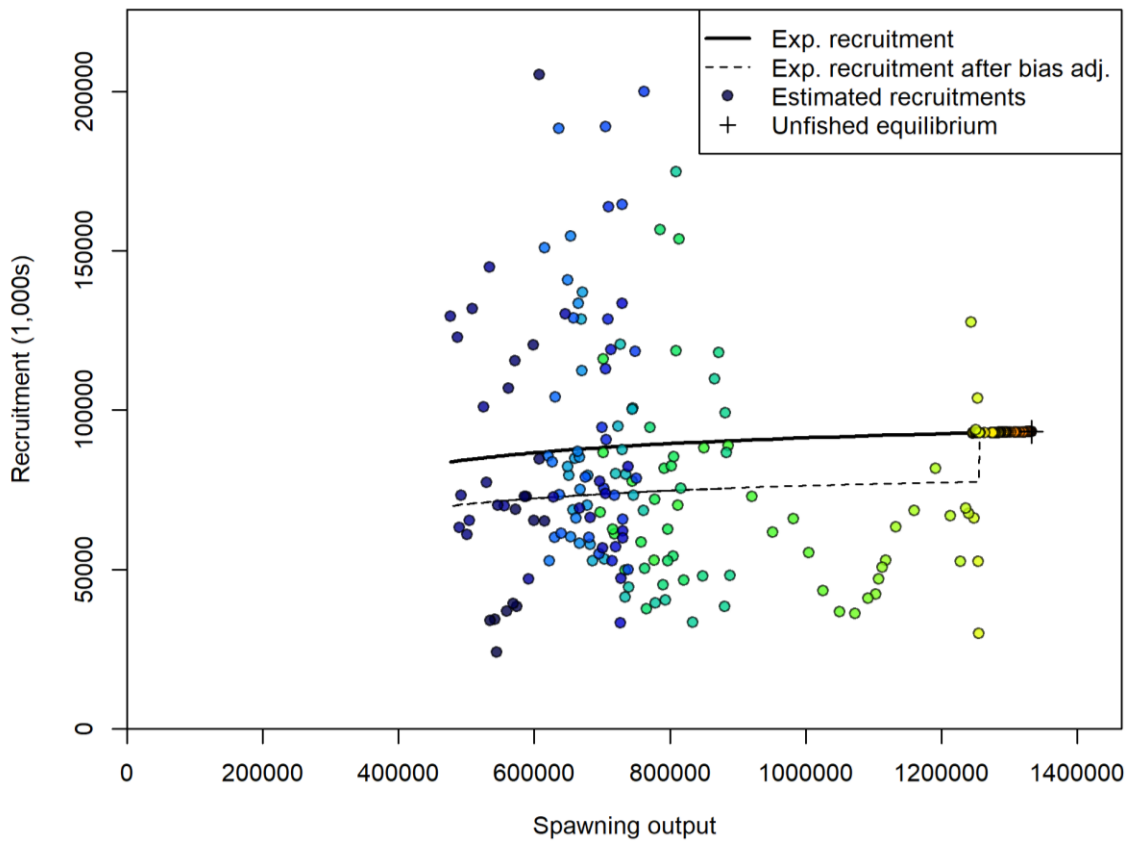


Figure A.13: Assumed spawner-recruitment relationship and individual recruitment estimates.

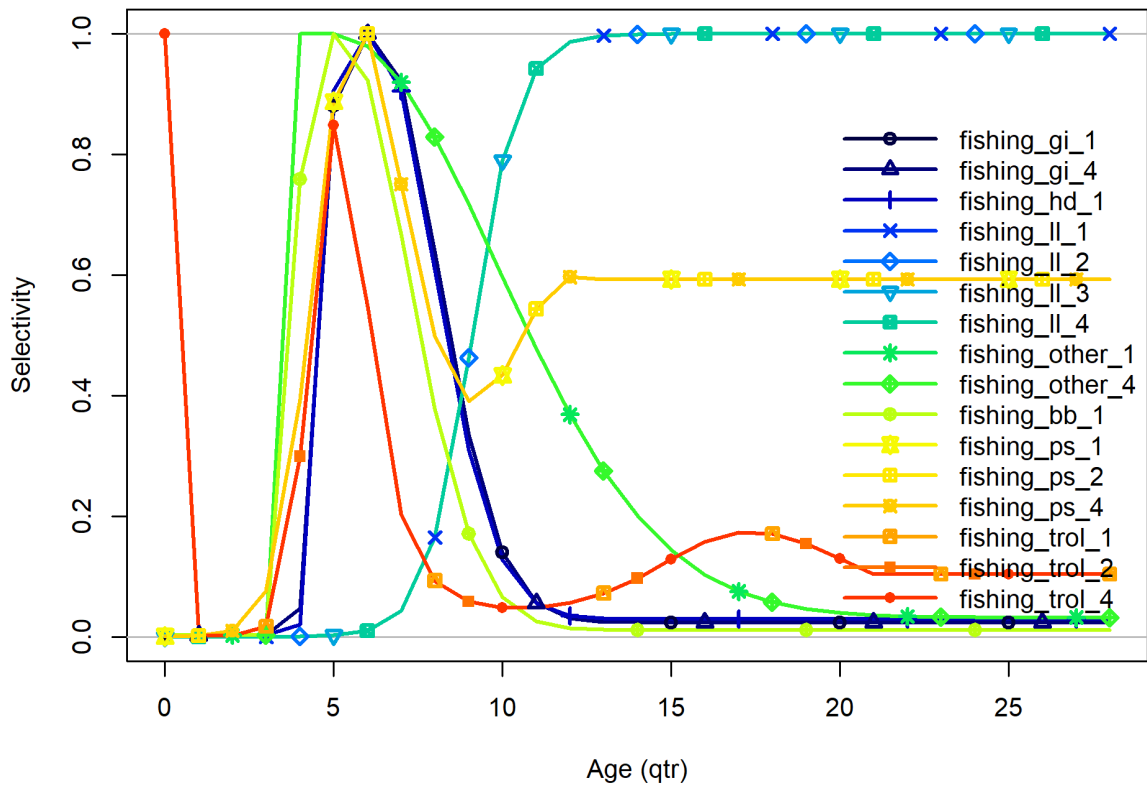


Figure A.14: Age-based selectivity by fleet. There are no length-based selectivities. Note that ages are in pseudo-years, i.e. quarters.

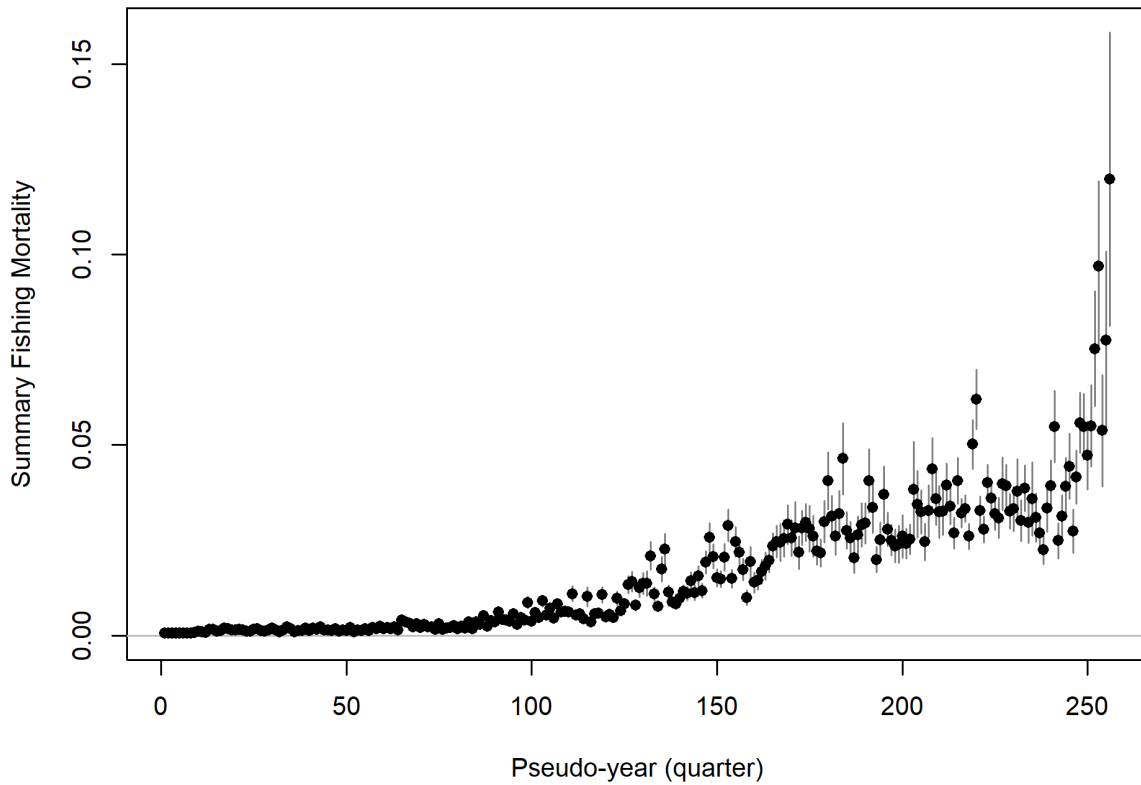


Figure A.15: Summarised fishing mortality by pseudo-year.

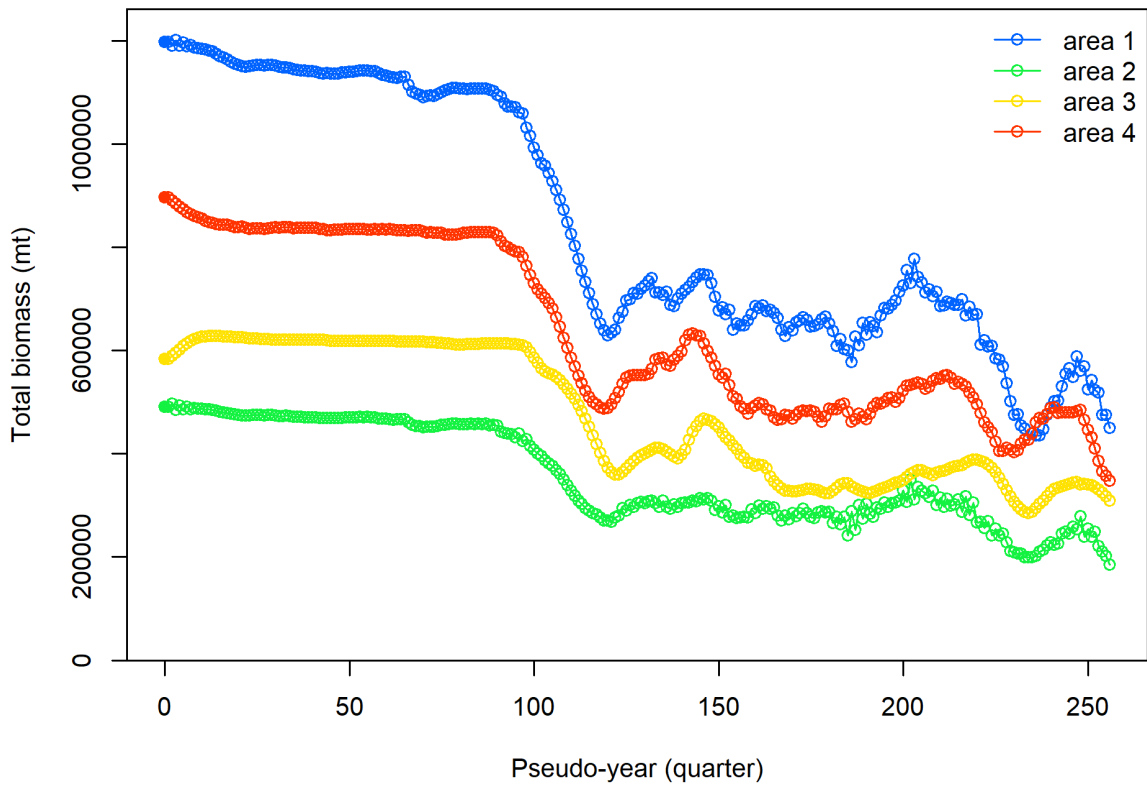


Figure A.16: Estimated total biomass trend by pseudo-year and region.

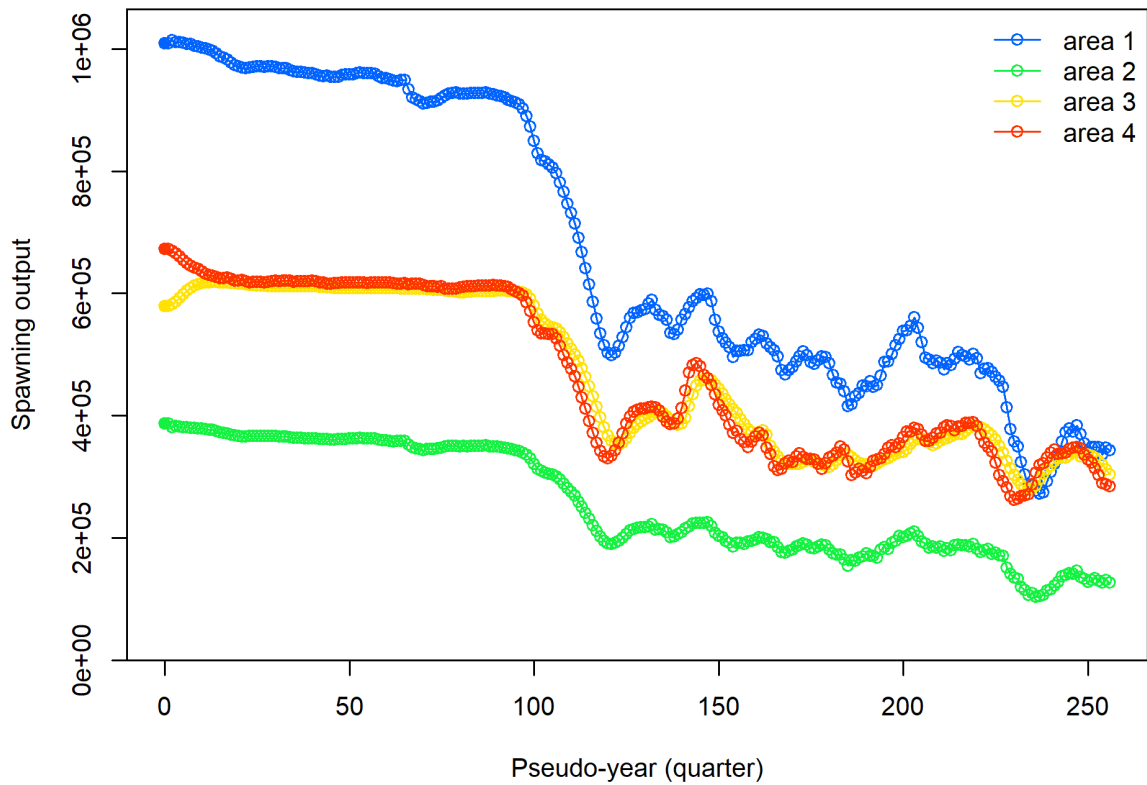


Figure A.17: Estimated trend in spawning output by pseudo-year and region.

Table A.1: Parameters estimated by each model, including the minimum and maximum bounds, initial values, mean and standard deviation of the normal priors. Also provided for the Base model are the parameters estimates ('Value'), standard deviations, and likelihood contributions of the priors ('Pr_Like').

| Parameter | Value | St. Dev. | Min | Max | Init | Prior | Pr_SD | Pr_Like |
|-----------------------------|-----------|----------|-----|-----|-------|-------|-------|----------|
| RecrDist_Area_1 | 1.13E+00 | 1.79E-01 | -5 | 5 | 1.18 | 1.5 | 0.25 | 1.08E+00 |
| RecrDist_Area_4 | 8.67E-01 | 1.79E-01 | -5 | 5 | 0.82 | 0.5 | 0.25 | 1.08E+00 |
| MoveParm_A_from_1to_1 | 1.72E+00 | 2.39E+00 | -12 | 12 | 1.87 | 0 | 4 | 9.23E-02 |
| MoveParm_B_from_1to_1 | 1.60E+00 | 2.31E+00 | -12 | 12 | 2.20 | 0 | 4 | 8.04E-02 |
| MoveParm_A_from_1to_2 | 2.46E+00 | 2.39E+00 | -12 | 12 | 3.08 | 0 | 4 | 1.90E-01 |
| MoveParm_B_from_1to_2 | 8.64E-01 | 2.31E+00 | -12 | 12 | 1.08 | 0 | 4 | 2.33E-02 |
| MoveParm_A_from_1to_4 | -4.18E+00 | 2.61E+00 | -12 | 12 | -4.95 | 0 | 4 | 5.47E-01 |
| MoveParm_B_from_1to_4 | -2.47E+00 | 2.32E+00 | -12 | 12 | -3.28 | 0 | 4 | 1.90E-01 |
| MoveParm_A_from_2to_1 | 2.49E+00 | 3.07E+00 | -12 | 12 | 0.53 | 0 | 4 | 1.94E-01 |
| MoveParm_B_from_2to_1 | 9.24E-01 | 2.87E+00 | -12 | 12 | 0.39 | 0 | 4 | 2.67E-02 |
| MoveParm_A_from_2to_2 | -2.49E+00 | 3.07E+00 | -12 | 12 | -0.53 | 0 | 4 | 1.94E-01 |
| MoveParm_B_from_2to_2 | -9.24E-01 | 2.87E+00 | -12 | 12 | -0.39 | 0 | 4 | 2.67E-02 |
| MoveParm_A_from_3to_3 | -4.77E-01 | 3.57E+00 | -12 | 12 | -0.03 | 0 | 4 | 7.10E-03 |
| MoveParm_B_from_3to_3 | 1.52E+00 | 2.84E+00 | -12 | 12 | 1.49 | 0 | 4 | 7.20E-02 |
| MoveParm_A_from_3to_4 | 4.77E-01 | 3.57E+00 | -12 | 12 | 0.03 | 0 | 4 | 7.10E-03 |
| MoveParm_B_from_3to_4 | -1.52E+00 | 2.84E+00 | -12 | 12 | -1.49 | 0 | 4 | 7.20E-02 |
| MoveParm_A_from_4to_1 | -3.02E+00 | 2.79E+00 | -12 | 12 | -3.86 | 0 | 4 | 2.86E-01 |
| MoveParm_B_from_4to_1 | -4.30E+00 | 2.60E+00 | -12 | 12 | -1.94 | 0 | 4 | 5.79E-01 |
| MoveParm_A_from_4to_3 | -1.73E+00 | 2.97E+00 | -12 | 12 | 0.86 | 0 | 4 | 9.39E-02 |
| MoveParm_B_from_4to_3 | 1.12E+00 | 2.39E+00 | -12 | 12 | -1.02 | 0 | 4 | 3.94E-02 |
| MoveParm_A_from_4to_4 | 4.76E+00 | 2.61E+00 | -12 | 12 | 2.99 | 0 | 4 | 7.08E-01 |
| MoveParm_B_from_4to_4 | 3.18E+00 | 2.39E+00 | -12 | 12 | 2.96 | 0 | 4 | 3.16E-01 |
| SR_LN(R0) | 1.14E+01 | 4.91E-02 | -2 | 25 | 11.49 | 10 | 5 | 4.16E-02 |
| AgeSel_1P_1_fishing_gi_1 | 5.26E+00 | 3.30E-01 | 1 | 12 | 8.49 | 7 | 3 | 1.67E-01 |
| AgeSel_1P_3_fishing_gi_1 | -6.66E-01 | 9.46E-01 | -10 | 9 | -0.81 | -1 | 3 | 6.21E-03 |
| AgeSel_1P_4_fishing_gi_1 | 1.88E+00 | 3.31E-01 | -5 | 9 | 1.84 | 3 | 1 | 6.30E-01 |
| AgeSel_1P_6_fishing_gi_1 | -3.71E+00 | 5.38E-01 | -9 | 5 | -1.62 | -2 | 1 | 1.45E+00 |
| AgeSel_3P_1_fishing_hd_1 | 5.19E+00 | 3.70E-01 | 1 | 40 | 22.57 | 10 | 5 | 4.64E-01 |
| AgeSel_3P_3_fishing_hd_1 | -1.07E+00 | 1.98E+00 | -10 | 9 | 3.83 | -1 | 3 | 2.90E-04 |
| AgeSel_3P_4_fishing_hd_1 | 1.85E+00 | 3.87E-01 | -5 | 9 | 3.37 | 3 | 1 | 6.61E-01 |
| AgeSel_3P_6_fishing_hd_1 | -3.48E+00 | 5.48E-01 | -9 | 5 | 0.15 | -2 | 1 | 1.09E+00 |
| AgeSel_4P_1_fishing_ll_1 | 9.10E+00 | 6.83E-02 | 8 | 18 | 12.75 | 14 | 2 | 3.00E+00 |
| AgeSel_4P_2_fishing_ll_1 | 2.00E+00 | 2.21E-02 | 2 | 6 | 3.44 | 4 | 1 | 2.00E+00 |
| AgeSel_8P_1_fishing_other_1 | 4.00E+00 | 1.20E-01 | 1 | 40 | 5.42 | 5 | 3 | 5.60E-02 |
| AgeSel_8P_3_fishing_other_1 | -3.00E+00 | 1.00E+00 | -10 | 9 | -3.08 | -3 | 1 | 2.00E-07 |
| AgeSel_8P_4_fishing_other_1 | 3.84E+00 | 1.90E-01 | -5 | 9 | 3.47 | 5 | 1 | 6.72E-01 |
| AgeSel_8P_6_fishing_other_1 | -3.41E+00 | 8.13E-01 | -9 | 9 | -3.13 | -3 | 1 | 8.45E-02 |
| AgeSel_10P_1_fishing_bb_1 | 4.20E+00 | 1.09E-01 | 1 | 10 | 2.81 | 3 | 1 | 7.14E-01 |
| AgeSel_10P_3_fishing_bb_1 | -2.05E+00 | 9.88E-01 | -7 | 5 | -0.73 | -2 | 1 | 1.41E-03 |
| AgeSel_10P_4_fishing_bb_1 | 2.07E+00 | 1.53E-01 | -5 | 9 | 3.03 | 3 | 1 | 4.28E-01 |

| | | | | | | | | |
|------------------------------------|-----------|----------|-----|----|-------|-------|-----|----------|
| AgeSel_10P_6_fishing_bb_1 | -4.43E+00 | 5.33E-01 | -9 | 9 | -2.33 | -3 | 1 | 1.03E+00 |
| AgeSpline_GradHi_fishing_ps_1_11 | -3.07E-02 | 4.11E-02 | -1 | 1 | -0.31 | -0.5 | 0.2 | 2.75E+00 |
| AgeSpline_Val_1_fishing_ps_1_11 | -3.66E+00 | 1.82E-01 | -10 | 10 | -3.40 | -3 | 0.5 | 8.69E-01 |
| AgeSpline_Val_3_fishing_ps_1_11 | -9.30E-03 | 1.04E-01 | -10 | 10 | -0.06 | -1 | 2 | 1.23E-01 |
| AgeSpline_Val_4_fishing_ps_1_11 | 3.15E-01 | 9.65E-02 | -10 | 10 | -0.11 | 0 | 1 | 4.95E-02 |
| AgeSpline_Val_5_fishing_ps_1_11 | 3.91E-01 | 1.11E-01 | -10 | 10 | -0.36 | -0.5 | 2 | 9.92E-02 |
| AgeSpline_GradHi_fishing_trol_1_14 | -2.02E-01 | 9.57E-02 | -1 | 1 | -0.09 | -0.1 | 0.1 | 5.20E-01 |
| AgeSpline_Val_1_fishing_trol_1_14 | -4.77E+00 | 7.08E-01 | -10 | 10 | -6.70 | -5 | 2 | 6.60E-03 |
| AgeSpline_Val_2_fishing_trol_1_14 | 6.40E-01 | 3.81E-01 | -10 | 10 | -3.24 | -2.5 | 0.5 | 1.97E+01 |
| AgeSpline_Val_3_fishing_trol_1_14 | 2.71E-01 | 3.57E-01 | -10 | 10 | -2.62 | -3 | 0.5 | 2.14E+01 |
| AgeSpline_Val_5_fishing_trol_1_14 | -2.08E-01 | 4.03E-01 | -10 | 10 | 0.20 | -0.5 | 1 | 4.27E-02 |
| TG_report_fleet:_1 | -4.88E+00 | 1.16E+00 | -10 | 10 | -2.82 | -2.82 | 2 | 5.30E-01 |
| TG_report_fleet:_2 | -5.45E+00 | 1.99E+00 | -10 | 10 | -5.43 | -5.43 | 2 | 2.08E-05 |
| TG_report_fleet:_3 | -6.45E+00 | 1.69E+00 | -10 | 10 | -6.05 | -6.05 | 2 | 1.99E-02 |
| TG_report_fleet:_4 | -6.11E+00 | 8.51E-01 | -10 | 10 | -1.55 | -1.55 | 2 | 2.60E+00 |
| TG_report_fleet:_5 | -5.45E+00 | 9.41E-01 | -10 | 10 | -1.89 | -1.89 | 2 | 1.58E+00 |
| TG_report_fleet:_6 | -2.38E+00 | 1.30E+00 | -10 | 10 | -0.61 | -0.61 | 2 | 3.93E-01 |
| TG_report_fleet:_7 | -4.38E+00 | 1.03E+00 | -10 | 10 | -1.28 | -1.28 | 2 | 1.21E+00 |
| TG_report_fleet:_8 | -4.06E+00 | 6.64E-01 | -10 | 10 | 4.60 | 4.60 | 2 | 9.37E+00 |
| TG_report_fleet:_9 | -2.09E+00 | 1.09E+00 | -10 | 10 | 1.54 | 1.54 | 2 | 1.65E+00 |
| TG_report_fleet:_10 | -5.61E+00 | 1.04E+00 | -10 | 10 | -2.81 | -2.81 | 2 | 9.77E-01 |
| TG_report_fleet:_13 | 1.69E+00 | 1.67E+00 | -10 | 10 | 1.43 | 1.43 | 2 | 8.63E-03 |
| TG_report_fleet:_15 | -4.73E+00 | 1.10E+00 | -10 | 10 | -2.32 | -2.32 | 2 | 7.25E-01 |
| TG_report_fleet:_16 | -2.78E+00 | 1.52E+00 | -10 | 10 | -1.93 | -1.93 | 2 | 9.12E-02 |